Electronic Thesis and Dissertation Repository

3-6-2015 12:00 AM

The Study of Mixing and Initial Granule Formation During High Shear Granulation of Pharmaceutical Powders

Aveen Alkhatib, *The University of Western Ontario*

Supervisor: Dr. Lauren Briens, *The University of Western Ontario*
A thesis submitted in partial fulfillment of the requirements for the Doctor of Philosophy degree in Chemical and Biochemical Engineering
© Aveen Alkhatib 2015

Follow this and additional works at: https://ir.lib.uwo.ca/etd

Part of the Other Chemical Engineering Commons

The Study of Mixing and Initial Granule Formation During High Shear Granulation of Pharmaceutical Powders

(Thesis format: Integrated Article)

by

Aveen Alkhatib

Graduate Program in Engineering Science
Department of Chemical and Biochemical Engineering

A thesis submitted in partial fulfillment
of the requirements for the degree of
Doctor of Philosophy

The School of Graduate and Postdoctoral Studies
The University of Western Ontario
London, Ontario, Canada

Abstract

Wet granulation is the agglomeration of particles using a liquid binder to form granules. The process is extensively used in the pharmaceutical industry to manufacture tablets, as granulation minimizes segregation, dust, and improves flowability. Granule uniformity is important in pharmaceutical manufacturing, as the tablet must contain a uniform distribution of excipients in the product in order to comply with United States Food and Drug Administration (FDA) regulations. The research presented in this thesis focuses on the influence of formulation and process parameters on granule formation. Sugar spheres were initially used to study segregation during the dry mixing phase of high shear granulation. The effect of formulation, specifically the effect of any hygroscopic components, was studied through drop penetration measurements using heterogeneous powder beds of varying hygroscopicity. The results were compared to theoretical models in the literature and led to improvements in the models through the introduction of a semi-empirical parameter. The effects of both process parameters and formulation were then combined in a final study. The conclusions from this research provide guidance for the selection of process parameters to promote the formation of optimal granule nuclei which can then grow into final granules with specific properties and provide information on the effect of formulation that can be used in development.

Keywords

Co-Authorship Statement

Chapters 4, 5, 6, and 7 are research studies will be submitted to peer-reviewed journals. The individual contributions of the authors of each manuscript are stated.

Chapter 4

The effect of operational parameters on mixing in wet high shear granulation

Authors: L. Briens and A. Alkhatib

A. Alkhatib conducted all experimental work. The manuscript was jointly written and revised by A. Alkhatib and L. Briens. Guidance for the work was provided by L. Briens.

Chapter 5

Granule nuclei formation in pharmaceutical powder beds of varying hygroscopic properties

Authors: A. Alkhatib and L. Briens

A. Alkhatib conducted all experimental work and performed all data analysis. The manuscript was jointly written and revised by A. Alkhatib and L. Briens. Guidance for the work was provided by L. Briens.

Chapter 6

Modelling liquid binder drop penetration into heterogeneous powder beds

Authors: A. Alkhatib and L. Briens

A. Alkhatib conducted all experimental work and performed all data analysis. The manuscript was jointly written and revised by A. Alkhatib and L. Briens. Guidance for the work was provided by L. Briens.

Chapter 7

Influence of process parameters and powder properties on initial granule nuclei formation during high shear granulation

Authors: A. Alkhatib and L. Briens

A. Alkhatib conducted all experimental work and performed all data analysis. The manuscript was jointly written and revised by A. Alkhatib and L. Briens. Guidance for the work was provided by L. Briens.

Acknowledgments

I would like to begin by thanking my supervisor, Dr. Lauren Briens, for providing me the opportunity to work on a project that I enjoyed. I would also like to thank her for her patience and support during my studies throughout my doctoral degree. Also, a thank you to my past and current lab members: Ryan Logan, Allison Crouter, Taylor Sheehan and Breanna Bowden-Green for your support, coffee breaks, and motivational speeches. A big thank you to Souheil Afara and Brian Dennis for their willingness to help at all times. I would also like to thank the Natural Sciences and Engineering Research Council (NSERC) of Canada for the financial support of this research.

My time at Western has had a number of ups and downs. Less than 2 years into my program, my family and I were struck with the sudden illness of my big brother, Weesam. As family is the most important thing to me, I took time off to care for my brother and my family. A couple of months later, my youngest brother, Shwan passed away suddenly and 42 days later Weesam had succumbed to his illness. My brothers were my strength, my cheerleaders, and my best friends. Weesam, being a vascular surgeon (and ex-chemical engineer), always had a way of pushing you when you were ready to give up. He had a "tough love" approach that motivated his siblings. He wanted to see us succeed in our careers and lives. He is the hardest working individual I have ever known, yet the most kind and humble. Shwan, my younger brother, always had a positive twist on everything, making sure to see the best in everyone he met. He thrived on making someone's day a little better, be it with a smile or a simple compliment. He truly had an innocent heart of gold. Shwan also wanted me to never give up, but instead of the "tough love" approach, opted for a softer technique; pushing me to better myself and reminding me to be kind to others. They were both extraordinary young men that will forever be missed.

I know, without a doubt they would have wanted me to continue my studies. Thus, without hesitation, I returned to Western to complete my PhD.   The lessons they have taught me have shaped my time here at Western. They remind me that what truly matters in life is how we treat others, to try to make someone's day a little better, and to continue to never give up

until we achieve our goals. Weesam and Shwan's lessons continue to inspire me to better myself and I hope to always make them proud throughout my life.

I could not have completed my PhD work without the immense love and support of my parents, and my sister Cheen. You have been my rock, giving me the strength to keep going. I also would like to acknowledge, Ben, Trish and their adorable sons Charlie and Leo Shwan for giving me and my family happiness. I would also like to acknowledge Noshin and Farah for all the late night talks, support, and beautiful friendships I have with both of you. You both are my sisters and I am so lucky to have you both in my life. Finally, I would like to thank Amu Kais and Khala Khalida for the weekly phone calls and selfless love I have received from both of you.

This thesis is dedicated to my brothers

Weesam Alkhatib (Jan 22, 1978- April 14, 2012)

Shwan Alkhatib (April 30, 1986-March 2, 2012)

May your souls be in peace and happiness

"You know why else I want to win?

So good people can be happy. Just for a day.

Because good people deserve good things, even if just for a day"

–Shwan Alkhatib

Table of Contents

List of Tables

List of Figures

List of Abbreviations

FDA	Food and Drug Administration
DEM	Discrete Element Modeling
PEPT	Positron Emission Particle Tracking
NIR	Near-Infrared Spectroscopy
AAE	Audible Acoustic Emissions
DOE	Design of Experiments
Ψ_a	Dimensionless spray flux
$\dot{A}$	Flux of liquid exposed to powder
d_d	Average drop size
$\dot{V}$	Volumetric flow rate
DDA	Decreasing drawing area
CDA	Constant drawing area
τ_{DDA}	Theoretical drop penetration time assuming DDA
τ_{CDA}	Theoretical drop penetration time assuming CDA
V_o	Drop volume
R_{pore}	Effective size of pores in powder bed
μ	Liquid viscosity
γ_{LV}	Liquid-vapor surface tension
θ_d	Dynamic contact angle

ε_{eff}	Effective bed voidage
R_{eff}	Effective pore radius
Φ	Shape factor
d_{32}	Surface mean particle diameter
Wcs	Work of cohesion for a solid
W_{CL}	Work of cohesion for a liquid
W_A	Work of adhesion for an interface
N_1/N_2	Impeller speed for granulator 1 and 2
D_1/D_2	Diameter of impeller for granulator 1 and 2
X_i	Mass percentage of small particles from sample at location i
$\overline{X}$	Observed mean of sample
N	Sample size
y_s	Standard deviation
ANOVA	Analysis of variance
Fr	Froude number
MCC	Microcrystalline cellulose
HPMC	Hydroxypropyl methylcellulose
SEM	Scanning electron microscope
QbD	Quality by Design
PSD	Particle size distribution

Chapter 1

1   Introduction to solid dosage manufacturing

Tablets are one of the most common dosage forms for pharmaceutical applications. Compared to other forms, solid dosage forms are relatively easier to ingest for the patient as well sustain a longer shelf life, giving tablets a major advantage for delivery to the patient [1, 2]. As a result, almost two-thirds of all dosage forms are tablets [3].

The manufacturing of tablets is generally carried out using one of three main processes: 1) direct compression, 2) dry granulation or roller compaction, and 3) wet granulation. The simplest process for tablet manufacturing is direct compression where a powder formulation is fed through a tablet feeder and compressed into a tablet for oral consumption. The second type of tableting process, dry granulation, feeds a raw material through rollers that compact the powder into a ribbon and are then milled into granules. The granules are then compressed into a tablet form in a press. The final process, and the focus of this research, uses wet granulation for tablet manufacturing. During wet granulation, powder is agglomerated into granules using a liquid binder. When liquid binder initially contacts the powder bed, granule nuclei are formed. Agitation via an impeller in high shear wet granulation allows the granule nuclei to grow through coalescence and then consolidate to a final product [4]. Granules are then typically dried, milled, and fed through a tablet press for compaction.

For tablets to comply with specifications from regulatory agencies such as the Food and Drug Administration (FDA), tablets must contain the correct proportion in a uniform distribution of all formulation components including excipients and the active drug. As a result, it is also crucial for granules produced through wet granulation to contain representative amounts of the formulation components.

The formulation used in wet granulation is typically a mix of powders with differing physical and chemical properties. The powder is first dry mixed in the granulator bowl by an impeller. Assuming that the powder is well mixed, the liquid binder spray is then started for the granulation. Powder segregation during the dry mixing phase can result in

the formation of granule nuclei which do not contain the correct proportions of the formulation components which can then develop into final granules that do not meet the specified properties and must be discarded. It is therefore important to study powder mixing during the dry mixing phase as well as the initial nucleation phase of granulation. Previous research on powder mixing using impellers, as well as granule formation for different formulations, has been reported. However the combination of both factors remains poorly understood and requires further study to be able to improve high shear wet granulation.

1.1   Thesis Objectives

The overall objective of the research presented in this thesis was to improve the understanding of the influence of process parameters and formulation properties on granule nuclei formation during high shear wet granulation.   Specific objectives contributing to the overall objective were addressed in Chapters 4 through 7.

Chapter 2: This chapter presents a literature survey on powder mixing including mixing mechanisms and different techniques that can be used to monitor mixing.

Chapter 3: This chapter reviews pharmaceutical drug manufacturing with an emphasis on high shear wet granulation include mechanisms of granule formation and subsequent granule growth.

Chapter 4: The objective the research presented in this chapter was to use a design of experiments to examine the effect of impeller speed on particle size differences, mixing time and loading order on possible particle segregation during the dry mixing just prior to the start of wet high shear granulation. It was hypothesized that segregation can occur during this mixing and can affect the formation of granule nuclei and therefore also final granule properties.

Chapter 5: The objective of the research presenedt in this chapter was to examine liquid binder drop penetration and subsequent granule nuclei formation using a mixture of two common commercially used excipients, hygroscopic microcrystalline cellulose (MCC) and non-hygroscopic α- lactose monohydrate. It was hypothesized that liquid binder viscosity and the presence of a hygroscopic component in the mixture would affect drop penetration times and granule morphology.

Chapter 6: The objective of the research presented in this chapter was to examine the models available in the literature for predicting drop penetration times using more complex powder bed systems of MCC and α-lactose monohydrate, two excipients commonly used in commercial formulations. It was hypothesized that these models may not provide accurate predictions for the complex powder mixtures of pharmaceutical formulations.

Chapter 7: The objective of this research presented in this chapter was to combine the research on mixing with that on drop penetration to examine conditions that could influence granule nuclei formation in high shear wet granulation.

Chapter 8: This chapter presents a summary of the research from this thesis and the impact this research can have on pharmaceutical manufacturing.

1.2   References

1. H.C. Ansel, Introduction to Pharmaceutical Dosage Forms, 4th Edition. Lea and Febiger: Philadelphia, Pa., USA (1985).

2. L. L. Augsburger, S. W. Hoag, Pharmaceutical dosage forms: Tablets (Vol. 3). Informa healthcare. (2008).

3. S. K. Niazi, Handbook of Pharmaceutical Manufacturing Formulations: Liquid Products (Vol. 3). CRC press. (2004).

4. S.M. Iveson, J.D. Litster, K. Hapgood, B.J. Ennis, Nucleation, growth and breakage phenomena in agitated wet granulation processes: a review, Powder Technology, 117 (2001) 3-39.

5. R.L. Stewart, J. Bridgwater, D.J. Parker, Granular flow over a flat-bladed stirrer, Chemical Engineering Science, 56 (2001) 4257-4271.

6. S.L. Conway, A. Lekhal, J.G. Khinast, B.J. Glasser, Granular flow and segregation in a four-bladed mixer, Chemical Engineering Science, 60 (2005) 7091-7107.

7. S. Radl, E. Kalvoda, B.J. Glasser, J.G. Khinast, Mixing characteristics of wet granular matter in a bladed mixer, Powder Technology, 200 (2010) 171-189.

8. T.M. Chitu, D. Oulahna, M. Hemati, Rheology, granule growth and granule strength: Application to the wet granulation of lactose-MCC mixtures, Powder Technology, 208 (2011) 441-453.

9. L. Shi, Y. Feng, C.C. Sun, Initial moisture content in raw material can profoundly influence high shear wet granulation process, International Journal of Pharmaceutics, 416 (2011) 43-48.

10. K.P. Hapgood, B. Khanmohammadi, Granulation of hydrophobic powders, Powder Technology, 189 (2009) 253-262.

Chapter 2

2   Introduction to Mixing

Powder mixing is a crucial manufacturing process in many industries such as cosmetics, food, chemicals, detergents, and pharmaceuticals. It is important to produce a homogenous mixture of two or more components. This is especially critical in the pharmaceutical industry as tablets and granules must comply with content uniformity criteria as stated by the United States Food and Drug Administration (FDA). Mixing of powders can influence subsequent steps in the manufacturing of pharmaceutical tablets as non-homogenous mixture blends can result in tablets with a non-uniform distribution of excipients and actives in the product. Difficulties in powder mixing arise from differing particle sizes, shape, and densities. This review will aim to achieve the following:

- Provide an overview on general mixing and segregation
- Discuss various mixing mechanisms
- Summarize the mixing of bladed impellers
- Discuss the modelling and monitoring of mixing

2.1   Mixing definitions

Definitions and general remarks regarding the mixing of dry solid particles are summarized thoroughly in a review by Poux et al. [1]. A mixture where each particle is near a particle of a different composition is defined as an ideally ordered mixture. Mixtures can be defined as random or orderly, where a perfectly random mixture requires particles of equal size and weight and an ideally ordered mixture does not include this requirement. A complete and incomplete mixture can also be described in terms of statistics. A completely mixed state occurs when particles of different colors are mixed where the probability of drawing a particle of a specific color at any point is the same throughout the mixer. Thus incomplete mixing occurs when the probability of drawing a particle of a specific color throughout the mixer is not identical.

Authors have also attempted to characterize mixing states using the concept of sample size. Ordered mixtures cannot exceed the homogeneity of a single ordered unit.

Consequently, the sample size of a single ordered unit is used to define homogeneity in a specific mixing process. The concept of using a single ordered unit to define the degree of mixing in a powder system has been used by several authors [1].

It is clear that defining homogeneity and mixing states in powder mixing is difficult and varies depending on the study. Thus, the term homogeneity needs to be defined on an appropriate scale specific to the system of interest.

2.1.1   Mixing Factors

Poor mixing of particles can result in non-homogeneous powder beds, leading to variability of tablet content. Super and sub-potent tablets can then both lead to a decrease in value and risks of toxicity to patients. Segregation is defined as the separation of powder particles during the vibration of a powder bed or the flow of powder and is a main problem during powder mixing and tablet manufacturing. It is known that segregation results due to particle size, shape, and density differences in a powder mixture [2, 3]. The three main mechanisms causing segregation are *percolation*, *density segregation,* and *trajectory segregation* [2].

Segregation of powders due to particle size differences is known to occur due to the percolation of particles. Percolation can be defined as the random occupation of different items of a chosen lattice. A thorough review on percolation theory is given by Hans Leuenberger [4]. In the case of pharmaceutical powders, percolation occurs when smaller particles are allowed to travel through macro-voids created by the powder mixture of differing particle sizes, thus leading to particle segregation. Percolation can be described as either site percolation or bond percolation, where site percolation assumes sites (macro-voids) are occupied at random, thus unoccupied sites may be empty or occupied by an excipient. Bond percolation assumes all sites are occupied and a random bond between two particles can possibly form. When discussing percolation throughout this review, site percolation is to be assumed.

Particles become more difficult to mix as the shape deviates from a sphere. Acicular or flat particles prolong mixing time due to aggregation and finer materials fall through

macro- voids created by the powder mix, leading to percolation. Powders of similar particle size and shape tend to have better flow than irregular shaped particles as spherical particles minimize inter-particle contact and irregular particles have poorer flow properties. High internal and surface friction angles on flat, angular, or rough particles with low friction angles tend to cause segregation. Shape differences can cause segregation, but occur more easily with particle size differences.

Particle density differences can lead to segregation of powders. Gravitational forces pull the more dense particles to the bottom of the powder bed and the less dense particles migrate towards the top of the bed. Rippie et al. [5] found that density alone does not cause significant segregation, but combined with different particle sizes, segregation increased. Segregation may occur with large particle differences in density, but is relatively unimportant compared to particle size and shape differences [6].

During trajectory segregation, particles travel a distance proportional to the square of its diameter as long as the particles are of the same density and velocity. Therefore, in a mixer, larger particles will travel to the sides of a mixer bowl, and the small particles migrate to the center [2].

2.2   Mixing Mechanisms

In order to achieve ideal mixing, particles should move randomly and in three dimensions. "Dead" regions, where mixing does not take place in the mixing unit, should be avoided and particles should move individually. Mixers can be characterized by one or a combination of three phenomena [2, 7, 8]:

- Diffusion: via the motion of a particle with respect to its neighbours. Particles roll over each other on a sloping surface of a powder. The powder is raised past the angle of inclination at which a particle will begin to slide, overcoming frictional forces.
- Convection: via the motion of a group of particles in relation to their neighbours. Particle movement arises as displacement with respect to other particles inside the

mixing device. Thus, spatial homogeneity is improved due to the observation of particle movement with respect to neighbouring particles.

- Shearing: via a change of distribution layers of ingredients in space. Occurs with convective mixing when slip planes are formed where velocity gradients are high; these planes collapse, with further mixing occurring. The effect is seen in mixers that involve a moving blade and general rotation.

2.2.1   Mixer Types

Mixers can be classified by the mixing mechanism (diffusion, convection or shearing) and the mixing action. Mixing actions can range from mixers with moving vessels to fixed vessels and fluidized beds [1]. Table 2.1 summarizes important characteristics and mixing mechanisms for some of these mixers. This review will focus on high speed impeller mixers, which involve convection and shear as the main mixing mechanisms.

Table 2.1: Description of various mixers

Mixer Type	Mixing Mechanism	Mixing Action
Rotating Drum	Diffusion and Shear	• Vessel is rotated along an axis, usually horizontal. • Radial and axial mixing occurs, though radial mixing occurs much quicker. • Used for free-flowing materials as emptying the drum is relatively easy to do. • Segregation of powers during emptying occurs.
Orbiting Screw Mixer	Convection and Diffusion	• Involve an inverted cone with an orbiting screw attached to the inside of the device. • The screw rotates and mixes the powders; materials move in an upward direction in the screw and general flow is downwards throughout the cross section of the mixer.
Double Cone Mixer	Shear and Diffusion	• Batch mixer where particles roll and fold over each other
High-speed granulators	Convection and Shear	• Involve a mixer bowl with an attached impeller. Blades push particles around the mixer at low speeds; at high speeds a toroidal movement of the particles take place as centrifugal effects become important to the system

2.3   Mixing with bladed impellers

In the pharmaceutical industry, efficient mixing is of critical importance in order to achieve uniform distribution of actives and excipients which would eliminate the chance of sub-or super potent tablets. Currently, manufacturing practices involve mixing of specific batches at predetermined times usually chosen via trial and error. However, the ability to predict mixing behaviour and how this influences granule nuclei behaviour can significantly reduce processing time thus saving in operating cost. Studies have been conducted to examine the effects of mixing in a bladed mixer, similar to a granulator.

Zhou et al. [9] examined particle flow in a cylindrical bladed mixer using monosize 5 mm diameter spheres. The effect of loading or initial arrangement of the particles was found to affect the mixing kinetics, but not the quality of the final mixture. Three different

initial arrangements were investigated with a horizontal layering arrangement showing the fastest mixing time. Koller et al. [10] also investigated initial arrangements on mixing. A binary powder mixture of acetyl salicylic acid and lactose monohydrate was used with horizontal layering so that one component initially formed the top powder layer with the other component at the bottom. Mixing was found to occur in two stages: (i) a convective vertical mixing between the layers followed by (ii) diffusive mixing. The convective mixing stage "overshoots" the vertical movement of the powders resulting in an intermediate state with the two horizontal layers partially reversed from the initial positions. The degree of this "overshoot" was affected by the loading and attributed to differences in the particle sizes and shapes.

Fill levels have been shown to affect mixing in bladed mixers. At high fill levels, Koller et al. [10] found that diffusive mixing primarily impacts the surface composition of the powder bed. The large convective movement of the horizontally loaded layers was not observed. Stewart et al. [11] observed that recirculation regions became much smaller as the fill level was increased. From this, they concluded that in a bed with particles of different sizes, densities and shapes, segregation will occur causing some particles to be over represented at the powder bed surface.

Segregation in a bladed mixer was studied by Conway et al. [12] using mixtures of glass beads of varying diameter. Larger particles segregated to the powder surface and then to the bowl perimeter. This pattern was observed independently of powder loading. Impeller velocities only up to 50 rpm were tested. Higher impeller velocities are typically used in high shear granulators, and therefore would be expected that the high centrifugal effects would segregate the large particles near the bowl perimeter.

The mixing behaviour of dry particles has been found to be different from that of wet particles. Radl et al. [13] found that mixing of wet particles was very heterogeneous as many different flow patterns were formed within the powder bed. This resulted in higher mixing rates for wet particles compared to dry powders. Lekhal et al. [14] confirmed different mixing of wet and dry particles. They attributed the difference to changes in the powder bed porosity as a result of agglomerate formation and increased cohesiveness. In

high shear granulation, as the liquid binder addition begins, the flow and mixing of the powder within the bowl should then change. The powder surface layer flow and composition may correspondingly change, affecting further granule formation.

Powder flow during high shear granulation was observed by Litster et al. [15]. Two distinct regions of flow were observed: bumping and roping (Figure 2.1). At low impeller speeds, the powder proceeds in the "bumping" regime. The powder surface remains relatively horizontal with little vertical powder turnover resulting in poor powder flow. As impeller speed increases, powder flow undergoes the "roping" regime, where powder is forced upward and tumbles down the bed surface. Good powder flow and vertical turnover is observed in this regime. Logan et al. [16] observed the transition from bumping to roping to occur at an impeller speed of 300 rpm using a Fielder PMA 1 granulator.
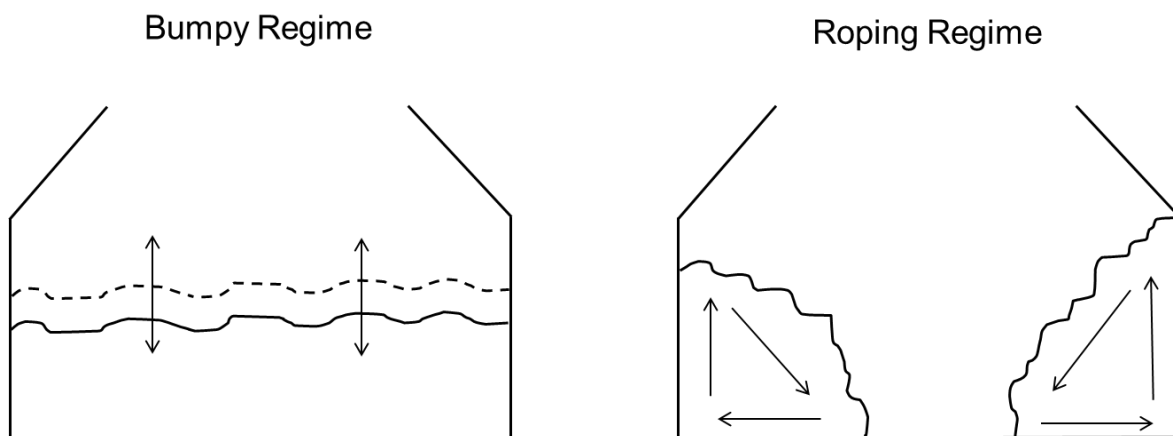
Figure 2.1: Bumping and roping powder flow regimes adapted from Litster et al. [15]

2.4   Modelling Techniques for Mixing

Several computational modeling techniques have been used in pharmaceutical manufacturing processes [9, 11, 13, 17-23]. The primary computational modeling technique for studying particle flow in a bladed mixer is Discrete Element Modelling (DEM).

2.4.1   Discrete Element Modelling (DEM)

Discrete element modeling can simulate the dynamics of individual particles in a system based on first principles. The DEM technique was initially introduced by Cundall et al. [17] and has since been utilized by many researchers in order to obtain a more detailed understanding of powder behaviour in a mixer [9, 18-23]. DEM calculates the location, velocity, and acceleration of individual particles as well as the forces acting on the particle. The calculated force is based on Newton's second law where the motion of each particle is described by respective equations. DEM technology has been used for various operating equipment in the pharmaceutical industry.

Remy et al. [18] used DEM simulations to study the granular flow in an agitated four bladed mixer. Blade orientation was found to influence the flow patterns and mixing kinetics. Also, frictional characteristics strongly influenced the behaviour of the granules inside the mixer. Another study by Remy et al. [19] examined the effect of mixer properties and fill level on granular flow in a bladed mixer. Fill levels were shown to influence the granular flow behaviour, with a critical fill level being characterized where above this level, the behaviour of the particles was found to be invariant of fill level. Wall friction was also shown to influence granular behaviour.

Agitation torque within in the high shear mixer and its effect on particle motion was studied by Sato et al. [20]. The motion and torque of the agitator blade was numerically analyzed using DEM where the torque, velocity profiles, and forces acting on the particles were calculated under different agitator rotational speeds. Results showed that particles experienced greater force at the bottom of the mixer, compared to the middle or upper sections. Particle flow changed as a function of agitator rotational speed and also indicated different velocity profiles.

2.5   Monitoring and measuring mixing

Dry mixing of a powder blend can have a significant effect on the subsequent steps in tablet formation [24]. However, process design and operation has proven to be difficult as judgment is largely based on experience rather than science. As a result, various methods

including process analytical technologies (PAT) and modeling techniques have been studied. A homogeneous mixture of all excipients during the blending process is needed, therefore pharmaceutical manufacturers invest a great amount of time, labour and resources to understand and perfect this process.

Current manufacturing practices for ensuring blending homogeneity involves collecting manual samples at pre-determined points of the process and analyzing by chromatography or UV-Vis spectroscopy [25]. A review by Poux et al. [1] investigated powder mixing in vessels, with an emphasis on practices used by different industries such as pharmaceutical, food, detergents and cosmetics. Traditional methods of sampling involve the use of a sampling probe that is inserted into the mixture and samples are collected at varying depths and locations. This sampling technique is highly invasive and can lead to distortions of the mixture which would ultimately lead to inaccurate samples that do not represent the bulk mixture. As a result, current research has focused on developing on-line monitoring methods that have the advantage of receiving information of the mixture without the need to stop the process, while also being non-invasive.

2.5.1   Positron Emission Particle Tracking (PEPT)

Positron emission particle tracking (PEPT) involves a single radioactively marked and tracked particle. The marked particle is added to the mixer and a positron camera consisting of two gamma-ray detectors is then placed in the mixer. The lone positron – emitting radionuclide particle is traced via emitted positrons that annihilate with electrons thus producing gamma rays. These gamma rays are co-linear and move in opposite directions. Detectors on either side of the mixer record the positions of the gamma rays. The gamma rays can be traced through opaque material, and therefore the motion of these particles can be detected within the mixer. Thus, it is possible to study three-dimensional granular flow and flow within the material bed in the mixer. A study by Parker et al. [26] provides more detail on the PEPT technique.

Particle behaviour inside a mixer has been studied by several researchers using PEPT technology. Stewart et al. [11] used PEPT to examine the mixing behaviour of glass spherical beads at various fill levels and impeller speeds in a vertical mixer with two

opposing blades. Mixing behaviour was found to be dependent on the particle's location inside the bowl. At the walls, particles in the path of the blades travelled upward and formed heaps then finally passed over the mixer blade. Away from the wall, particles moved radially producing 3-D recirculation regions.

Two dimensional flow in a horizontal bladed mixer has also been studied by several research groups by observing the flow using photography through the end wall of the bed. They found that there were differences between flow at the end wall and in the main bed [27-30].

2.5.2   Near-Infrared Spectroscopy (NIR)

Near infrared spectroscopy has been used as an on-line technique for monitoring the homogeneity of pharmaceutical powder blends [10, 31-33]. A study by Blanco et al. [31] used NIR to monitor blending with mixtures consisting of a heterogeneous powder blend where a method for calculating the mean square differences was developed. NIR was also used to monitor powder blending in a V-blender where experiments detected spectral changes until eventually converging to a point of variance, leading to blend homogeneity [33]. A V-blender was also utilized by Hailey et al. [32] to detect powder blending using NIR technology. An automated system was developed that used fiber-optics and a graphical user interface using the NIR technology. The software controls the blender and spectrophotometer operations while producing statistical spectral data analysis in real time. Acetyl salicylic acid and α-lactose were used in a convective mixer where NIR was utilized for powder blend monitoring [10]. Fill levels and filling protocols were varied which eventually led to uniform powder blend according to NIR technology.

2.5.3   Audible acoustic emissions (AAE)

During the granulation process, sound is produced from particle-particle and particle-wall/equipment collisions. These sound waves change in frequency and intensity which can then be used to monitor granulation processes. Audible acoustic emissions (AAE) have the advantage of collecting real time data, while exhibiting non-invasive

characteristics. There is no need to alter the manufacturing equipment as sensors can be placed on the outside walls.

Audible acoustic emissions have been developed as monitoring techniques for high shear granulation [34, 35]. Collisions of the granules against the surface of the granulator bowl produce sounds that can be captured and analyzed for use as a monitoring method. Particle properties such as size, density and porosity, change as granulation proceeds, thus influencing the sound emission of the process.

A study by Tily et al. [36] used acoustic emissions to monitor the mixing process of dry powder mixtures. The mixing was studied using equipment that closely mimicked that of orbital mixers used in industry. It was demonstrated that AAE from particle-wall collisions could be used to monitor a solid mixing process.

Non-invasive acoustic emission monitoring of aspirin, citric acid, and Avicel in a bench top convective mixer were studied by Allan et al. [37]. Intensity of the AAE signal increased with impeller speed, mass of powder, decreasing density of the particles, and particle size. Also, as the mixture became more homogenous, it was observed that the AAE signal reached a plateau.

Acoustic emissions have been applied in bench top and small scale mixers to study both dry and wet mixing. AE has also been used for end-point determination in industrial high shear granulation.

2.5.4   Thermal Tracer

The use of thermal tracers to study the mixing quality of powder blends in a bladed mixer was developed by Saberian et al. [38]. Particles were cooled and mixed with particles at room temperature. Thermocouples were placed in various ports inside the bladed mixer and temperature of the powder was measured using a data acquisition system. Mixing quality was defined as the inverse of the dimensionless standard deviation of the temperatures taken throughout the trial. It was found that in order to achieve a good distribution of powders throughout the system, dry mixing needed to proceed for 90

seconds. This technique allows for a quick and easy method for measuring mixing quality in dry powder blends using a bladed mixer.

2.6   References

1. M. Poux, P. Fayolle, J. Bertrand, D. Bridoux, J. Bousquet, Powder mixing- Some practical rules applied to agitated systems, Powder Technology, 68 (1991) 213-234.

2. H.J. Venables, J. Wells, Powder mixing, Drug development and industrial pharmacy, 27 (2001) 599-612.

3. F.J. Muzzio, P. Robinson, C. Wightman, D. Brone, Sampling practices in powder blending, International Journal of Pharmaceutics, 155 (1997) 153-178.

4. H. Leuenberger, The application of percolation theory in powder technology, Advanced Powder Technology, 10 (1999) 323-352.

5. E.G. Rippie, M.D. Faiman, M.K. Pramoda, Segregation kinetics of Particulate solids systems. 4. Effect of particle shape on energy requirements, Journal of Pharmaceutical Sciences, 56 (1967) 1523-&.

6. V. Swaminathan, D.O. Kildsig, Polydisperse powder mixtures: Effect of particle size and shape on mixture stability, Drug Development and Industrial Pharmacy, 28 (2002) 41-48.

7. K. Van Scoik, Theory of Mixing Solids, Abbott Laboratories, Arden House Conference, 1992.

8. J. Bridgwater, Mixing of powders and granular materials by mechanical means-A perspective, Particuology, 10 (2012) 397-427.

9. Y.C. Zhou, A.B. Yu, J. Bridgwater, Segregation of binary mixture of particles in a bladed mixer, Journal of Chemical Technology and Biotechnology, 78 (2003) 187-193.

10. D.M. Koller, A. Posch, G. Hoerl, C. Voura, S. Radl, N. Urbanetz, S.D. Fraser, W. Tritthart, F. Reiter, M. Schlingmann, J.G. Khinast, Continuous quantitative monitoring of powder mixing dynamics by near-infrared spectroscopy, Powder Technology, 205 (2011) 87-96.

11. R.L. Stewart, J. Bridgwater, D.J. Parker, Granular flow over a flat-bladed stirrer, Chemical Engineering Science, 56 (2001) 4257-4271.

12. S.L. Conway, A. Lekhal, J.G. Khinast, B.J. Glasser, Granular flow and segregation in a four-bladed mixer, Chemical Engineering Science, 60 (2005) 7091-7107.

13. S. Radl, E. Kalvoda, B.J. Glasser, J.G. Khinast, Mixing characteristics of wet granular matter in a bladed mixer, Powder Technology, 200 (2010) 171-189.

14. A. Lekhal, S.L. Conway, B.J. Glasser, J.G. Khinast, Characterization of granular flow of wet solids in a bladed mixer, Aiche Journal, 52 (2006) 2757-2766.

15. J.D. Litster, K.P. Hapgood, J.N. Michaels, A. Sims, M. Roberts, S.K. Kameneni, Scale-up of mixer granulators for effective liquid distribution, Powder Technology, 124 (2002) 272-280.

16. R. Logan, L. Briens, Investigation of the effect of impeller speed on granules formed using a PMA-1 high shear granulator, Drug Development and Industrial Pharmacy, 38 (2012) 1394-1404.

17. P.A. Cundall, O.D. Strack, A discrete numerical model for granular assemblies, Geotechnique, 29 (1979) 47-65.

18. B. Remy, J.G. Khinast, B.J. Glasser, Discrete Element Simulation of Free Flowing Grains in a Four-Bladed Mixer, Aiche Journal, 55 (2009) 2035-2048.

19. B. Remy, B.J. Glasser, J.G. Khinast, The Effect of Mixer Properties and Fill Level on Granular Flow in a Bladed Mixer, Aiche Journal, 56 (2010) 336-353.

20. Y. Sato, H. Nakamura, S. Watano, Numerical analysis of agitation torque and particle motion in a high shear mixer, Powder Technology, 186 (2008) 130-136.

21. S.S. Manickam, R. Shah, J. Tomei, T.L. Bergman, B. Chaudhuri, Investigating mixing in a multi-dimensional rotary mixer: Experiments and simulations, Powder Technology, 201 (2010) 83-92.

22. E. Sahni, R. Yau, B. Chaudhuri, Understanding granular mixing to enhance coating performance in a pan coater: Experiments and simulations, Powder Technology, 205 (2011) 231-241.

23. Y.C. Zhou, A.B. Yu, R.L. Stewart, J. Bridgwater, Microdynamic analysis of the particle flow in a cylindrical bladed mixer, Chemical Engineering Science, 59 (2004) 1343-1364.

24. M. Summers, M. Aulton, Granulation, Pharmaceutics, The science of dosage form design, Churchill Livingstone, Spain, (2002) 364-378.

25. R.E. Schirmer, Modern methods of pharmaceutical analysis, CRC press 1990.

26. D.J. Parker, C.J. Broadbent, P. Fowles, M.R. Hawkesworth, P. McNeil, Positron emission particle tracking- a technique for studying flow within engineering equipment, Nuclear Instruments & Methods in Physics Research Section a-Accelerators Spectrometers Detectors and Associated Equipment, 326 (1993) 592-607.

27. K. Malhotra, A.S. Mujumdar, Particle mixing and solids flowability in granular beds stirred by paddle-type blades, Powder Technology, 61 (1990) 155-164.

28. K. Malhotra, A.S. Mujumdar, H. Imakoma, M. Okazaki, Fundamental particle mixing studies in an agitated bed of granular materials in a cylindrical vessel, Powder Technology, 55 (1988) 107-114.

29. K. Malhotra, A.S. Mujumdar, M. Miyahara, Estimation of particle renewal rates along the wall in a mechanically stirred granular bed, Chemical Engineering and Processing, 27 (1990) 121-130.

30. K. Malhotra, A. Mujumdar, M. Okazaki, Particle flow patterns in a mechanically stirred two-dimensional cylindrical vessel, Powder Technology, 60 (1990) 179-189.

31. M. Blanco, R. Gozalez Bano, E. Bertran, Monitoring powder blending in pharmaceutical processes by use of near infrared spectroscopy, Talanta, 56 (2002) 203-212.

32. P.A. Hailey, P. Doherty, P. Tapsell, T. Oliver, P.K. Aldridge, Automated system for the on-line monitoring of powder blending processes using near-infrared spectroscopy .1. System development and control, Journal of Pharmaceutical and Biomedical Analysis, 14 (1996) 551-559.

33. S.S. Sekulic, H.W. Ward, D.R. Brannegan, E.D. Stanley, C.L. Evans, S.T. Sciavolino, P.A. Hailey, P.K. Aldridge, On-line monitoring of powder blend homogeneity by near-infrared spectroscopy, Analytical Chemistry, 68 (1996) 509-513.

34. M. Whitaker, G.R. Baker, J. Westrup, P.A. Goulding, D.R. Rudd, R.M. Belchamber, M.P. Collins, Application of acoustic emission to the monitoring and end point determination of a high shear granulation process, International Journal of Pharmaceutics, 205 (2000) 79-91.

35. L. Briens, D. Daniher, A. Tallevi, Monitoring high-shear granulation using sound and vibration measurements, International Journal of Pharmaceutics, 331 (2007) 54-60.

36. P. Tilly, S. Porada, C. Scruby, S. Lidington, Monitoring of mixing processes using acoustic emission, Fluid Mixing III. Rugby, Warks: The Institution of Chemical Engineers, (1988).

37. P. Allan, L.J. Bellamy, A. Nordon, D. Littlejohn, Non-invasive monitoring of the mixing of pharmaceutical powders by broadband acoustic emission, Analyst, 135 (2010) 518-524.

38. M. Saberian, Y. Segonne, C. Briens, J. Bousquet, J.M. Chabagno, O. Denizart, Blending of polymers in high speed, vertical mixers: development of a thermal tracer measurement procedure, Powder Technology, 123 (2002) 25-32.

Chapter 3

3   Introduction to pharmaceutical manufacturing

Pharmaceutical drug manufacturing is more of an art than a science. The US government invests billions of dollars in research and development of new drug discoveries. However, research to improve drug manufacturing methods is relatively ignored. The cost of pharmaceutical manufacturing development can account for 30-35% of the total cost to bring a drug to the market [1]. Even with a high percentage of pharmaceutical costs resulting from development, drug manufacturing is mainly left to "trial and error" methods which prove to be inefficient and costly. The lack of efficient manufacturing of prescription drugs is one of the factors that leads to high drug costs [2].

Cost of bringing a drug to market is estimated to be between 0.8 to 1.7 billion dollars (US) [2]. In order to reduce this cost, it is crucial to improve on drug manufacturing. A critical idealized path for drug development is shown in Figure 3.1. Basic research in drug discovery and development has been highly funded by the US government. The *critical path of drug development* begins with preclinical development and proceeds to Food and Drug Administration (FDA) approval and launch. Rigorous evaluation of the drugs is conducted in preclinical development, and as a consequence, a low percentage of possible candidates proceed to market application and FDA approval [2].

Basic Research

↓

Discovery
Physical Design

↓

Preclinical Development
Small Scale-Production

↓

Clinical Development
Manufacturing Scale-Up

↓

FDA Approval and Launch
Mass Production

Figure 3.1: Idealized "critical path of drug development" from basic research to FDA approval and launch. Industrialization steps are also included and are largely ignored in pharmaceutical development (Adapted from FDA [2]).

The *critical path of drug development* is focused on improving product development processes and has been largely ignored. The path includes: assessing safety, demonstrating medical utility, and industrialization. For the sake of this review, industrialization will be discussed.

Industrialization involves the pathway of taking a lab concept to a product ready to be manufactured. Details of industrialization are summarized in Figure 3.1 and include: physical design, small scale-production, manufacturing scale-up and mass production. These challenges in industrialization are highly underrated in the scientific community and are often the rate-limiting steps for the development of new technologies in drug manufacturing [2]. In order to reduce the cost of pharmaceutical drug, it is essential for research to focus on improvements in downstream process manufacturing. Knowledge gained from this can lead away from "trial and error" methods and more towards systematic manufacturing, resulting in consistent drugs with lower cost.

3.1   Pharmaceutical tablet manufacturing

Pharmaceutical tablets are formed by the compression of a desired formulation into a tablet mould. The solid oral dosage form is easy to ingest and relatively more stable with a longer shelf life compared to other dosage forms. Due to such advantages, almost two-thirds   of   all   dosage   forms   are   produced   as   a   tablet   [3].

Dry mixing

Granulation

Drying

Milling

Blending

Tableting

Coating

Figure 3.2: Schematic of pharmaceutical tablet manufacturing pathway (Adapted by Summers et al. [4])

Figure 3.2 illustrates a schematic for typical pharmaceutical downstream tablet manufacturing. For every step in the processes, a batch wise operation is conducted. After each step, the process is stopped and tests are carried out to ensure the product complies with specific conditions. After this, the process continues until completion.

The process begins with the dry mix of excipients in the formulation for a specified amount of time. After dry mixing, a liquid binder is introduced to the powder bed and particles agglomerate and grow in size; called granulation. The agglomerate granules are then dried, typically using a fluidized bed, to a specified moisture content. Milling then ensures that the dried granules are within a desired size distribution. A second mixing step is needed to add excipients such as glidants and lubricants that cannot be initially

added in the process. Finally, the formulation is tableted and coated before packaging distribution.

One of the most important steps in this pathway is wet granulation. Parameters such as wet massing time, formulation components, spray rate, and impeller speed can all affect granule formation. The granule formation can then affect the subsequent manufacturing steps. Improper formation of granules can lead to sub or super-potent tablets which need to be discarded, leading to costly and inefficient processes. Therefore, extensive research focuses to further understand this manufacturing step. This review will introduce the essentials of granulation using a high shear granulator. Granulation as well as wetting and nucleation will be discussed.

3.2   High Shear Granulation

High shear wet granulation is the process of the agglomeration of particles using a liquid binder to form multi-particle granules used in downstream processing. The granules are important for preventing segregation, improving flowability and compaction, as well as for stabilizing mixtures [5]. Poor granulation causes problems in downstream processes that eventually lead to substandard tablets that must be discarded. Wet high shear granulation is a common step in the manufacture of many pharmaceutical tablets. The granulator bowl is charged with specific powder excipients. After an initial mixing period, the liquid binder is sprayed onto the powder bed to form granule nuclei that grow until the process is stopped. The wet granules are then allowed to dry to a desired moisture content, where these dry granules can be utilized in tablet formation.

Three classifications of equipment used in the granulation process are categorized according to shear strength [6]:

(a) *Low shear granulators* (ribbon blenders, twin shell with agitator bar, planetary mixer, dough mixer, fluid bed without a roto-granulator attachment)
(b) *Medium shear granulators* (fluid bed granulators with a roto-granulator attachment)
(c) *High shear granulators*

The granulation process can be influenced by the use of granulators with varying shear strength. Depending on the equipment used, granules can be formed with various characteristics [7-9]. Different grades of material were granulated using direct compression, a fluidized bed or a high shear granulator [7]. Granules using high shear granulation produced hard granules and good tablets. Using direct compression, the granules resulted in poor flowability; fluid-bed granulation resulted in good flow and tablet formation.

High shear granulators are commonly used to produce pharmaceutical granules. Advantages of this process over other granulation processes include: short processing time, use of less binder solution, production of less friable granules, and production of reproducible granules with a uniform particle size distribution [6].

3.3   Granulation Mechanism

During high shear granulation, binder is added to the powder bed and distributed via an impeller and chopper. The binder is distributed to the particles where wet films are formed on the surface of the exposed powder. A proposed mechanism for water distribution between particles includes three states: *pendular*, *capillary,* and *funicular* [4]. The *pendular state* involves particles held together at low moisture levels with lens-shaped rings of liquid. Surface tension forces due to the air-water interface and hydrostatic pressure of the liquid bridge results in adhesion of the particles. The *capillary state* is achieved when the air between particles dissipates and capillary suction holds the particles together. The *funicular state* is an intermediate step between the capillary and pendular states.

The formation of granules in wet high shear granulators has been studied by several research groups. A thorough review has been presented by Iveson et al. [10]. Summers et al. [4] propose granulation to occur in three stages: *nucleation, transition* and *ball growth*.

> (a) *Nucleatio*n: When binder is added to the powder bed, particle-particle interaction and adhesion occurs due to the formation of liquid bridges.

Initially, the particle-particle interactions are in a *pendular* state. However with further agitation, the liquid bridges form the *capillary* state, which result in the granule nuclei.

(b) *Transition:* Growth of granules at this stage occur either by the addition of single particles added to the nuclei via pendular bridges or with the combination of two or more granule nuclei. In this stage, a large number of small granules at a wide size distribution are present. The transition stage is the ideal end point for pharmaceutical tablet manufacturing due to the presence of a large number of small granules.

(c) *Ball Growth*: Larger spherical granules are produced and the mean particle size increases with an increase in granulation time. Coalescence of granules continue, producing over- massed and unusable agglomerates. This stage can be termed as over-granulation.

There are three main mechanisms of ball growth: *coalescence*, *breakage* and *abrasion transfer*:

(a) *Coalescence:* Large granules are formed by the combination of two or more granules.

(b) *Breakage*: As granules break, they may adhere to other granules resulting in the agglomeration and growth of a granule.

(c) *Abrasion transfer*: Attrition of materials from granules occurs due to the agitation of the granule bed. The broken material from this agitation adheres to other granules, resulting in larger granules.

In addition to the mechanisms summarized above, Ennis et al. [7] proposed a competing mechanism to describe granule formation. Wet granulation is theorized to occur in three distinct phenomena simultaneously: wetting and nucleation, consolidation and growth, and attrition and breakage [7]. Figure 3.3 illustrates the proposed phenomena.
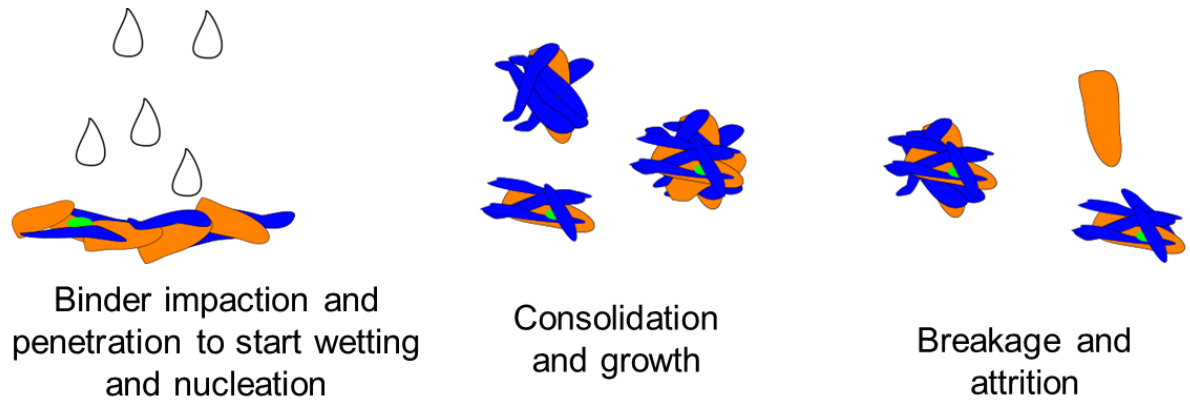
Figure 3.3: Granulation mechanism adapted from Ennis et al. [7]

(a) *Wetting and Nucleation:* Liquid binder impacts the powder surface in the process bowl, ideally as small droplets, and then penetrates into the powder surface to form initial granule nuclei.

(b) *Consolidation and Growth:* Collisions between particles, granules, or the equipment walls leads to granule agglomeration and growth.

(c) *Breakage and Attrition:* Breakage of granules can occur due to impact between granules, the equipment, or product handling.

The proposed mechanism by Ennis et al. [7] provides the advantage of distinguishing between granule growth and breakage. The quantitative measurement in the mechanism proposed by Summers et al. [4] is difficult. Also, the distinct steps proposed depend arbitrarily on the cut off sizes between granule and non-granulated material, which depend on the user's interest and ability to count small particles. Therefore the mechanism proposed by Ennis et al. [7] is more commonly used to describe granule formation.

3.4   Wetting and Nucleation

Recent studies have focused on wetting and nucleation during granulation, attempting to quantify this important step [8, 11, 12]. Figure 3.4 considers the nucleation process when liquid binder is added to a powder mix. Nucleation takes place in the "spray zone" in a

high shear mixer, where the powder bed surface is exposed to the liquid spray [11]. Droplets impact the powder bed and penetrate into the mix, forming initial granule nuclei described in the wetting and nucleation process. The size distribution of the nuclei is crucial to developing granules of optimum particle size that are sufficient for solid oral dosage production. To develop processes that are easy to control and reproduce, nuclei formation and binder dispersion are both considered in the nucleation zone [11]. Nuclei formation is dependent on the formulation properties while binder dispersion is dependent on the process parameters. Both need to be considered when developing an efficient and reproducible granulation process.

A study by Hapgood et al. [11] defined two types of wet nucleation regimes: drop controlled nucleation and mechanical mixing regimes. Ideally it is desired to operate in the drop controlled regime, where one drop of binder forms one nucleus. If not, the granulation process operates in the mechanical mixing regime. In order to operate in the desired drop controlled regime, two conditions must be satisfied:

1) Drops must not overlap on the powder surface (flux of droplets onto powder bed)
2) Droplets must penetrate into the powder bed quickly (kinetics of droplets into powder bed)

The first condition is quantified by the dimensionless spray rate, which is dependent on the process operating parameters, while the second condition is controlled by the drop penetration time, which is dependent on the powder formulation properties.
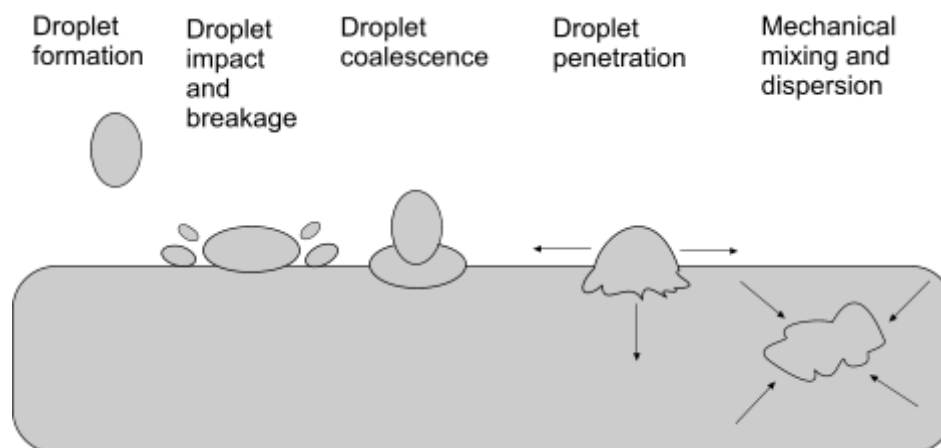
Figure 3.4: Five steps of nucleation adapted from Hapgood et al. [8].

3.4.1 Dimensionless spray rate

To operate in the desired drop controlled regime, it is essential that the droplets not overlap each other on the powder surface. If overlapping occurs, this can lead to an undesirable wide particle size distribution. Litster et al. [13] proposed a dimensionless spray flux (ψ_a) to describe the flux of droplets onto a powder bed, where $\dot{A}$ is the flux of powder exposed to the spray zone, d_d is the average drop size, and $\dot{V}$ is the volumetric flow rate.

$$\Psi_a = \frac{3\dot{V}}{2\dot{A}d_d} \tag{3.1}$$

Litster et al. [13] used a single flat spray nozzle to study the effect of the dimensionless spray flux on granule nucleation. Lactose monohydrate powder passed under a spray nozzle once at varying speeds. Liquid binders of water and 7 wt% HPC solution were used. After one pass under the spray nozzle, samples were collected to study the initial granule nuclei formation. It was found that at high Ψ_a, powder caking occurred and resulted in a broad size distribution of granules. At low Ψ_a, the system was found to operate in the *drop controlled regime,* where the nuclei size distribution was narrow and allowed for one droplet to form one granule nuclei. The development of a dimensionless spray flux allows for particle design where equipment design is independent of the

variable. Thus, allowing for a broader application of this variable in different granulation systems to determine the critical drop controlled regime.

3.4.2   Drop penetration time

The kinetics of droplets penetrating into a powder bed is the second criterion to achieve the ideal drop controlled nucleation regime. The powder bed is assumed to comprise of capillary voids where the orientation is dependent on powder formulation. When a droplet contacts the powder bed, capillary pressure differences allow for the penetration of liquid through the voids, forming the initial granule nuclei.

Drop imbibition into a powder bed can be characterized by two limiting cases: *decreasing drawing area (DDA)* and *constant drawing area (CDA)* (Figure 3.5) [14]:
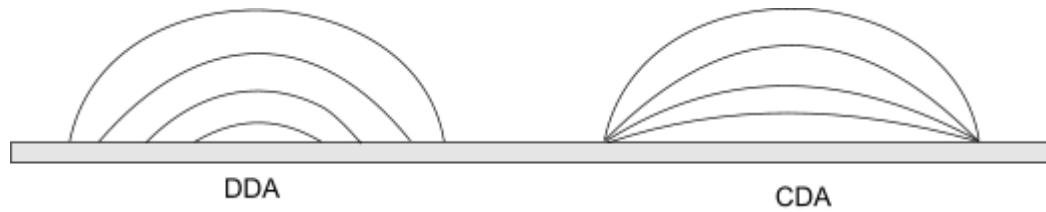
Figure 3.5: Limiting cases for drop imbibition adapted from Marmur et al. [14]

The decreasing drawing area occurs when the contact angle remains constant and the drop radius decreases during drop imbibition [15]:

$$\tau_{DDA} = 9\tau_{CDA} \tag{3.2}$$

where τ_{DDA} is the drop penetration time assuming DDA, and τ_{CDA} is the drop penetration time assuming CDA. The constant drawing area occurs when drop radius remains constant and the contact angle decreases as the droplet penetrates into the powder bed [9]. Equation 3.3 used to calculate the drop penetration time assumes CDA imbibition and is modeled on the basis of droplet penetration via capillary action in a porous bed.

$$\tau_{CDA} = 1.35 \frac{V_o^{2/3}}{\varepsilon^2 R_{pore}} \frac{\mu}{\gamma_{LV} \cos \theta_d} \qquad (3.3)$$

where V_o is the drop volume, ε is the powder bed porosity, R_{pore} is the effective size of the pores in the powder bed, μ is the liquid viscosity, γ_{LV} is the liquid-vapor surface tension and θ_d is the dynamic contact angle of the liquid in a solid capillary.

Equation 3.3 was developed by Middleman et al. [9] and modeled the drop penetration time of a droplet into a powder bed. The model is based on a bundle of parallel cylindrical capillaries by applying the Washburn equation. Constant drawing area (CDA) is assumed to be present in the model [14]. Hapgood et al. [8] improved on Middleman's model by introducing an effective voidage (ε_{eff}), which includes the bed voidage, tap voidage, macro-voids of the powder, and an effective pore radius (R_{eff}):

$$\tau_{CDA} = 1.35 \frac{V_o^{2/3}}{\varepsilon_{eff}^2 R_{eff}} \frac{\mu}{\gamma_{LV} \cos \theta_d} \qquad (3.4)$$

where

$$R_{eff} = \frac{\varphi d_{3,2}}{3} \frac{\varepsilon_{eff}}{(1-\varepsilon_{eff})} \qquad (3.5)$$

and φ is the shape factor, $d_{3,2}$ is the surface mean particle diameter and $\varepsilon_{eff} = \varepsilon_{tap}(1-\varepsilon+\varepsilon_{tap})$.

The drop penetration time depends on the powder bed voidage, the size and orientation of the voids, and the properties of the powders [9]. Powders with large voids promote short penetration times. Irregularly packed powders with large macro-voids decrease penetration as the macro-void space blocks the fluid flow. As particle shape, size, and size distribution affect the packing and structure of the powder bed, the powder in initial contact with the liquid binder will affect the formation of granule nuclei.

The wettability of a powder can influence the formation of initial granule nuclei. A comprehensive review on powder wettability is provided by Lazghab et al. [16]. Iveson et al. [10] demonstrate that liquid binder can preferentially wet more hydrophilic particles. Therefore, if the powder surface in initial contact with the liquid binder contains a mixture of powders with different surface properties, granule formation and

growth with hydrophilic particles would be promoted over granules containing hydrophobic particles.

Several research groups have performed single drop nucleation experiments, where one single drop of binder is released onto a loose powder bed, usually in a petri dish [8, 17,- 26]. A study by Agland et al. [26] used large glass beads to conduct single drop experiments, where velocity and liquid binder were varied. They found that at low impact velocities, the drops penetrated through the powder bed by capillary forces. At high impact velocities, they spread on the powder bed surface.

Competing spreading versus infiltration mechanisms were recognized by Charles-Williams et al. [24]. Different size lactose particles and binders were used in single drop penetration studies with static dry and pre-wetted powder beds. Empirical relationships for infiltration and spreading rates were dependent on both powder and liquid properties. The study also showed that with porous surfaces, the infiltration rate had a larger degree of dependence due to spreading with changes in viscosity.

Several studies investigated single drop behavior with hydrophobic and hydrophobic/hydrophilic powder bed combinations [17, 20- 23]. Liquid marbles with a powder shell were developed, proposing a solid spreading nucleation where hydrophobic particles spread over the binder droplet upon impact onto the powder bed. As the drop height increased, the surface coverage of the drop increased as well having an effect on this solid spreading nucleation [22, 23].

3.4.3   Drop Controlled Regime Map

Depending on formulation properties and process parameters, mechanisms during granulation can vary. Litster et al. [13] proposed nucleation to occur in the *drop controlled regime, mechanical, or intermediate regime*. As discussed earlier, the drop controlled regime is ideal, where one droplet will form one granule nuclei. In order to operate in this regime, two conditions must be satisfied: (i) kinetics of the droplet imbibition must be fast, and (ii) powder flux through the spray zone must be fast enough as to not overlap. If these criteria are not satisfied, then the granulation process proceeds

in the mechanical regime. Poor wetting powders or highly viscous binder fluids can contribute to longer drop penetration times. Also, "pooling" of powder may occur when the powder flux is too slow. Pooling refers to drop coalescence on the powder surface, leading to undesirable broad granule size distribution. An intermediate regime can occur due to the significance of both drop penetration kinetics and shear force dispersion. This regime is the most difficult to control [10].

A nucleation regime map proposed by Hapgood et al. [11] can help determine the nucleation regime occurring during granulation. The liquid spray flux and the drop penetration time are used to determine if operation is occurring in the drop controlled, intermediate, or mechanical dispersion regimes.

Validation of the nucleation regime map can potentially allow for the prediction of formulation and operating conditions needed during granulation. Validation of the regime map was conducted using water and lactose systems [11]. It was shown that at short drop penetration times, decreasing ψ_a values exhibited a shift towards the drop controlled regime and thus a narrower nuclei distribution. High ψ_a values led to broad size distributions from the overlap of droplets in the nucleation zone. Long drop penetration times resulted in no effect on the change in spray flux. The nucleation regime map developed by Hapgood et al. [11] is a good tool for controlling wetting and the nucleation regime during wet granulation.

3.5   Powder Properties

Nucleation thermodynamics has been studied by several research groups. As stated earlier, nucleation is the first and most important step in achieving optimum granules. The physical and chemical properties of the powders have been shown to affect granule formation. Wetting thermodynamics has focused on two main aspects [10]:

(a) The contact angle between the binder liquid and solid, and

(b) The spreading coefficients of the solid phase over the liquid phase and vice versa

The contact angle between the binder liquid and solid has been shown to have a direct effect on granule formation by various researchers. A study by Aulton et al. [27] used varying amounts of salicylic acid powder (contact angle of $\theta=103°$) mixed in a fluidized bed with lactose powder (contact angle of $\theta=30°$). Generally, contact angles below 90° are considered to be hydrophilic, while anything above this value is considered to be hydrophobic [17]. It was found that during fluidized bed granulation, mean granule size decreased as the contact angle of the powder mixture increased.

The contact angle of various powders has also been shown to directly affect the granulation kinetics of processes. Sand powders of varying contact angles were granulated with a binder of 1% carboxyl methyl cellulose (CMC) solution in a fluidized bed [28]. It was found that as the contact angle increased, hence increasing the level of hydrophobicity, the granule growth rate decreased. At contact angles above 90°, granule growth was minimal.

Surface free energies can also be used to describe wetting and nucleation. The spreading coefficient, λ, can be used to determine the affinity for a liquid to spread over a solid. It is related to adhesion and cohesion given by:

Work of cohesion for a solid: $W_{CS}=2\gamma_{SV}$ (3.6)

Work of cohesion for a liquid: $W_{CL}=2\gamma_{LV}$ (3.7)

Work of adhesion for an interface: $W_A=\gamma_{SV}+\gamma_{LV}-\gamma_{SL}$ (3.8)

$W_A=\gamma_{LV}(\cos\theta+1)$ (3.9)

where γ is the surface free energy, θ is the solid-liquid contact angle and subscripts "S", "V" and "L" are solid, vapour and liquid phases respectively. The work of cohesion is the work needed to separate a unit cross sectional area from itself, while the work of adhesion is the work required to separate a unit area from an interface. The spreading coefficient is the difference between the work of cohesion and adhesion. The value of the spreading coefficient indicates whether the spreading is thermodynamically favorable.

A study by Krycer et al. [29] validated that differences in granule properties are correlated with spreading coefficients. Krycer et al. [29] introduced a "work of spreading" term given by:

$$\Lambda^{*}_{LS}=\lambda_{LV}(\cos \theta \text{-}1) \tag{3.10}$$

Optimal spreading occurs when the work of spreading is closest to zero. Granules composed of paracetamol with 4 wt% hydroxypropyl methylcellulose (HPMC) had a work of spreading closest to zero and were least friable. Granules using a 4wt % sucrose solution were shown to have a more negative coefficient of spreading and were more friable.

3.5.1   Hydrophobic Powders

As stated earlier, wettability of powders is an important consideration in the formation of granule nuclei and subsequent granulation of powder formulations. To promote even distribution of liquid binder throughout the powder bed, liquid must sufficiently wet the powder during liquid spray.

Poorly wetting systems prevent the penetration of liquid into the powder bed and subsequent granule nuclei formation. The use of hydrophobic powders during granulation and on the formation of granule nuclei has recently been studied by various research groups, as these powders have been shown to result in poorly wetting systems [17, 20, 22, 30].

"Solid-spreading nucleation" has been used to describe the spreading of a liquid droplet onto hydrophobic powders. Conventional granulation assumes that the liquid droplet spreads over the solid particles. Solid-spreading nucleation occurs when hydrophobic powders spread over liquid droplets or liquid droplets roll on the hydrophobic powder bed [22].

The use of hydrophobic powders in granulation has led to an interest in "liquid marble" formation. Liquid marbles form when hydrophobic powders contact water, forming a structurally sound spherical shell [22]. The driving forces behind the formation of liquid

marbles originally was thought to be related to solid spreading nucleation, where the spreading coefficient (λ_{SL}) predicted if a liquid marble would form or not [30]. However a study by Hapgood et al. [22] suggests that the bulk motion of liquid may be crucial in liquid marble formation as well.

3.5.2   Hygroscopic Powders

Hygroscopic powders have the tendency to "swell" and hold on to water molecules from the surrounding environment. Microcrystalline cellulose is one of the most widely used pharmaceutical powders due to its ease for compressibility during tablet manufacturing. It is also known to be hygroscopic [28, 33].

Microcrystalline cellulose is produced by the partial hydrolysis of wood pulp and commonly used as an excipient in the cosmetic, food and pharmaceutical industries [31, 32].
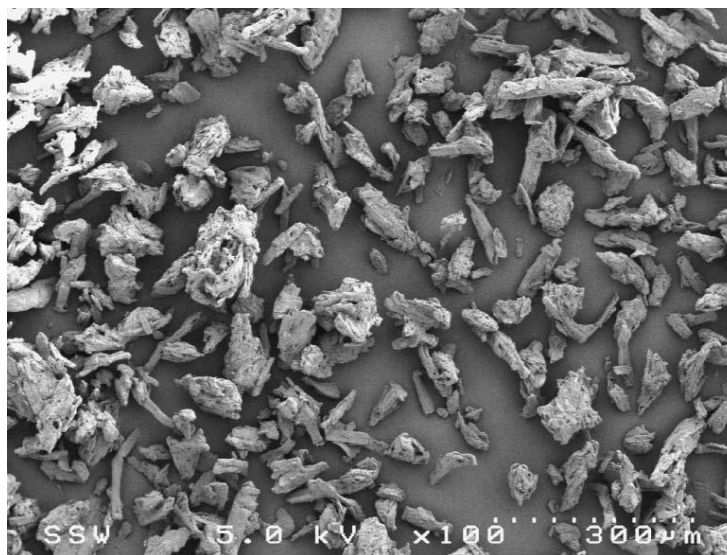
Figure 3.6: SEM images of microcrystalline cellulose

MCC is partially hydrolyzed using a dilute mineral acid solution of α-cellulose. The MCC then undergoes a filtration process, purifying the material. The resulting suspension of microcrystals or crystallites is then spray dried, where the resulting MCC

powder particles are left behind [32]. Water-isotherms have shown MCC to uphold up to 26% of water based on dry weight, giving MCC its hygroscopic characteristic [32].

Many studies have incorporated MCC into wet granulation processes [33-38]. Chitu et al. [33] studied the effects of a MCC-lactose binary formulation on granule growth kinetics and granule morphology. It was found that increasing the amount of MCC resulted in a higher binder amount needed to granulate. This can be attributed to the hygroscopic nature of MCC and its tendency to swell and take in a high amount of liquid binder. Kristensen et al. [34] also determined that the binder liquid needed for optimum granulation depended on the amount of MCC in the powder formulation, where the effects of hygroscopicity contributed to the change in liquid binder needed for optimum granulation.

3.6   References

1. P. Suresh, P.K. Basu, Improving pharmaceutical product development and manufacturing: impact on cost of drug development and cost of goods sold of pharmaceuticals, Journal of Pharmaceutical Innovation, 3 (2008) 175-187.

2. F.D.A. Administration, Innovation or stagnation: challenge and opportunity on the critical path to new medical products, Food and Drug Administration, critical path report, (2004).

3. S.K. Niazi, Handbook of Pharmaceutical Manufacturing Formulations: Liquid Products (Volume 3 of 6), CRC press2004.

4. M. Summers, M. Aulton, Granulation, Pharmaceutics, The science of dosage form design, Churchill Livingstone, Spain, (2002) 364-378.

5. D. Daniher, L. Briens, A. Tallevi, End-point detection in high-shear granulation using sound and vibration signal analysis, Powder Technology, 181 (2008) 130-136.

6. R. Gokhale, Y. Sun, A.J. Shukla, High-shear granulation, Drugs and the pharmaceutical sciences, 154 (2005) 191.

7. B. Ennis, J. Litster, Particle size enlargement, Perry's Chemical Engineers' Handbook, 7th edn, McGraw-Hill, New York, (1997) 20-56.

8. K.P. Hapgood, J.D. Litster, S.R. Biggs, T. Howes, Drop penetration into porous powder beds, Journal of Colloid and Interface Science, 253 (2002) 353-366.

9. S. Middleman, Modeling axisymmetric flows: dynamics of films, jets, and drops, Academic Press1995.

10. S.M. Iveson, J.D. Litster, K. Hapgood, B.J. Ennis, Nucleation, growth and breakage phenomena in agitated wet granulation processes: a review, Powder Technology, 117 (2001) 3-39.

11. K.P. Hapgood, J.D. Litster, R. Smith, Nucleation regime map for liquid bound granules, Aiche Journal, 49 (2003) 350-361.

12. W.J. Wildeboer, E. Koppendraaier, J.D. Litster, T. Howes, G. Meesters, A novel nucleation apparatus for regime separated granulation, Powder Technology, 171 (2007) 96-105.

13. J.D. Litster, K.P. Hapgood, J.N. Michaels, A. Sims, M. Roberts, S.K. Kameneni, T. Hsu, Liquid distribution in wet granulation: dimensionless spray flux, Powder Technology, 114 (2001) 32-39.

14. A. Marmur, The radial capillary, Journal of colloid and interface science, 124 (1988) 301-308.

15. M. Denesuk, G.L. Smith, B.J.J. Zelinski, N.J. Kreidl, D.R. Uhlmann, Capillary penetration of liquid droplets into porous materials, Journal of Colloid and Interface Science, 158 (1993) 114-120.

16. M. Lazghab, K. Saleh, I. Pezron, P. Guigon, L. Komunjer, Wettability assessment of finely divided solids, Powder Technology, 157 (2005) 79-91.

17. K.P. Hapgood, L. Farber, J.N. Michaels, Agglomeration of hydrophobic powders via solid spreading nucleation, Powder Technology, 188 (2009) 248-254.

18. A.C. Lee, P.E. Sojka, An Experimental Investigation of Nucleation Phenomenon in a Static Powder Bed, AIChE Annual Meeting. Nashville, TN, 2009.

19. S.H. Schaafsma, P. Vonk, P. Segers, N.W.F. Kossen, Description of agglomerate growth, Powder Technology, 97 (1998) 183-190.

20. T. Nguyen, W. Shen, K. Hapgood, Drop penetration time in heterogeneous powder beds, Chemical Engineering Science, 64 (2009) 5210-5221.

21. N. Eshtiaghi, J.J.S. Liu, K.P. Hapgood, Formation of hollow granules from liquid marbles: Small scale experiments, Powder Technology, 197 (2010) 184-195.

22. K.P. Hapgood, B. Khanmohammadi, Granulation of hydrophobic powders, Powder Technology, 189 (2009) 253-262.

23. N. Eshtiaghi, J.S. Liu, W. Shen, K.P. Hapgood, Liquid marble formation: Spreading coefficients or kinetic energy?, Powder Technology, 196 (2009) 126-132.

24. H.R. Charles-Williams, R. Wengeler, K. Flore, H. Feise, M.J. Hounslow, A.D. Salman, Granule nucleation and growth: Competing drop spreading and infiltration processes, Powder Technology, 206 (2011) 63-71.

25. J.O. Marston, S.T. Thoroddsen, W.K. Ng, R.B.H. Tan, Experimental study of liquid drop impact onto a powder surface, Powder Technology, 203 (2010) 223-236.

26. S. Agland, S.M. Iveson, The impact of liquid drops on powder bed surfaces, Chemeca 99: Chemical Engineering: Solutions in a Changing Environment, (1999) 218.

27. M. Aulton, M. Banks, Influence of the hydrophobicity of the powder mix on fluidised bed granulation, International Conference on Powder Technology in Pharmacy, Basel, Switzerland, Powder Advisory Centre, 1979.

28. A. Hemati, R. Cherif, K. Saleh, V. Pont, Fluidized bed coating and granulation: influence of process-related variables and physicochemical properties on the growth kinetics, Powder Technology, 130 (2003) 18-34.

29. I. Krycer, D.G. Pope, J.A. Hersey, An evaluation of tablet binding agents part I. Solution binders, Powder Technology, 34 (1983) 39-51.

30. P. McEleney, G. Walker, I. Larmour, S. Bell, Liquid marble formation using hydrophobic powders, Chemical Engineering Journal, 147 (2009) 373-382.

31. R.C. Rowe, P.J. Sheskey, S.C. Owen, A.P. Association, Handbook of pharmaceutical excipients, Pharmaceutical press London2006.

32. P. Kleinebudde, The crystallite-gel-model for microcrystalline cellulose in wet-granulation, extrusion, and spheronization, Pharmaceutical Research, 14 (1997) 804-809.

33. T.M. Chitu, D. Oulahna, M. Hemati, Rheology, granule growth and granule strength: Application to the wet granulation of lactose-MCC mixtures, Powder Technology, 208 (2011) 441-453.

34. J. Kristensen, T. Schaefer, P. Kleinebudde, Direct pelletization in a rotary processor controlled by torque measurements. II: Effects of changes in the contest of microcrystalline cellulose, Aaps Pharmsci, 2 (2000) art. no.-24.

35. L. Shi, Y. Feng, C.C. Sun, Initial moisture content in raw material can profoundly influence high shear wet granulation process, International Journal of Pharmaceutics, 416 (2011) 43-48.

36. L. Shi, Y. Feng, C.C. Sun, Massing in high shear wet granulation can simultaneously improve powder flow and deteriorate powder compaction: A double-edged sword, European Journal of Pharmaceutical Sciences, 43 (2011) 50-56.

37. L. Shi, Y. Feng, C.C. Sun, Origin of profound changes in powder properties during wetting and nucleation stages of high-shear wet granulation of microcrystalline cellulose, Powder Technology, 208 (2011) 663-66

38. T. Suzuki, H. Kikuchi, S. Yamamura, K. Terada, K. Yamamoto, The change in characteristics of microcrystalline cellulose during wet granulation using a high-shear mixer, Journal of Pharmacy and Pharmacology, 53 (2001) 609-616.

Chapter 4

4 The effect of operational parameters on mixing in wet high shear granulation

4.1 Introduction

Pharmaceutical tablet production typically includes wet granulation, the process through which powder particles are agglomerated using a liquid binder into granules. This process is complex and involves three mechanisms that occur simultaneously: nucleation and binder distribution, consolidation and growth, and attrition and breakage. During wet high shear granulation, powders are initially dry mixed in the granulator using the impeller before the liquid binder is added to start the granulation. The liquid binder is sprayed from above onto the moving powder bed below. The liquid droplets impact and penetrate into the powder bed to form granule nuclei. The composition of the powder exposed to the liquid binder spray therefore affects the formation of granule nuclei.

Litster et al. [1] reported two powder flow regimes during granulation: bumping and roping flow. Bumpy flow occurs at lower impeller speeds and is characterized by slow powder rotation in the bowl with almost no vertical movement. As the impeller speed increases, the powder transitions from bumping to roping flow. In roping flow, the powder rotates quickly around the centre axis and forms a toroid that also provides vertical movement or mixing of the powder. It has been shown that roping flow is required for optimal formation of granules. During bumpy flow, the slow rotation and minimal vertical movement does not allow adequate granule consolidation and growth resulting in undersized granules that may not contain the required ratios of the powder components.

Zhou et al. [2] examined particle flow in a cylindrical bladed mixer using monosize 5 mm diameter spheres. The loading or initial arrangement of the particles was found to affect the mixing kinetics, but not the quality of the final mixture. Three different initial arrangements were investigated with a horizontal layering arrangement showing the fastest mixing time. Koller et al. [3] also investigated initial arrangements. A binary

mixture of acetyl salicylic acid and lactose monohydrate was used with horizontal layering. Mixing was found to occur in two stages: first, a convective vertical mixing between the layers, followed by diffusive mixing. The convective mixing stage showed an overshoot, where the vertical movement of the powders resulted in an intermediate state with the two horizontal layers partially reversed from the initial positions. The degree of this overshoot was affected by the loading and attributed to differences in the particle sizes and shapes.

Fill levels have been shown to affect mixing in bladed mixers. At high fill levels, Koller et al. [3] found that diffusive mixing primarily impacts the surface composition of the powder bed. Large convective movement of the horizontally loaded layers was not observed. Stewart et al. [4] observed that recirculation regions became much smaller as fill levels increased. From this, they concluded that in a bed with particles of different sizes, densities and shapes, segregation will occur causing some particles to be over represented at the powder bed surface.

Segregation in a bladed mixer was studied by Conway et al. [5] using mixtures of glass beads of varying diameter. It was found that the larger particles segregated to the powder surface and then to the bowl perimeter. This pattern was observed independently of powder loading. Impeller speeds only up to 50 rpm were tested. Higher impeller speeds of about 300 to 1000 rpm are typically used in high shear granulators, and these higher speeds could affect particle segregation.

When liquid binder is introduced to the dry powder mix to promote granule growth, the liquid spray initially contacts the powder bed surface. Granule uniformity is therefore influenced by the composition of the powder bed surface, where ideally an even distribution of all excipients and active should be incorporated into the granule. A study by Oka et al [6] found non-homogeneity of granules to form due to powder segregation at the powder bed surface. Samples were collected at the surface of the powder bed to determine the surface composition at impeller speeds of 225 and 300 rpm using a design of experiments. Percolation of smaller particles to the bottom of the powder bed allowed for the larger particles to the bed surface and therefore non-homogeneity of granules.

Experimental design is used in the pharmaceutical industry as a tool in pre-formulation to determine significant process parameters in the manufacturing process [7]. The purpose of experimental design is to plan and execute a series of experiments in an ordered manner to maximize the amount of information with a minimum number of experiments. Process parameters are assigned low and high level settings as variables are changed simultaneously in order to observe changes in the system. This design also allows for the interactions of parameters to be observed, which would not be seen in a one factor at a time design.

Experimental design has been used extensively in pharmaceutical studies to evaluate granulation [8-10]. Ranjbarian et al. [8] used a three factor design of experiments to evaluate the influence of impeller speed, binder mass and granulation time on the mean size of granules produced in a lab scale conical high shear granulator. The mean granule size varied linearly with binder mass, but varied with a quadratic trend with increasing impeller speed. Fonteyne at al. [9] used a two-level full factorial experimental design to study the effects of screw speed, powder feed rate, water content and barrel temperature on granule characteristics. Temperature, liquid amount and powder feed rate all affected the granules while high barrel temperature and feed rate resulted in larger granules. Soyeux et al. [10] used a fraction three factorial design to examine the effect of binder volume, water volume and mixing time on granule properties thereby assessing the performance of a new maltodextrin binder.

The aim of this work was to use a design of experiments to examine the effect of impeller speed on particle size ratio, dry mixing time and loading order during dry mixing to determine possible particle segregation just prior to the start of wet high shear granulation. Samples were collected both radially as well as at the bed surface in order to determine particle segregation. The effect of impeller speed in the bumpy and roping regimes on particle flow and particle segregation were considered using a lab-scale high shear granulator. It was hypothesized that segregation can occur during this mixing and can affect the formation of granule nuclei and therefore also final granule properties.

4.2　　　Materials and Methods

4.2.1　　Equipment

An Aeromatic-Fielder PMA-1 high shear granulator (GEA Pharma Systems, Wommelgem Belgium) shown schematically in Figure 4.1 was used for all the trials. This vertical shaft granulator has a bottom mounted three bladed impeller (Figure 4.2) and a bowl volume of 10 L. A side chopper was removed from the bowl and not used for this study. An impeller speed of 300 or 700 rpm (corresponding to tip speeds of 4.3 and 10 m/s respectively) was selected based on the specified trial. The height to diameter (H/D) fill level for all trials was 0.13 which corresponded to a static powder bed height of about 3.6 cm.
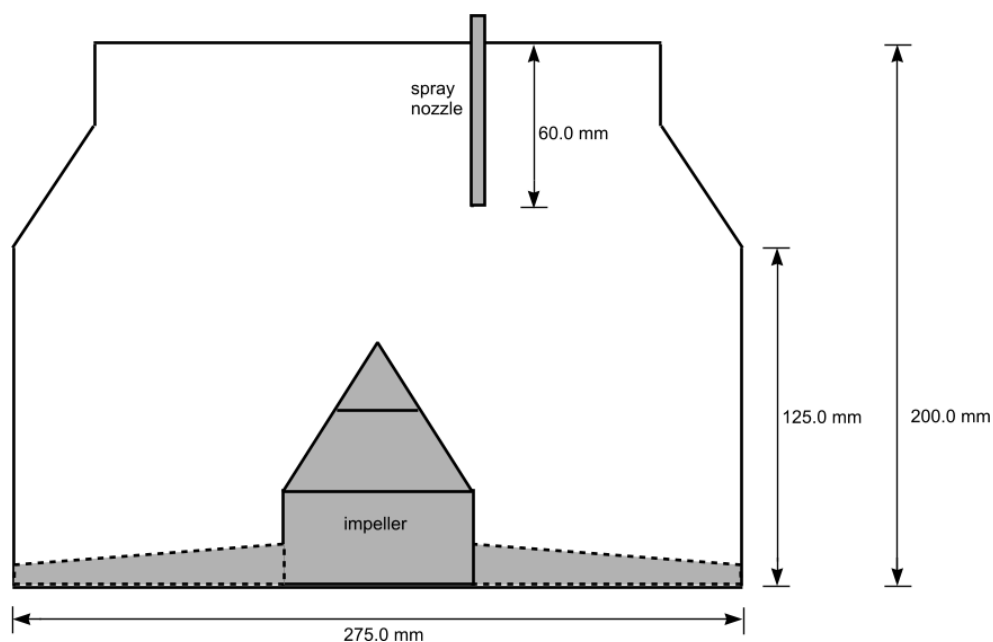
Figure 4.1: Schematic diagram of the PMA-1 high shear granulator
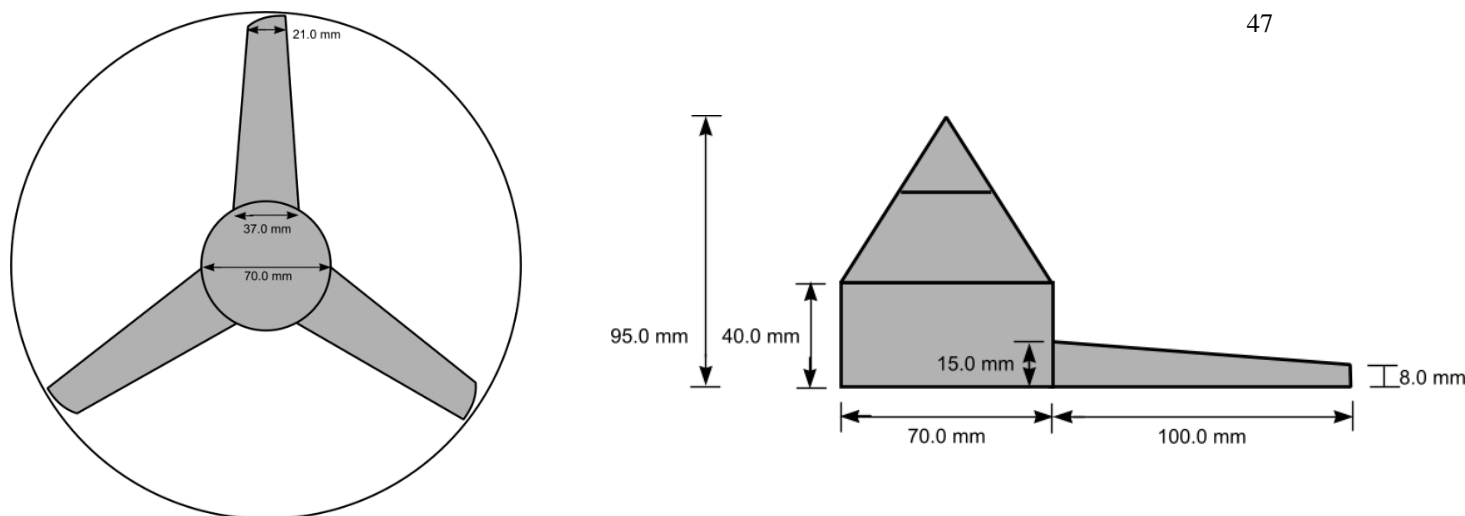
Figure 4.2: Schematic diagram of the granulator impeller (a) top view and (b) side view

4.2.2   Formulation

Three different size cuts of sugar spheres (Paulaur Corporation, USA) were used for the trials: 20-25 mesh (850-710 µm), 40-50mesh (425-300 µm) and 60-80 mesh (250-180 µm). These size cuts allowed binary mixtures to be created with average particle size ratios of 1.7 (60-80 mesh and 40-50 mesh) and 3.7 (60-80 mesh and 20-25 mesh). Sugar spheres were stored in seal tight containers to ensure constant moisture content of particles.

The particle size ratio of commonly used pharmaceutical excipients α-lactose monohydrate and microcrystalline cellulose is estimated at around 2.5.   Therefore, a range of ratios below and above this value, ratios of 1.7 and 3.7 were used.

4.2.3   Experimental Design

StatEase Design Expert 8 statistical software (Stat-Ease, Inc. Minnesota, USA) was used to generate a three factor two-level factorial design of experiments with the factors of particle size ratio (1.7 and 3.7), dry mix time (10 and 300 s) and loading order of the two mesh cuts for the binary mixture (Table 4.1).

Table 4.1: Trials for design of experiments (DOE). Particle size ratios high and low values were 3.7 and 1.7 respectively. Dry mix time high and low values were 10 s and 300 s respectively. Large or small particles were loaded first horizontally to the granulator bowl as per the experimental design

Trial	Particle size ratio (-)	Dry mix time (s)	Loading order, first particle size
1	3.7	300	Large
2	1.7	300	Large
3	1.7	10	Large
4	3.7	10	Small
5	3.7	300	Small
6	3.7	10	Large
7	1.7	10	Small
8	1.7	300	Small

The design of experiments was conducted separately for impeller speeds of 300 rpm and 700 rpm ensuring that the factors were examined under both "bumpy" and "roping" flow regimes.

For the Niro-Fielder PMA-25 granulator used by Litster et al. [1], the transition between the "bumpy" and "roping" flow regimes was found to be 250 to 300 rpm for dry lactose monohydrate and 150 to 200 rpm for wet lactose monohydrate powder. The PMA-1 granulator used in this study was geometrically similar to the PMA-25 granulator and a scale-up criterion for impeller speed based on the Froude number can be used to estimate the regime transition:

$$\frac{N_2}{N_1} = \sqrt{\frac{D_1}{D_2}}$$
(4.1)

where N is the impeller speed and D is the diameter of the impeller. Based on this scale-up criterion, the transition from "bumpy" to "roping" regimes would occur just above 300 rpm for the PMA-1 granulator. This transition was confirmed by Logan et al. [11].

4.2.4   Sampling Methods

A systematic method was developed to collect samples from the trials and analyze segregation of the particles. Samples were collected using a template at locations shown in Figure 4.3. The locations ensured that samples were withdrawn from various radial positions. Samples were collected both radially and at the surface of the powder bed to study particle segregation throughout the entire depth of the powder bed and at the powder bed surface.

Radial samples were collected using a side sampling thief probe with an outer diameter of 0.015 m and a sampling port 0.035 m high by 0.015 m arc length, located 0.002 m from the flat probe tip. This relatively large sampling port located at the thief tip ensured that almost the entire bed depth was sampled at each location. The sample thief probe was inserted vertically into the powder bed to collect sample from the top to the bottom of the bed. Locations where the impeller blade hindered proper sampling were not used in data analysis; therefore the seven sample locations illustrated in Figure 4.3 were used. An average sample weight for all sampling locations for each trial was determined to be 2.11 g $\pm$ 0.59.
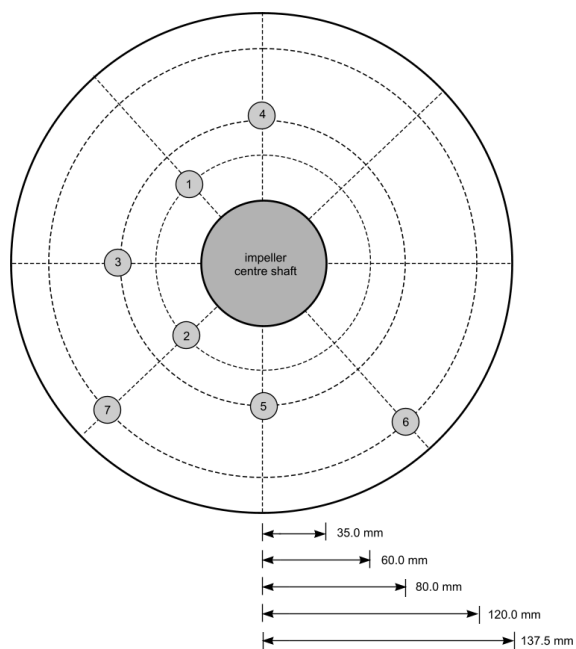
Figure 4.3: Locations for both radial and surface bed sampling. Radial sampling was collected using a sample thief probe where powder was collected vertically from the top to the bottom of the powder bed. Surface bed sampling was collected at the top of the powder bed using the same sampling locations.

To determine the composition of sugar spheres at the surface of the powder bed, surface bed samples were collected at the same locations illustrated in Figure 4.3. Samples were carefully collected from the top of the powder bed, where samples were extracted approximately 2-3 mm from the surface of the bed. Samples were collected using a 1/8 teaspoon scoop in order to allow for relatively consistent weight of sample withdrawn for each trial. An average sample weight for all sampling locations for each trial was determined to be $0.37 \text{ g} \pm 0.14$.

To study the extent of mixing, the relative mass amounts of spheres from the larger and smaller mesh cuts were determined through sieving using 50 and 100 mesh (300 and 150 μm) sieves for both radial and surface bed sampling methods. A constant density of sugar spheres of 0.8 g/cm^3 for all mesh sizes allowed for the relative mass for each trial to be compared. The percent standard deviation of the mass of small spheres collected from sample locations 1 to 7 from each trial was calculated as:

$$y_s = \frac{\sqrt{\frac{\sum_{i=1}^{N}(X_i - \overline{X})^2}{N-1}}}{} \cdot 100\% \qquad (4.2)$$

where X_i is mass percentage of small particles from a sample site location i (i=1-7), $\overline{X}$ is the observed mean of the samples from all locations for a trial, and N is the number of sampling locations (N=7). This sampling standard deviation (y_s) provides an indication of the segregation within the bowl for a given trial: the higher the sampling standard deviation, the higher the segregation of particles within the bowl. A sampling standard deviation of zero would indicate no segregation or a perfectly uniform distribution of the binary mixture.

4.3   Results

4.3.1   Radial Sampling

For the trials conducted at an impeller speed of 300 rpm, the standard deviation of the samples collected using radial sampling ranged from 1.2 to 6.7%. The least segregation occurred under conditions of a particle size ratio of 1.7, mixing time of 300 s and with small particles loaded first while the largest segregation occurred at a particle ratio of 3.7, 10 s mixing and with large particles loaded first. An analysis of variance (ANOVA) of the sampling standard deviation was conducted, where significant factors were determined when p-values <0.05, indicating a 95% confidence interval. ANOVA analysis at 300 rpm for factors particle size ratio (p=0.16), dry mix time (p=0.12) and particle load order (p=0.19) did not show statistical significance (p>0.05).

For the trials conducted at an impeller speed of 700 rpm, the standard deviation of the samples was overall lower and ranged from 0.6 to 5.2%. The least segregation occurred under conditions of a particle size ratio of 1.7, mixing time of 10 s and with large particles loaded first while the largest segregation occurred at a particle ratio of 3.7, 300 s mixing and with small particles loaded first. ANOVA indicated that the particle size ratio (p=0.004) and the particle loading order (p=0.012) significantly affected the segregation. Figures 4.4 and 4.5 illustrate these effects compared with the one factor plots at 300 rpm.
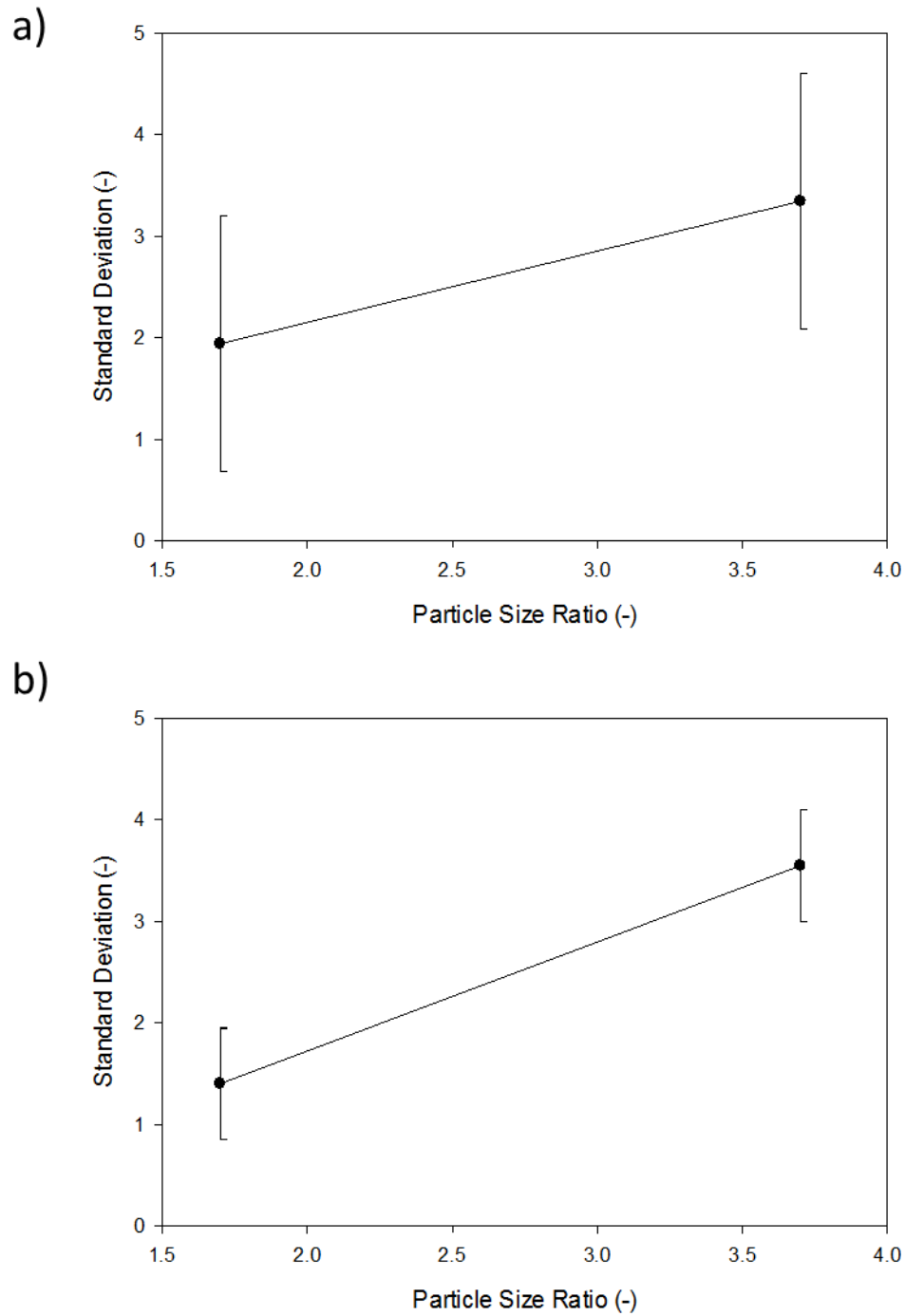
Figure 4.4: One factor plots for the influence of particle size ratio on particle segregation during mixing of the binary sugar spheres at an impeller speed of 300 rpm (a) and 700 rpm (b), where particle size ratio was determined to significantly affect particle segregation at 700 rpm via radial sampling.
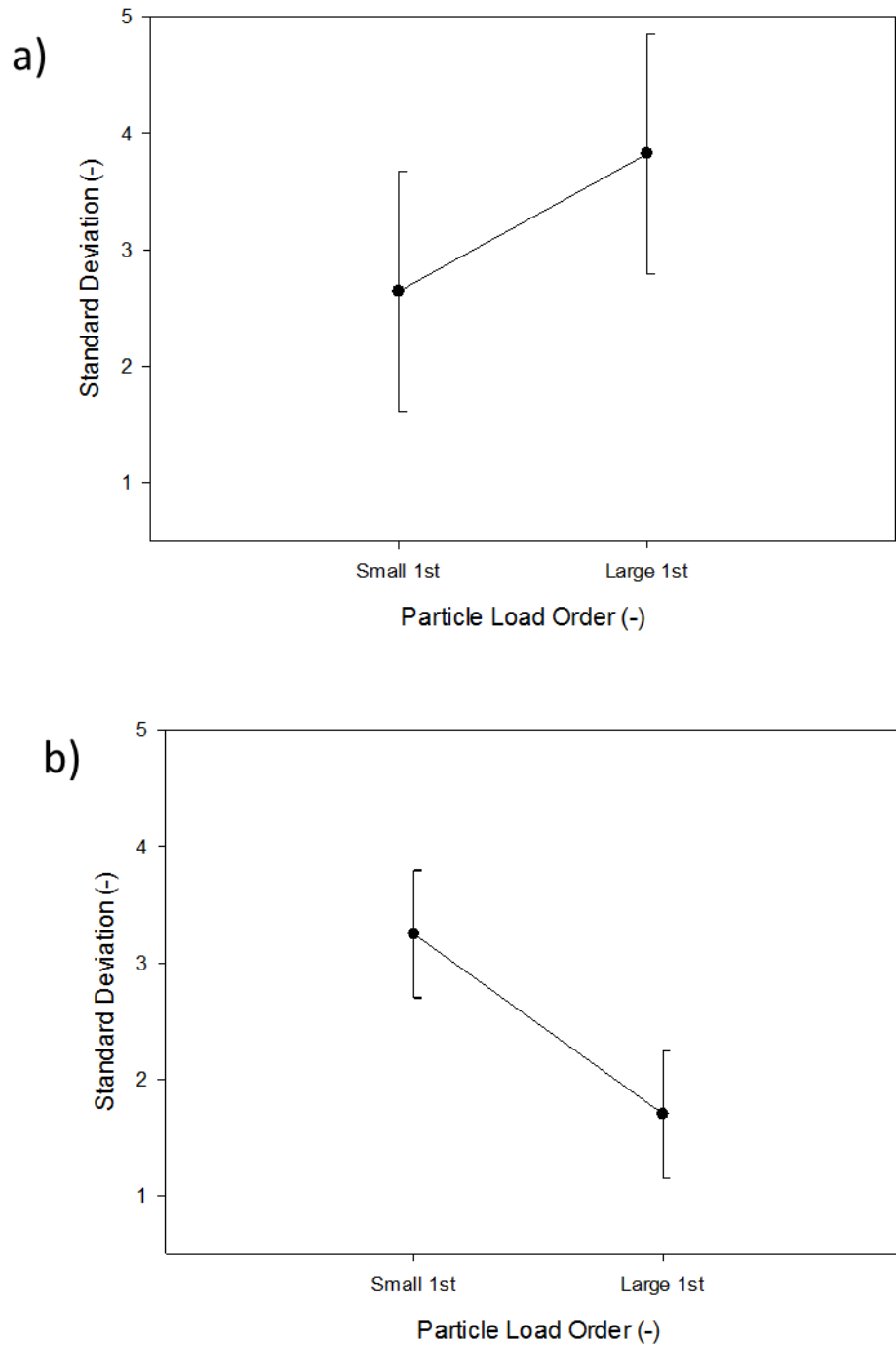
Figure 4.5 One factor plots for the influence of particle load order on segregation during mixing of the binary sugar spheres at an impeller speed of 300 rpm (a) and 700 rpm (b), where particle load order was determined to significantly affect particle segregation at 700 rpm via radial sampling.

4.3.2   Surface Bed Sampling

For the trials conducted at an impeller speed of 300 rpm, the standard deviation of the samples at the powder bed surface ranged from 1.03 to 6.93%. The least segregation occurred under conditions of a particle size ratio of 1.7, mixing time of 10 s and with small particles loaded first while the largest segregation occurred at a particle ratio of 3.7, 10 s mixing and with large particles loaded first. An analysis of variance (ANOVA) of the sampling standard deviation was conducted, where significant factors were determined when p-values <0.05, indicating a 95% confidence interval. ANOVA analysis indicated that particle size ratio (p=0.022) and the interaction of particle size with particle load order (p=0.029) significantly influenced particle segregation. Figures 4.6 and 4.7 illustrate the one factor plots and interaction plots at 300 rpm and 700 rpm.

For the trials conducted at an impeller speed of 700 rpm, the standard deviation of the samples was overall lower and ranged from 1.2 to 4.6%. ANOVA analysis at 700 rpm for factors particle size ratio (p=0.88), dry mix time (p=0.26) and particle load order (p=0.061) did not show statistical significance (p>0.05).
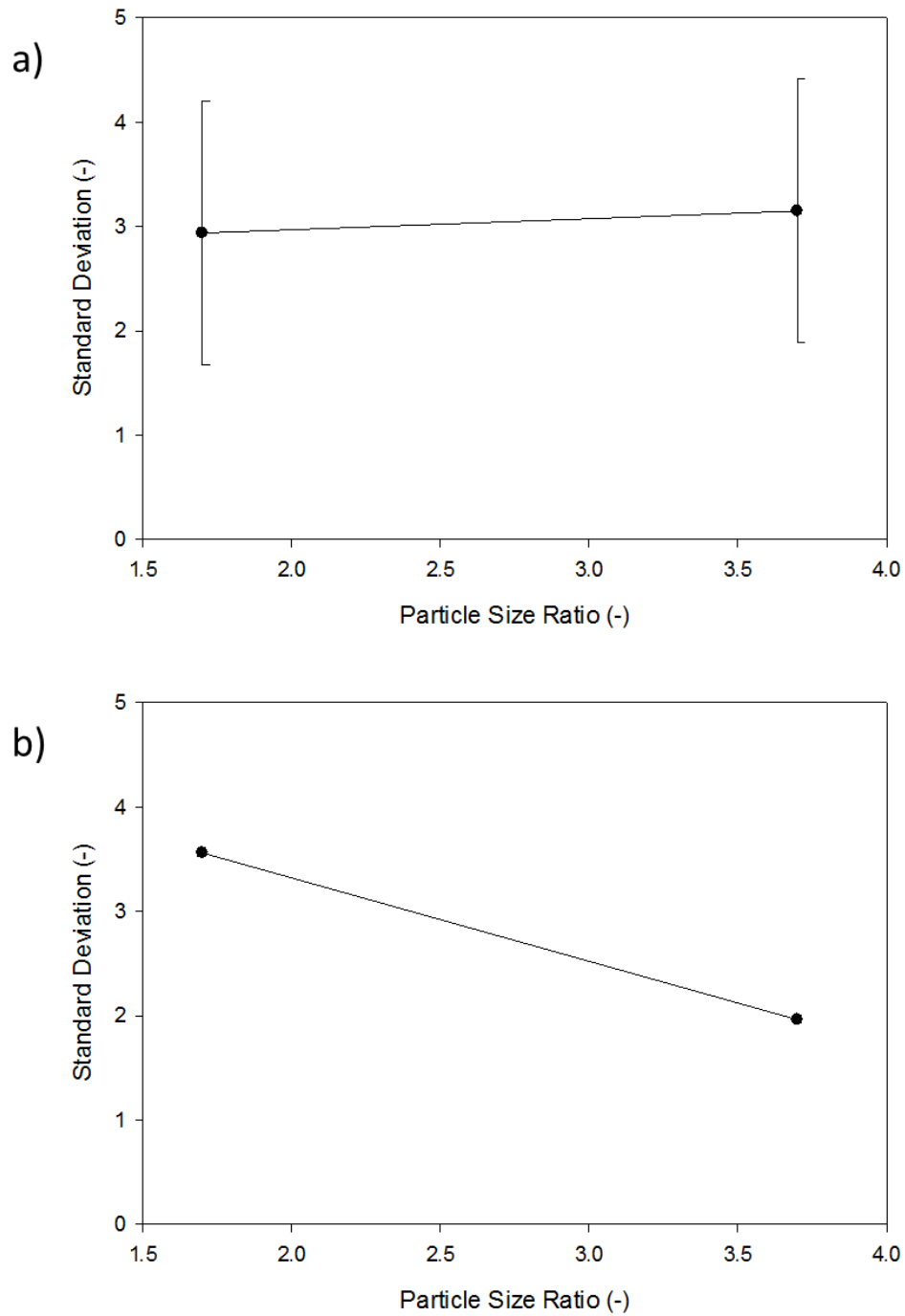
Figure 4.6: One factor plots for the influence of particle size ratio on segregation during mixing of the binary sugar spheres at an impeller speed of 300 rpm (a) and 700 rpm (b), where particle size ratio was determined to significantly affect particle segregation at 300 rpm when sampled at the bed surface.
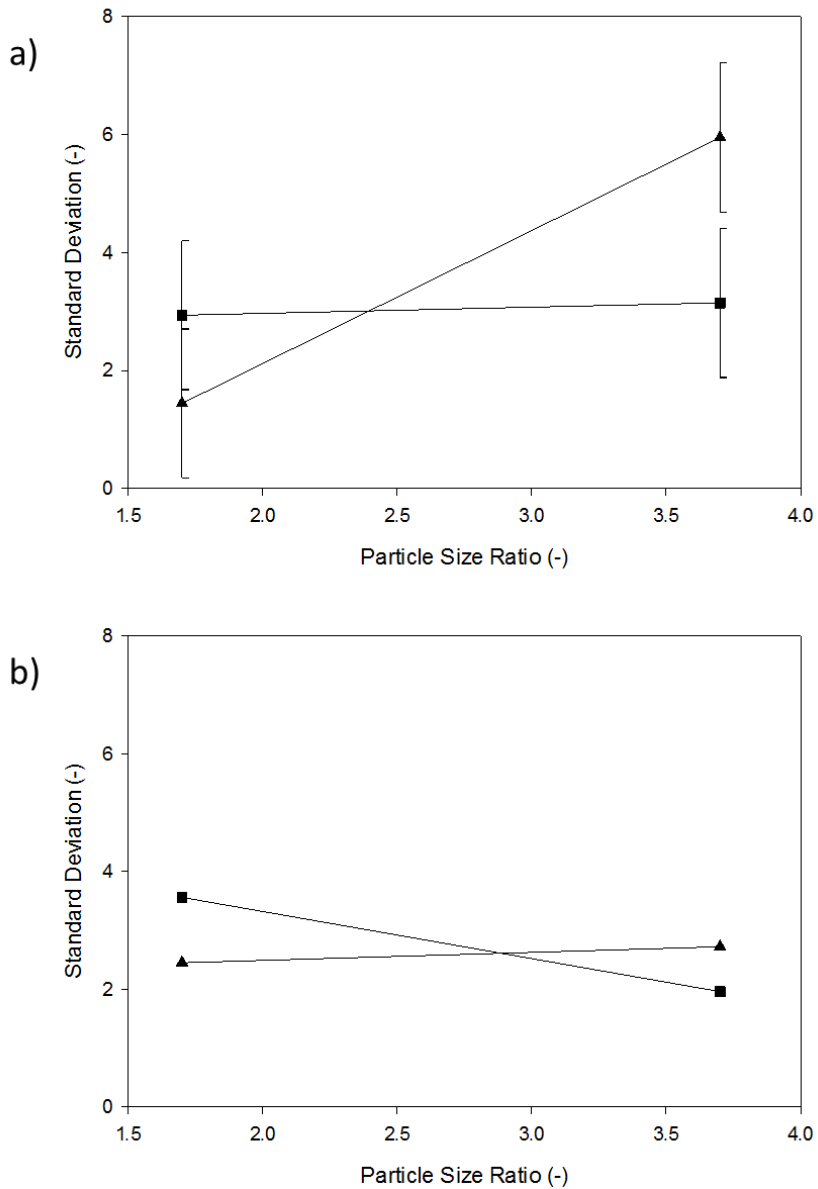
Figure 4.7: Interaction plot for the influence of particle size ratio and particle load order on segregation during mixing of the binary sugar spheres at an impeller speed of 300 rpm (a) and 700 rpm (b). Small particles loaded first (■) and large particles loaded first (▲) at high particle size ratio (3.7) resulted in larger segregation of particles at the powder bed surface compared with a low particle size ratio (1.7) at the powder bed surface at 300 rpm.

4.4   Discussion

4.4.1   Bumpy Regime (300 rpm)

Segregation is the separation of particles during flow of a powder or vibration of a powder bed. The main factors promoting segregation are size, density and shape [12]. The particles used in the trials were all spherical with a constant density of about 0.8 g/cm^3. However, particle sizes varied with ratios of 1.7 and 3.7. Segregation due to size can occur through percolation segregation: as powder flows, the smaller particles fall through voids between the larger particles due to gravitational forces resulting in segregation of the smaller particles near the bottom of the vessel [13, 14]. Trajectory segregation can also occur where, for the same density and velocity in free flight, the distance a particle travels is proportional to the square of its diameter. Therefore, trajectory segregation promotes segregation of larger particles near the walls of a mixer with the smaller particles in the centre due to centrifugal effects [5]. The effect of trajectory segregation can vary with location within the granulator bowl: the velocity of the particles increase near the impeller and the blade tips, while particles near the bed surface, although they have a lower velocity, have more opportunity for longer trajectories before a collision with another particle [12].

For the trials conducted at an impeller speed of 300 rpm, the standard deviation of the samples ranged from 1.2 to 6.7% indicating some particle segregation when samples were extracted radially using a sample thief probe. Figure 4.8 shows that the segregation resulted in more of the large particles near the centre of the bowl than at the perimeter. This segregation occurred at the high particle size ratio with only a short mix time and with the large particles loaded first.
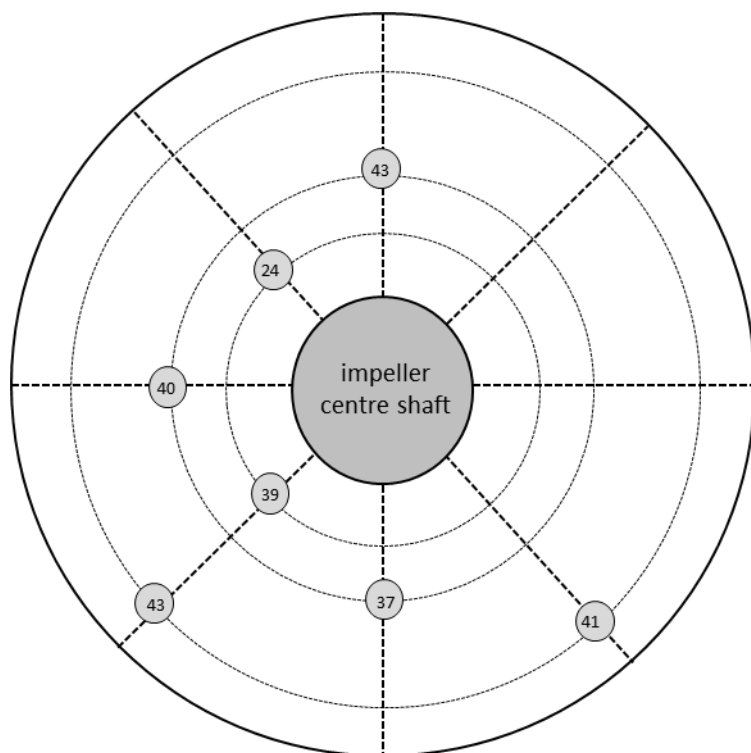
Figure 4.8: Radial sampling results for Trial 6 (particle size ratio 3.7, dry mix time 10s, large particles loaded first) at an impeller speed of 300 rpm; values indicate the mass percentage of smaller particles within each sample

At an impeller speed of 300 rpm, samples were also extracted at the surface of the powder bed. The standard deviation of the samples ranged between 1.03 to 6.93%, indicating some particle segregation at the powder bed surface. The two trials with the highest standard deviations both used a high particle size ratio (3.7), with larger particles loaded first. However, a short dry mix time of 10 s resulted in a higher standard deviation (6.93%) compared with the longer dry mix time of 300 s (4.7%). Figure 4.9a shows more of the smaller particles at the powder bed surface compared with Figure 4.9b, where overall less small particles were at the powder bed surface and larger particles were slightly overrepresented near the center of the bowl at the longer dry mix time.
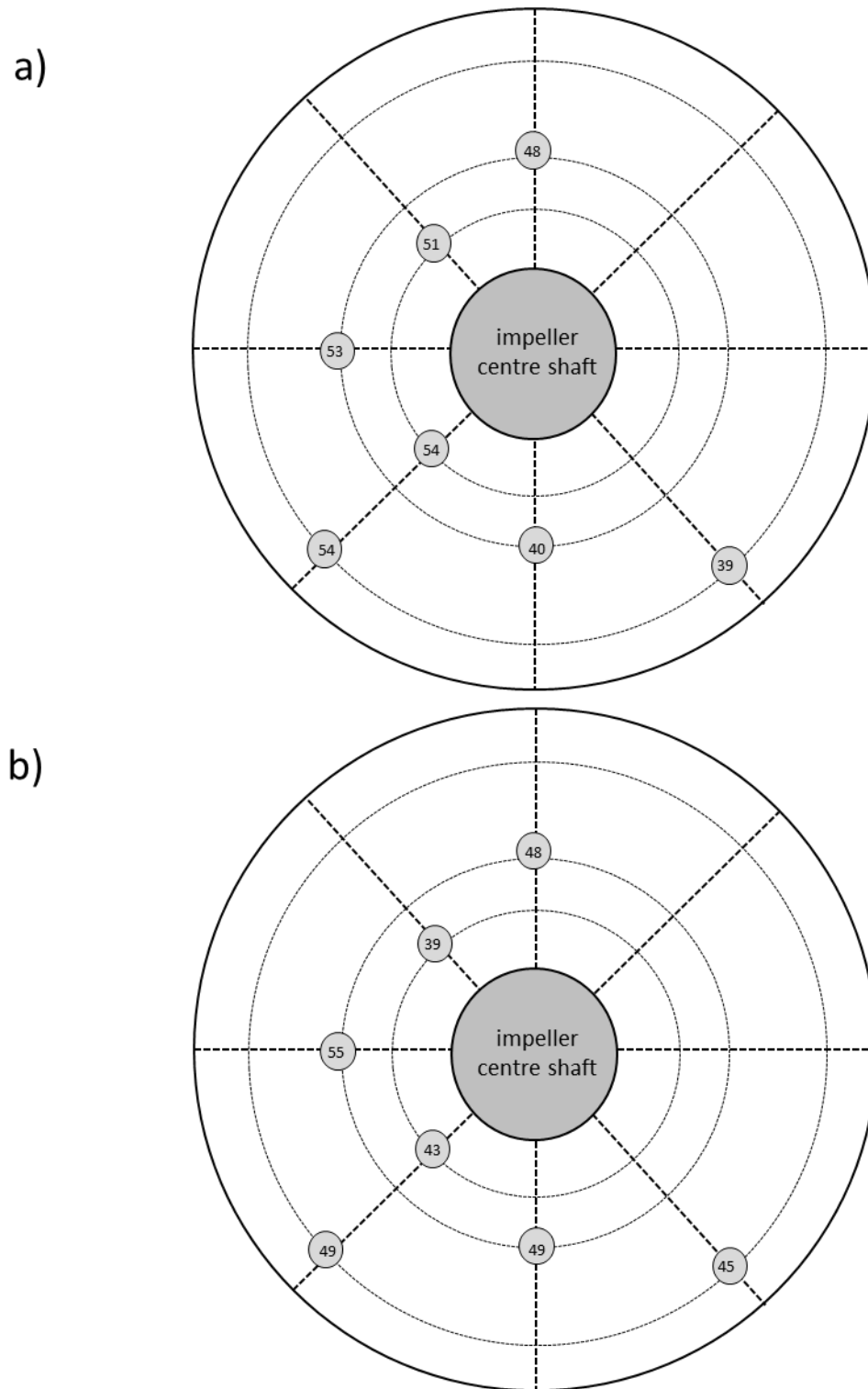
Figure 4.9: Surface bed sampling results for Trial 6 (a) at an impeller speed of 300 rpm and Trial 1 (b); values indicate the mass percentage of smaller particles within each sample at the powder bed surface

Percolation segregation, promoted by disturbances caused within the powder bed would allow for smaller particles to migrate to the bottom of the powder bed and larger particles to migrate to the top of the bed. However, at short dry mix times, percolation segregation effects do not fully develop compared to longer dry mix times. Therefore mainly small particles remain at the powder bed surface for shorter dry mix times compared with mixing times at 300 s, where larger particles percolate to the top of the powder bed.

Shear caused by the impeller blades can also lead to dilation of the powder bed, where dense matter has been observed to expand within the bed [15]. The expansion of the powder bed would then allow for an increase in bed voidage of the sugar sphere mixture during dry mixing. Percolation segregation would then be expected to be further promoted by the dilation of the bed, where more sites would allow for the smaller sugar spheres to travel towards the bottom of the powder bed and large particles to the top of the bed.

At an impeller speed of 300 rpm, the particles followed a bumpy flow regime. At this low impeller speed, centrifugal effects pushing the particles towards the bowl perimeter were minimal. In addition, although the impeller tip speed was 4.3 m/s, the powder velocity at the bed surface has been shown to be very slow, at about 0.25 m/s for a similar fill level and impeller rotation [16]. The bed, however, was disturbed by the movement of the impeller blades, which promoted any percolation segregation, where the longer dry mixing times would allow for larger percolation effects at the powder bed surface. Due to the geometry of the bowl and impeller, the effect of the impeller on the bed was larger near the centre of the bowl than near the perimeter as shown in Figure 4.10b. Percolation segregation of the smaller particles from the surface of the bed migrated to the bottom of the powder bed and larger particles to the powder bed surface. Surface bed sampling at longer dry mix times near the centre of the bowl then showed a higher mass percentage of larger particles at the powder bed surface (Figure 4.9b) and radial sampling also showed slightly larger particles at the center of the bowl (Figure 4.8). Percolation segregation was also shown in Oka et al. [6], where smaller particles percolated to the bottom of the powder bed, allowing for larger particles at the powder bed surface.

ANOVA indicated that the particle size ratio and the interaction of particle size ratio and particle loading order affected the segregation for the roping flow regime at an impeller speed of 300 rpm (Figures 4.6 and 4.7). An increase in particle size ratio showed an increase in particle segregation, where the effect of percolation segregation would be further promoted with larger differences between the size of the sugar spheres. The effect of both particle load order and particle size ratio on segregation was more pronounced when larger particles were loaded first at a high particle size ratio (Figure 4.7). The effect of percolation when smaller particles initially comprised the powder bed surface would allow for more migration of smaller particles the bottom of the bed, allowing for more particle segregation.
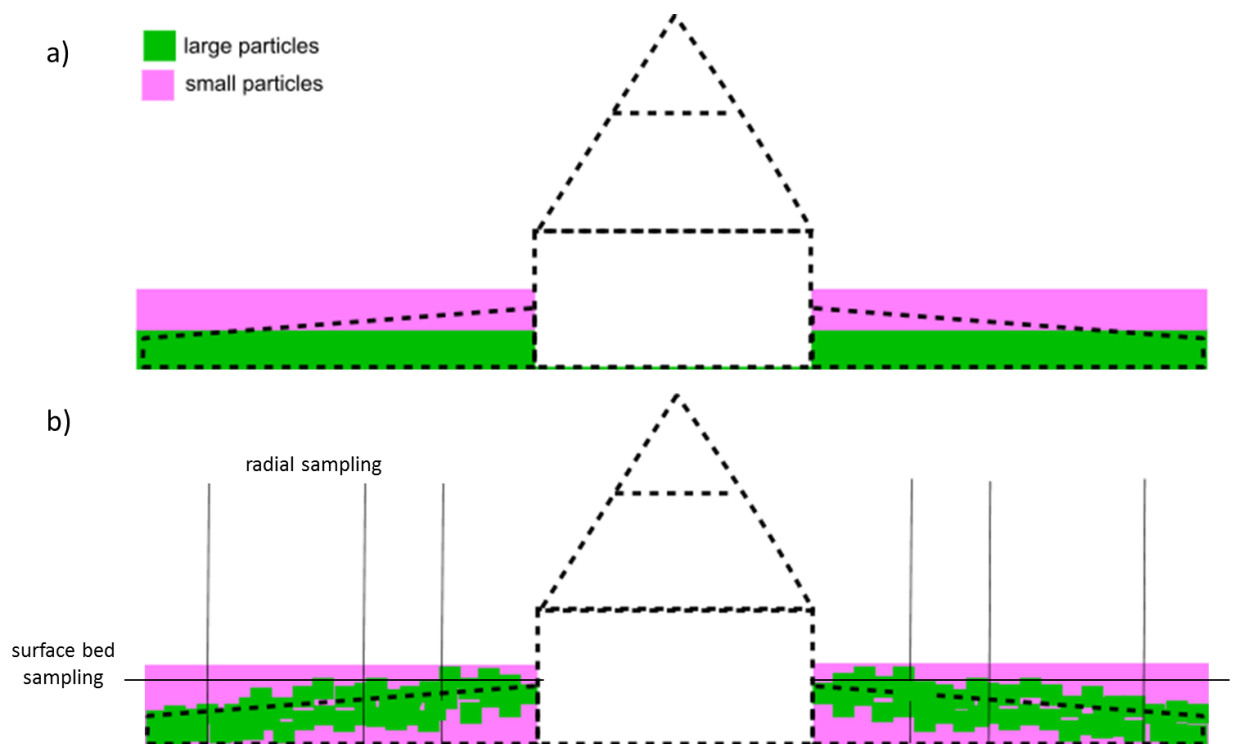
Figure 4.10: Schematic illustration of particle segregation at an impeller speed of 300 rpm during dry mixing of a binary sugar sphere mixture. Particles initially are loaded with small sugar spheres at the bed surface prior to mixing (a), and (b) particles segregate due to percolation segregation due to impeller blade disturbances.

4.4.2 Roping regime (700 rpm)

For the trials conducted at an impeller speed of 700 rpm, the standard deviation of the samples ranged from 0.6 to 5.2% indicating some particle segregation when samples were collected radially using a sample thief probe. Figure 4.11 shows that the segregation again resulted in more large particles near the centre of the bowl than at the perimeter when samples were drawn from the top to the bottom of the powder bed. This segregation occurred at the high particle size ratio with a long mix time and with the smaller particles loaded first. Different operating conditions promoted segregation at an impeller speed of 700 rpm compared to conditions at 300 rpm, highlighting the distinct flow patterns of the bumpy and roping flow regimes.
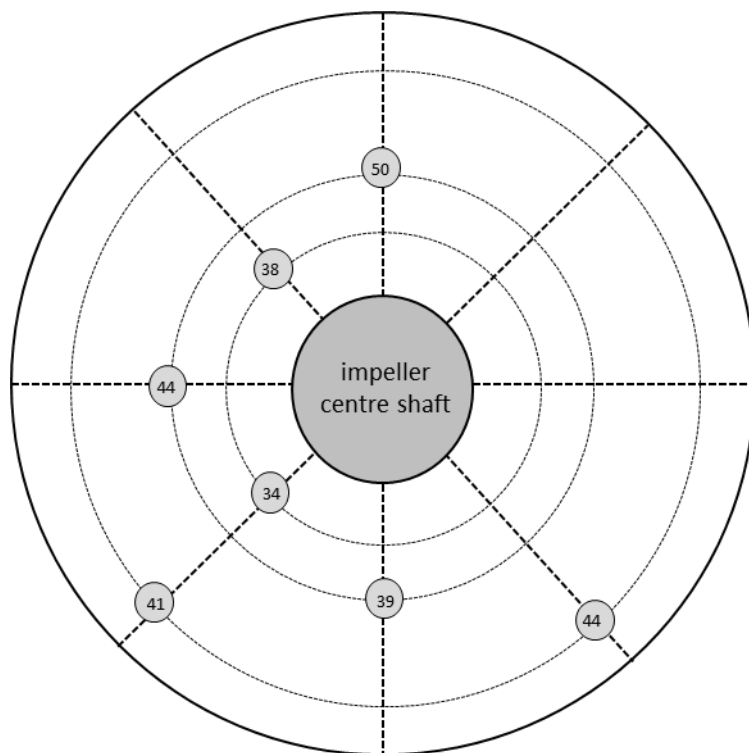
Figure 4.11: Radial sampling results for Trial 5 (particle size ratio 3.7, dry mix time 300 s, smaller particles loaded first) at an impeller speed of 700 rpm; values indicate the percentage of smaller particles within each sample

Figure 4.12 shows the mass percentage of small particles at each sampling location when samples were collected at the surface of the bed for the same operating conditions compared with Figure 4.11. Figure 4.12 shows relatively minimal difference at the powder bed surface, where overall larger particles were slightly overrepresented at the powder bed surface. The percent standard deviation was relatively low at 1.20% suggesting minimal segregation radially from the center to the perimeter of the bowl at the powder bed surface for the selected operating conditions.
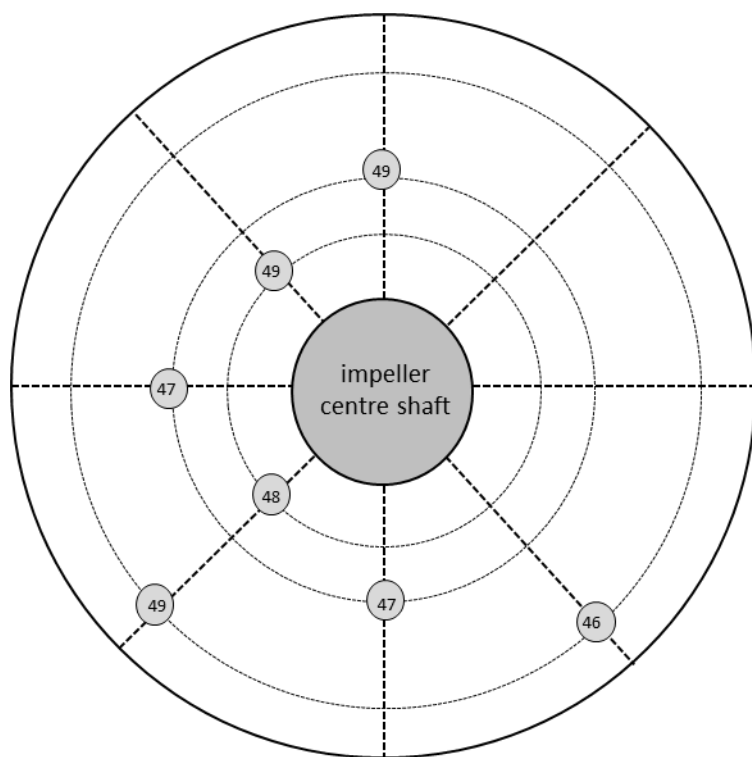
Figure 4.12: Surface bed sampling results for Trial 5 at an impeller speed of 700 rpm; values indicate the mass percentage of smaller particles within each sample at the powder bed surface

At an impeller speed of 700 rpm, the particles followed a roping flow regime which was confirmed from Logan et al. [11]. In this flow regime, the high centrifugal effects push the particles to the bowl perimeter. Also, particles flow inwards at the bed surface and outwards at the bottom of the bowl to form a toroid. Figure 4.13 is a schematic of the proposed particle flow that promotes segregation within the roping flow regime. The centrifugal effects initially pushed the particles to the bowl perimeter, especially the large

particles loaded last and located at the bed surface. This trajectory segregation would initially cause the large particles to segregate near the bowl perimeter. As the toroidal flow developed, the large particles would then flow toward the centre over the smaller particles. Their trajectory would continue downwards and then the centrifugal effects would again push them to the bowl perimeter. A toroid with larger particles at its surface and smaller particles within its structure would eventually develop. When samples were collected at the powder bed surface, samples comprised primarily of large particles (Figure 4.12), further supporting the toroidal formation with large particles at the surface of the toroid.
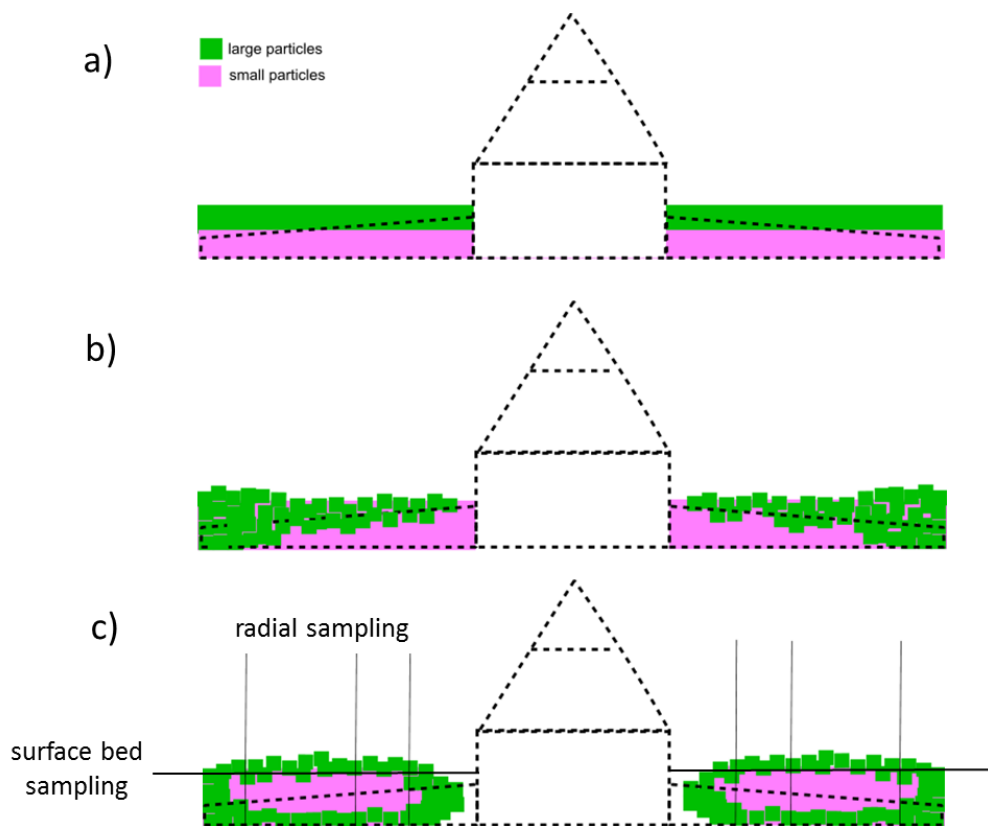
Figure 4.13: Schematic illustration of speculated particle segregation at an impeller speed of 700 rpm during dry mixing of a binary sugar sphere mix. Particles initially loaded with large sugar spheres at the bed surface prior to mixing (a). Immediately after impeller begins to rotate, trajectory segregation causes larger particles to travel to the bed perimeter (b). As time progresses, a toroidal formation develops (c) causing large particles to segregate to the toroidal surface of the powder bed

ANOVA indicated that the particle size ratio and the particle loading order significantly affected the segregation for the roping flow regime at an impeller speed of 700 rpm when powder was sampled radially using a sample thief probe (Figures 4.4 and 4.5). With the smaller particles loaded first, trajectory segregation would quickly force the large particles near the bed surface to the bowl perimeter and then to form a toroid with the larger particles at its surface. With the larger particles loaded first, the smaller particles would exhibit both percolation segregation towards the bottom of the bowl as well as trajectory segregation towards the bowl perimeter. A toroid with larger particles at its surface would eventually form, but only after a longer mixing time. A larger particle size ratio promoted trajectory segregation which quickly formed a toroid with larger particles at its surface.

4.4.3   Spray zone implication

The spray zone, shown in Figure 4.14, was identified using the liquid binder coloured with food colouring sprayed onto a non-moving powder bed. The spray zone was a wedge with an angle of about 60° and an area of about 8900 mm^2. Due to the geometry of the spray zone, particles located at the perimeter of the bowl would be exposed to the liquid binder spray for longer times. The particles that the liquid binder droplets initially contact within the spray zone form granule nuclei. Any radial segregation, especially at the powder bed surface would then affect the composition of the granule nuclei. From the sugar spheres results, at low impeller speeds or within the bumpy flow regime, more granule nuclei would be formed from smaller rather than larger particles. At higher impeller speeds, with the powder flowing as a toroid, more granule nuclei would be formed from the larger particles at the surface of the toroid.
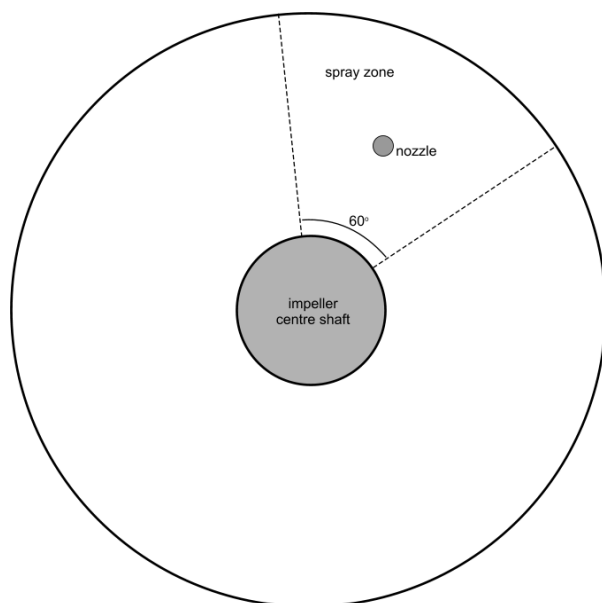
Figure 4.14: Schematic diagram of the measured liquid binder spray zone for an Aeromatic-Fielder high shear granulator. Spray nozzle is placed at the intermediate location in the bowl, where the angle of the spray zone is approximately measured at 60°

4.5   Conclusions

During high shear wet granulation, granule nuclei form when the liquid binder droplets impact upon the powder bed, and therefore the composition and uniformity of the powder bed surface are critical to the formation of granule nuclei with specific properties. Granule nuclei with disproportionate amounts of components of a formulation could grow to granules that also do not contain the correct proportions and therefore must be discarded. Sugar spheres were mixed in a high shear granulator under different impeller speeds, mixing times, loading order and size ratios to investigate the conditions that would lead to a powder bed with uniform distribution of the formulation components. To minimize powder segregation and therefore minimize the possibility of granule nuclei with disproportionate components, it was concluded that the larger formulation components should be added first to the bowl and then the initial dry mixing phase should be kept short and use a high impeller speed to ensure roping flow.

4.6   References

1. J.D. Litster, K.P. Hapgood, J.N. Michaels, A. Sims, M. Roberts, S.K. Kameneni, Scale-up of mixer granulators for effective liquid distribution, Powder Technology, 124 (2002) 272-280.

2. Y.C. Zhou, A.B. Yu, R.L. Stewart, J. Bridgwater, Microdynamic analysis of the particle flow in a cylindrical bladed mixer, Chemical Engineering Science, 59 (2004) 1343-1364.

3. D.M. Koller, A. Posch, G. Hoerl, C. Voura, S. Radl, N. Urbanetz, S.D. Fraser, W. Tritthart, F. Reiter, M. Schlingmann, J.G. Khinast, Continuous quantitative monitoring of powder mixing dynamics by near-infrared spectroscopy, Powder Technology, 205 (2011) 87-96.

4. R.L. Stewart, J. Bridgwater, D.J. Parker, Granular flow over a flat-bladed stirrer, Chemical Engineering Science, 56 (2001) 4257-4271.

5. S.L. Conway, A. Lekhal, J.G. Khinast, B.J. Glasser, Granular flow and segregation in a four-bladed mixer, Chemical Engineering Science, 60 (2005) 7091-7107.

6. S. Oka, H. Emady, O. Kaspar, V. Tokarova, F. Muzzio, F. Stepanek, R. Ramachandran, The effects of improper mixing and preferential wetting of active and excipient ingredients on content uniformity in high shear wet granulation, Powder Technology, (2015).

7. J. Gabrielsson, N.O. Lindberg, T. Lundstedt, Multivariate methods in pharmaceutical applications, Journal of chemometrics, 16 (2002) 141-160.

8. S. Ranjbarian, F. Farhadi, Evaluation of the effects of process parameters on granule mean size in a conical high shear granulator using response surface methodology, Powder Technology, 237 (2013) 186-190.

9. M. Fonteyne, J. Vercruysse, D. Cordoba Diaz, D. Gildemyn, C. Vervaet, J.P. Remon, T. De Beer, Real-time assessment of critical quality attributes of a continuous granulation process, Pharmaceutical Development and Technology, 18 (2013) 85-97.

10. P. Soyeux, A. Delacourte, B. Delie, P. Lefevre, B. Boniface, Influence and optimisation of operating parameters with a new binder in wet granulation. I: use in powder form, European Journal of Pharmaceutics and Biopharmaceutics, 46 (1998) 95-103.

11. R. Logan, L. Briens, Investigation of the effect of impeller speed on granules formed using a PMA-1 high shear granulator, Drug Development and Industrial Pharmacy, 38 (2012) 1394-1404.

12. H.J. Venables, J. Wells, Powder mixing, Drug development and industrial pharmacy, 27 (2001) 599-612.

13. M.S. Siraj, S. Radl, B.J. Glasser, J.G. Khinast, Effect of blade angle and particle size on powder mixing performance in a rectangular box, Powder Technology, 211 (2011) 100-113.

14 .K. Sakaie, D. Fenistein, T.J. Carroll, M. van Hecke, P. Umbanhowar, MR imaging of Reynolds dilatancy in the bulk of smooth granular flows EPL (Europhysics Lett). 84 (2008) 38001

15. B. Remy, J.G. Khinast, B.J. Glasser, Polydisperse granular flows in a bladed mixer: Experiments and simulations of cohesionless spheres, Chemical Engineering Science, 66 (2011) 1811-1824.

16. M. Cavinato, R. Artoni, M. Bresciani, P. Canu, A.C. Santomaso, Scale-up effects on flow patterns in the high shear mixing of cohesive powders, Chemical Engineering Science, 102 (2013) 1-9.

Chapter 5

5 Granule nuclei formation in pharmaceutical powder beds of varying hygroscopicity

5.1 Introduction

Wet granulation is the agglomeration of particles using a liquid binder to form large granules. The process is extensively used in the pharmaceutical industry to produce tablets, as granulation minimizes segregation and dust, while improving flowability of powders [1]. Granule uniformity is important in pharmaceutical manufacturing, as the tablet must contain a uniform distribution of excipients in the product to comply with regulations and ensure product efficacy.

The wet granulation process is complex with three stages occurring simultaneously: wetting and nucleation, consolidation and growth, and attrition and breakage [1]. A thorough review on these three stages of granulation is provided by Iveson et al. [2]. Since wet granulation processes occur simultaneously, it is difficult to predict the formation of ideal granules. Wetting and nucleation have received significant attention, as these have been shown to be crucial in obtaining granules with specified properties.

Ideal nucleation occurs when one drop forms one granule nucleus, called drop controlled nucleation [3]. The droplets falling upon into the powder surface must not overlap and must penetrate into the powder bed quickly with short drop penetration times. These two criteria are both required for drop controlled nucleation.

The drop penetration of several different fluids into powder beds has been studied by Hapgood et al. [3]. This study focused on homogenous powder beds (ballotini spheres, lactose, zinc oxide, and titanium oxide) with six different binders. The kinetics of drop penetration was found to depend on the powder particle size, viscosity, surface tension and contact angle of the liquid binder solution. Packing of the powder bed was also found to be crucial, as the orientation of the particles influenced the mechanism of liquid penetration. The formation of macro-voids prevented liquid migration through the

powder bed. The orientation of particles in the powder bed changed the void sizes causing liquid velocities to vary and eventually stop when a macro-void was encountered. Hapgood et al. [3] proposed that the presence of macro-voids resulted in longer drop penetration times as the liquid velocity through these voids was inhibited.

Drop penetration behaviour into heterogeneous powder beds was examined by Nguyen et al. [4]. Salicylic acid and lactose powders were used to study the effects of varying degrees of hydrophobicity on the kinetics of drop penetration. As the relative proportion of hydrophobic salicylic acid in the binary powder mixture increased, the drop penetration times increased and the average granule size decreased. The study analyzed powder of two extreme powder characteristics: one being highly hydrophobic and the other being hydrophilic. The formation of granule nuclei in highly hydrophobic powders followed a different mechanism than for hydrophilic powders as "liquid marbles" were formed: liquid droplets that did not penetrate into the powder, but formed granule nuclei by attracting the powder at the droplet interface [5-7].

The hygroscopicity of a powder refers to its ability to absorb moisture from its surroundings. Microcrystalline cellulose (MCC) and lactose monohydrate are commonly used excipients in pharmaceutical tablets. MCC is widely used in the industry due to its chemical inactivity and its lack of toxicity [8]. MCC is also widely known to be hygroscopic, where lactose monohydrate is known to be non-hygroscopic. Using hygroscopic powders such as MCC in a formulation affects granulation. Kristensen et al. [9] and Chitu et al. [10] found that the amount of liquid binder needed for granulation increased with the amount of MCC in the powder formulation. For granules to form, a critical amount of liquid must be available at the surface of the particles to form the required liquid bridges between the particles. Due to its hygroscopic property, MCC will internally absorb some of the liquid binder. More binder is therefore required to ensure a critical amount at the surface for the liquid bridges and granule nuclei formation.

Work by Rocca et al. [11] used a novel foam binder to study drop penetration of a 50/50 MCC and lactose monohydrate powder mix. It was found that penetration time as well as granule size were both influenced by the moisture content of the of the powder bed. Li et

al. [12] expanded on this by comparing the novel foam method to the conventional drop penetration method using a 50/50 MCC and lactose monohydrate powder mix. Both of these studies used the drop penetration method as supplementary work and did not comprehensively study the influence of MCC at varying fractions on drop penetration time and granule nuclei morphology.

There have only been limited studies on drop penetration and granule morphology using heterogeneous powders and also hygroscopic powders. This forms a significant gap of critical information about granulation as all commercial formulations include more than one component and many will also include a hygroscopic component. Therefore, the goal of this research was to examine liquid binder drop penetration and subsequent granule nuclei formation using a mixture of two common commercially used excipients, hygroscopic microcrystalline cellulose and non-hygroscopic lactose monohydrate.

5.2   Materials and Methods

5.2.1   Formulation

Microcrystalline cellulose (Avicel PH-101, FMC BioPolymer) and α-lactose monohydrate (EMD Emprove) powders were used in this study. All powder properties are summarized in Table 5.1. The surface mean diameter particle size ($d_{3, 2}$) was defined as the diameter of a sphere with the same surface to volume ratio as the measured non-spherical particle. Measurements were taken in triplicate using a Malvern Mastersizer 2000.

Table 5.1: Measured powder properties

wt/wt% MCC	wt/wt% α-lactose monohydrate	$d_{3,2}$ (μm)	ρ_{bulk} (g/cm^3)	ρ_{tap} (g/cm^3)	ε_{bed} (-)	ε_{tap} (-)	$\varepsilon_{effective}$ (-)
0	100	98.7±0.61	0.76±0.00	0.91±0.01	0.51±0.00	0.41±0.01	0.37±0.00
20	80	87±0.47	0.61±0.01	0.78±0.01	0.61±0.01	0.5±0.01	0.44±0.00
40	60	75.32±0.33	0.49±0.01	0.68±0.02	0.68±0.01	0.56±0.01	0.5±0.01
60	40	63.64±0.22	0.43±0.01	0.58±0.01	0.73±0.00	0.63±0.01	0.57±0.00
80	20	51.97±0.16	0.36±0.00	0.52±0.00	0.77±0.00	0.67±0.00	0.6±0.00
100	0	40.29±0.23	0.33±0.01	0.45±0.01	0.79±0.01	0.71±0.01	0.66±0.01

5.2.1.1 Density and Voidage

The true particle density of α-lactose monohydrate and MCC were obtained through comparison with literature values and calculations described by Nguyen et al. [4] for determining true particle densities of heterogeneous mixtures [13]. Values ranged between 1.55 g/cm^3 for pure α-lactose monohydrate particles to 1.58 g/cm^3 for pure MCC particles.

The effective bed voidage (ε_{eff}) was determined using Equation 5.1[3]:

$$\varepsilon_{eff} = \varepsilon_{tap}\left(1 - \varepsilon + \varepsilon_{tap}\right) \tag{5.1}$$

where ε_{tap} is the tap bed voidage, ε is the bed voidage, and ε_{eff} is effective bed voidage. The bed voidage can be determined using:

$$\varepsilon = 1 - \frac{\rho_{bulk}}{\rho_{true\ particle\ density}} \tag{5.2}$$

and tap bed voidage using:

$$\varepsilon_{tap} = 1 - \frac{\rho_{tap}}{\rho_{true\ particle\ density}} \tag{5.3}$$

Bulk density was determined by measuring the powder weight mass when loosely filled in a 100 mL graduated cylinder. Tap density was determined by agitating the powder in 100 mL graduated cylinders and determining the change in volume.

5.2.1.2   SEM Images

Images of the MCC and α-lactose monohydrate particles were obtained using a scanning electron microscope (Hitachi S-4500 field emission SEM with a Quartz XOne EDX system). Samples were placed on a plate and coated with gold prior to examination.

5.2.1.3   Liquid Binder Measurements

Liquids used for drop penetration trials were water and 2 wt%, 6 wt%, and 8 wt% hydroxypropyl methylcellulose (HPMC) solutions in water (Shin-Etsu Chemical Company, Grade 603). Solutions using HPMC were prepared by heating water to over 85° C, then gradually adding HPMC powder while stirring until the powder fully dissolved. Solutions were then brought back to room temperature (23°C) before conducting experiments. A blue dye that was confirmed not to significantly affect the liquid properties was added to the solutions to increase visibility during drop penetration experiments.

The density of liquid binders was measured using a Gamma-Sphere, Type X (Viscone Instruments, CH-5605 Dottikon): 10 mL liquid samples were measured and a 10 g sphere was inserted into the liquid sample. Displacement measurements were recorded to obtain density values. Viscosity measurements were conducted using a Brookfield Viscometer at 20 rpm with a 61 spindle. Dynamic surface tension was measured using a KRUSS Bubble Pressure Tensiometer and surface tension values were used at a surface age of 37 ms. Liquid binder properties are summarized in Table 5.2.

Table 5.2: Measured liquid binder solution properties

Liquid Solution	Viscosity (Pa s)	Density (g/cm^3)	Surface Tension (mN/m)
Water	0.0012±0.21	0.996±0.00	73.67±0.30
2 wt % HPMC	0.0042±0.42	1.002±0.01	56.13±0.16
6 wt % HPMC	0.0231±1.27	1.012±0.00	55.28±0.17
8 wt % HPMC	0.0429±0.85	1.017±0.00	55.14±0.36

5.2.2 Drop penetration time measurements

Drop penetration time was measured for single drop experiments using a procedure similar to that developed by Hapgood et al. [3]. A schematic of the drop penetration setup is shown in Figure 5.1.Mixtures of heterogeneous powder beds of MCC and lactose were determined on a weight basis. The powders were mixed manually for 30 seconds and then sieved through a 1.70 mm sieve into a petri dish. Excess powder was scraped level using a spatula. A 25 gauge needle syringe was mounted 0.5 cm above the powder bed. A liquid binder droplet of 0.0048 mL was gently dropped on the powder bed and a video of the drop penetration was filmed using a Canon EOS 60D camera with a macro lens, capturing images at 30 frames per second (fps). The procedure was repeated in triplicate. The drop penetration time was determined as the time at which the liquid droplet was no longer visible at the powder bed surface. The images were carefully examined for changes in grayscale to help determine this time. Granule nuclei were collected and their properties examined.
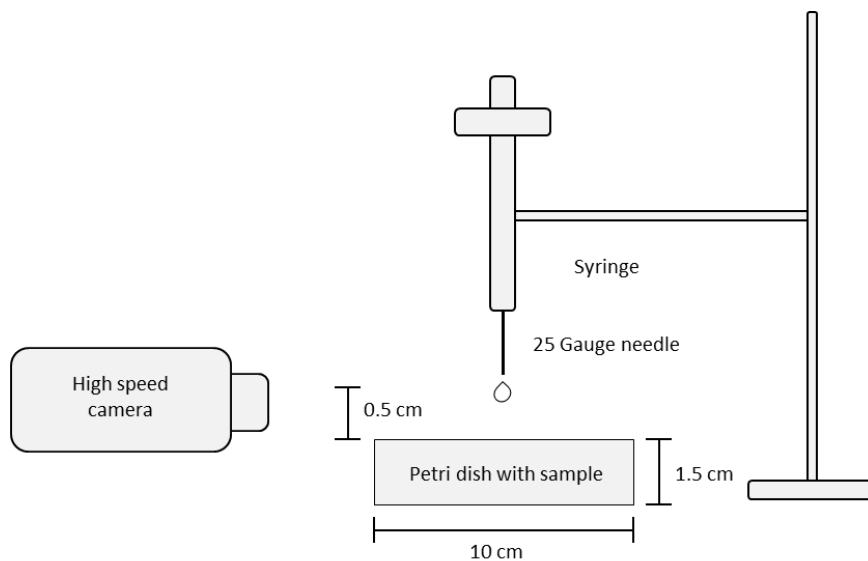
Figure 5.1: Schematic of the drop penetration set up

5.2.2.1   Granule Characterization

An image processing program (ImageJ Software, U.S. National Institutes of Health) was used to determine granule nuclei sizes through the Ferret diameter of individual granule nuclei. Colored images of the granule nuclei were set to black and white 8-bit images and binary processing was applied to the images. A measurement scale was set and the granule nuclei were analyzed using the FeretX and FeretY values to provide the Feret diameter of the granule.

5.3   Results

5.3.1   Drop penetration and granule nuclei for homogenous powder beds

Figure 5.2 shows the SEM images for both α- lactose monohydrate and MCC particles.
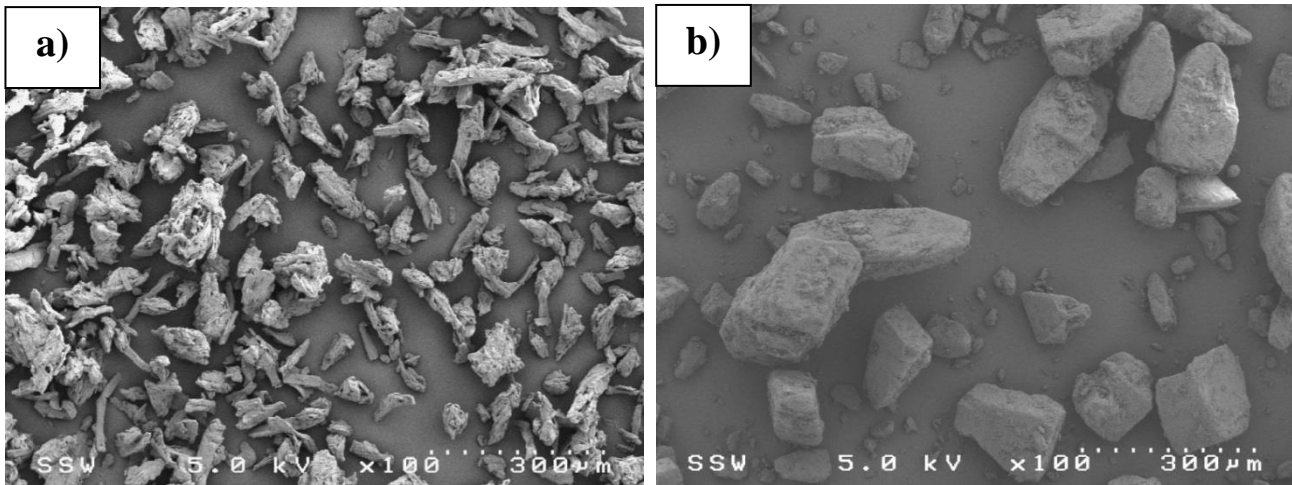
Figure 5.2: Scanning electron micrograph images of (a) microcrystalline cellulose and (b) α- lactose monohydrate

Figure 5.3 shows photos of a droplet of 2 wt% HPMC liquid binder solution penetrating into a powder bed of α-lactose monohydrate with a drop penetration time of just over 0.40 s.
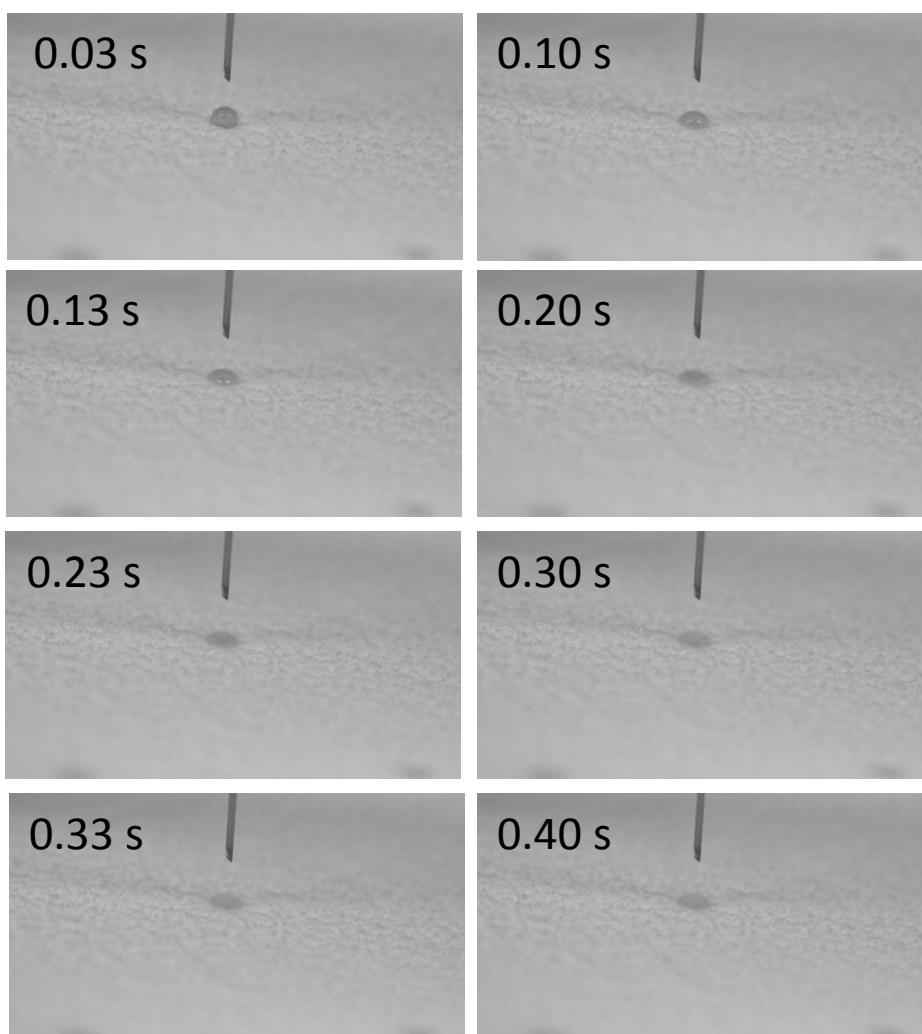
Figure 5.3: Images of penetration of a 2 wt% HPMC solution droplet into an α-lactose monohydrate powder bed taken with images at 30 fps

Drop kinetics of increasing liquid binder solution viscosity in contact with α-lactose monohydrate and MCC are shown in Figure 5.4. Regression analysis allowed for the line of best fit to the data for both α-lactose monohydrate and MCC. Drop penetration times into the α-lactose monohydrate beds were longer than those into MCC powder beds. Increasing the liquid solution viscosity increased drop penetration times for both powders.
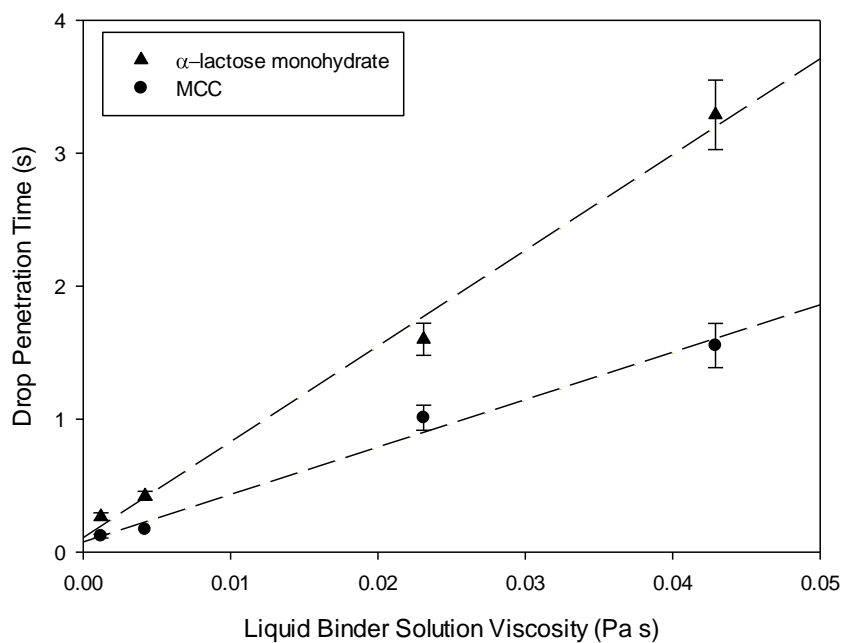
Figure 5.4: Drop penetration times into α-lactose monohydrate and MCC powder beds for varying liquid binder solution viscosities

Figure 5.5 shows that the sizes of granule nuclei changed when different viscosities of liquid binder solutions were used with α-lactose monohydrate and MCC powder beds. Regression analysis allowed for the line of best fit to the data for both α-lactose monohydrate and MCC. Granule nuclei formed from α-lactose monohydrate were larger than those formed from MCC.
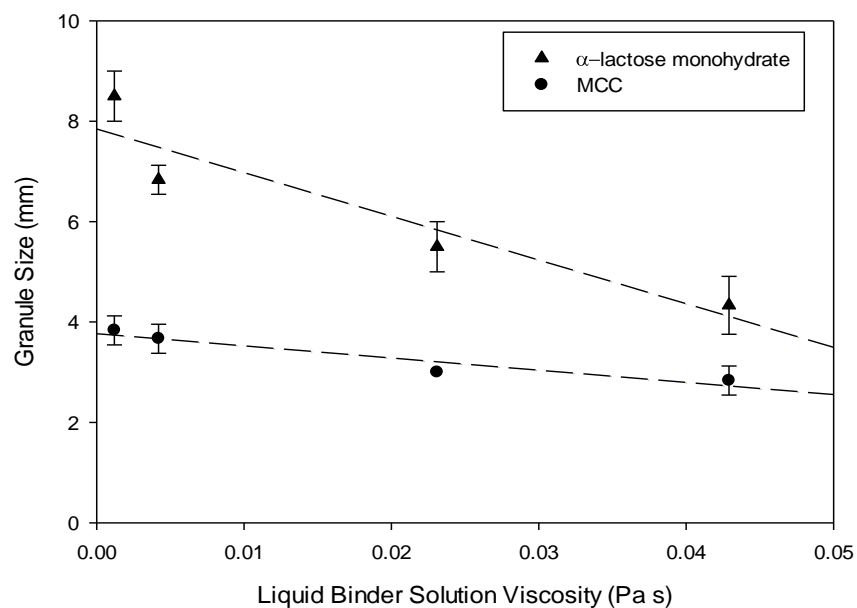
Figure 5.5: Effect of liquid binder solution viscosity on granule nuclei sizes with α-lactose monohydrate and MCC powder beds

The shapes of granule nuclei formed from MCC and α-lactose monohydrate powder beds were different (Figure 5.6). α-lactose monohydrate granule nuclei (Figure 5.6a) formed a ball shape while the MCC granule nuclei were disc-shaped (Figure 5.6b).
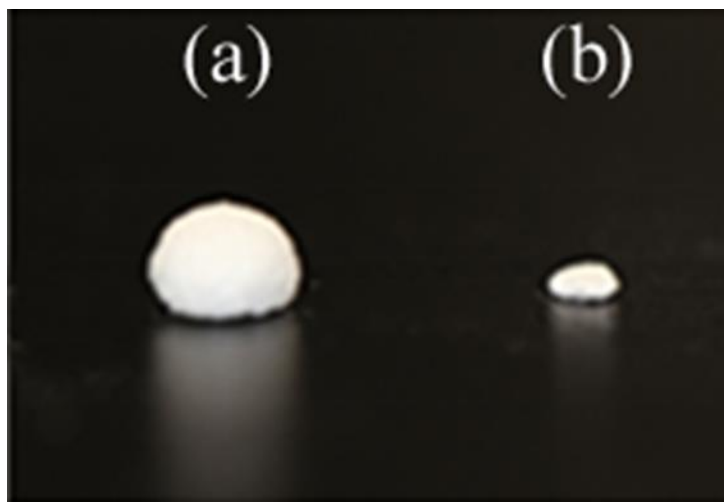
Figure 5.6: Photograph showing the shapes of granule nuclei formed from α-lactose monohydrate (a) and MCC (b) with 2 wt% HPMC liquid binder solution

5.3.2 Drop penetration and granule nuclei for heterogeneous powder beds

Figure 5.7 shows that the effective voidage of the powder beds increased approximately linearly from 0.37 for α-lactose monohydrate to 0.66 for MCC. Regression analysis allowed for the line of best fit to the data.
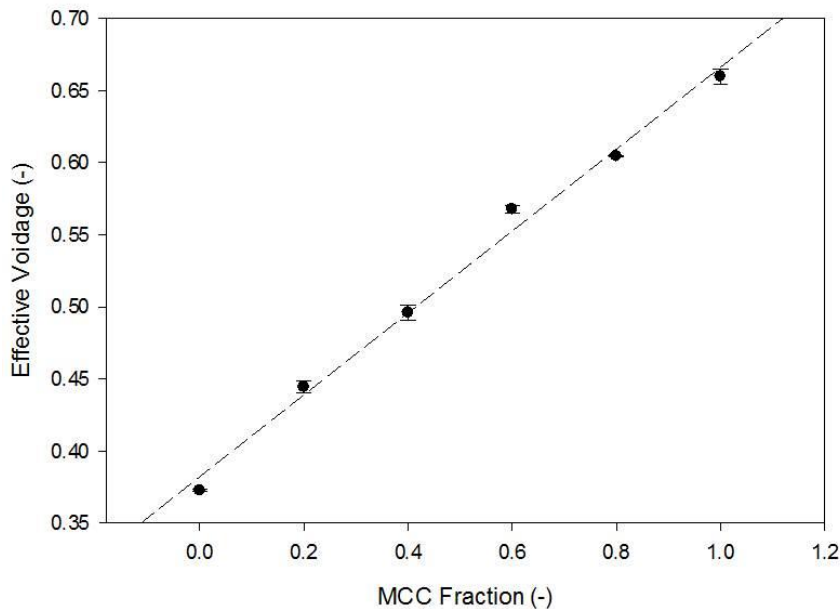
Figure 5.7: Effective bed voidage of the heterogeneous powder beds used for drop penetration measurements

Figure 5.8 shows that the drop penetration time into the heterogeneous powder bed decreased as the effective voidage increased. Regression analysis allowed for the line of best fit to the data.
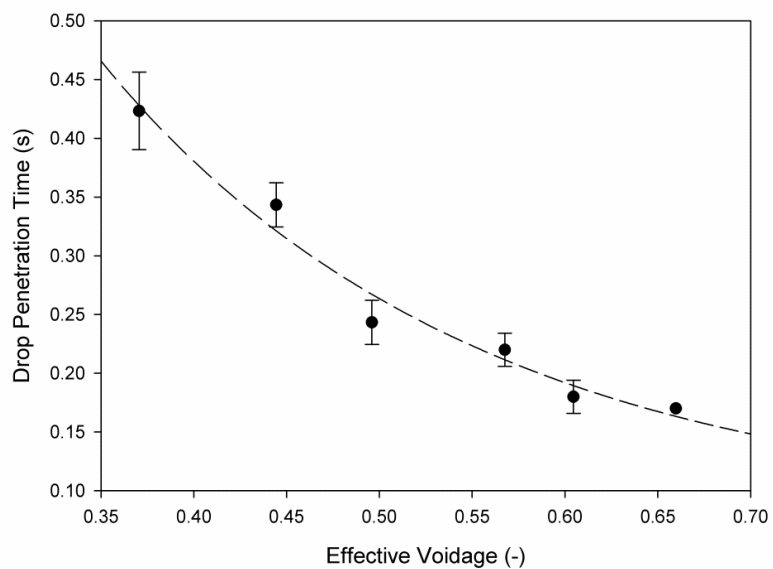
Figure 5.8: Drop penetration times of 2 wt% liquid solution into powder beds with varying effective voidage

Figure 5.9 shows that the granule nuclei size decreased significantly with increasing effective voidage. This decrease reflected the increasing amount of MCC within the bed. Regression analysis allowed for the line of best fit to the data.
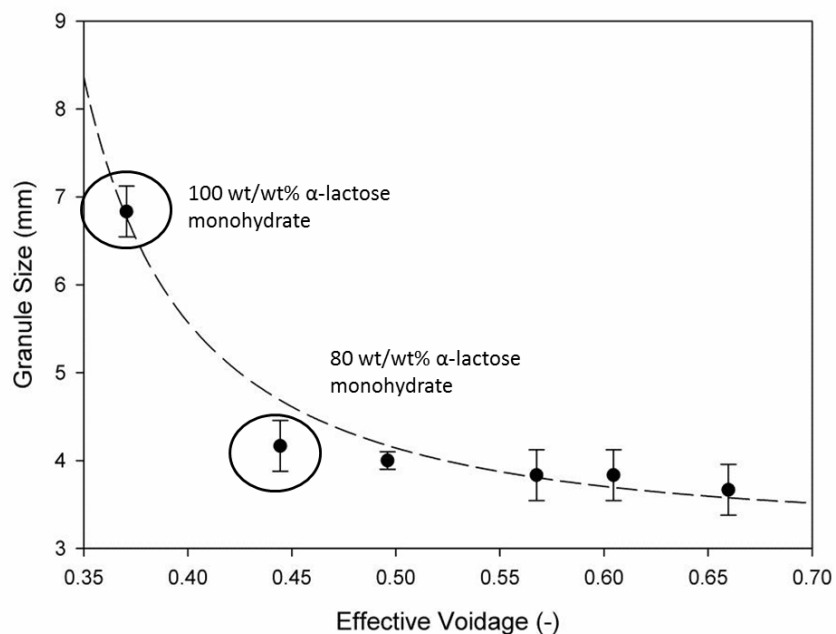
Figure 5.9: Granule nuclei size as a function of effective voidage of the heterogeneous powder beds

5.4   Discussion

5.4.1   Homogenous powder beds

The SEM images from Figure 5.2 show very different size, shape, and morphology of α-lactose monohydrate and MCC powders. The α-lactose monohydrate particles had a smooth surface and an estimated sphericity of 0.8 to 0.9. Microcrystalline cellulose particles were porous fibers with a rough surface texture and a sphericity of less than 0.5.

Figure 5.3 shows a droplet of 2wt% HPMC penetrating into an α-lactose monohydrate powder bed. As the droplet penetrated into the bed, its radius remained constant while the contact angle decreased. Therefore the drawing area of the droplet into the powder bed was approximately constant. Droplet penetration also followed a constant drawing area for the MCC beds and for the heterogeneous powder beds.

The average velocity a liquid travels through a porous matrix can be described using Equation 5.4:

$$U = \frac{dx}{dt} = \frac{R\gamma \cos \theta_d}{4\mu x} \qquad\qquad (5.4)$$

where U is the average velocity, x is the distance of liquid travelled, t is the time, μ is the viscosity of the liquid, γ is the surface tension of the liquid, R is the average radius of the voids formed between particles and θ_d is the dynamic contact angle measured between the powder bed and liquid solution. The surface tension (γ) of the liquid binders used in this study was relatively similar (Table 5.2) and therefore did not significantly contribute to any differences in the average velocity of the liquid into the powder bed. The dynamic contact angle (θ_d) for the two powders ranged from 49.09 to 83.1 and provided only small differences in the velocity [14]. Differences in the velocity that in turn affect the drop penetration times must therefore be due to the voidage of the powder beds, reflected through the average radius (R) of the voids, and due to the viscosity of the liquid binder solution.

Equation 5.4 indicates that the average liquid velocity should be proportional to the radius of the voids between particles. According to the relationship developed by Hapgood et al. [3], the average void radius for the MCC powder bed was estimated at 7.04×10^{-6}mm while the value for the α-lactose monohydrate powder bed was almost 1.5 times larger at 1.08×10^{-5}mm. Therefore, the average liquid velocity should be slower through a MCC powder bed than through a α-lactose monohydrate powder bed. However, Figure 5.4, shows that drop penetration times into MCC powder beds were lower than α-lactose monohydrate, indicating that the factors affecting the average liquid velocity and consequent drop penetration times were more extensive than indicated in Equation 4 and/or the relationship of the velocity with the drop penetration times may be complex.

Viscosity is inversely related to the average liquid velocity, as shown in Equation 5.4. For the experimental trials, the liquid binder solution viscosity ranged from 0.0012 Pa s to 0.0429 Pa s. This increase in viscosity would have decreased the velocity through the voids in the powder beds. As shown in Figure 5.4, the drop penetration time correspondingly increased.

Figure 5.5 shows the sizes of granule nuclei created when different viscosities of liquid binder solutions were used with the α-lactose monohydrate and with MCC powder beds. Granule nuclei formed from α-lactose monohydrate were expected to be larger than those formed from MCC as individual α-lactose monohydrate particles were almost 1.5 times larger than MCC fibers. The MCC powder, however, had an effective voidage of 0.66, almost double the effective voidage of 0.37 of the α-lactose monohydrate powder bed. This allowed a higher liquid flowrate through the voids in the MCC powder bed. The liquid binder therefore had more potential opportunities to contact particles and build liquid bridges between these particles to form larger granule nuclei containing more particles. The wetting of the particles and formation of liquid bridges, however, also depend on the hygroscopicity of the powder.

The hygroscopicity of a powder describes the amount of moisture uptake of a powder from the surrounding environment [15]. Classifications of hygroscopicity were established by Callahan et al. [16] where a Class I non-hygroscopic powder shows no change in moisture content when exposed to the surrounding environment, while a Class IV very hygroscopic powder shows a change in moisture content even with relatively low humidity in the surrounding environment. α-lactose monohydrate is classified as a non-hygroscopic powder with a relatively linear moisture adsorption isotherm while MCC is classified as hygroscopic [16]. Due to its hygroscopic properties, MCC partially absorbed the liquid binder solution when this liquid contacted a MCC particle. This reduced the amount of liquid that traveled through the voids between MCC particles. Fewer particles were therefore in contact and wetted by the liquid binder, reducing the number of liquid bridges and decreasing the granule nuclei size. In contrast, the non-hygroscopic lactose monohydrate particles did not absorb any of the liquid binder. The liquid was therefore available to continue to migrate through the voids, contacting more particles to incorporate into a larger granule nucleus.

Figure 5.5 also shows that the viscosity of the liquid binder solution affected the granule nuclei size. Smaller granules using higher viscosity liquids were also observed in Rocca et al. [11], where larger viscosity binders would migrate less readily through the voids, allowing for smaller nuclei. As the viscosity increased, the velocity of the liquid binder

migrating through the voids of the powder beds decreased. The liquid binder therefore had less potential opportunities to contact particles and build liquid bridges between these particles to form granule nuclei. The potential number of particles that the liquid contacted therefore decreased leading to fewer liquid bridges between particles and smaller granule nuclei. The effect of the liquid viscosity on the granule nuclei size was much smaller for the MCC than for the α-lactose monohydrate particles. Less liquid binder was available for migration through the voids in the MCC powder bed due to the partial absorption of the liquid by the hygroscopic particles. Consequently, the effect of viscosity on the granule nuclei size of the remaining liquid migrating through the voids was relatively small.

The shape of the granule nuclei formed was different for the two powders (Figures 5.6). This difference was partially attributed to the orientation of particles within the powder bed. Figure 5.10 shows possible schematic diagrams of the powder beds and the liquid droplet penetration and migration.
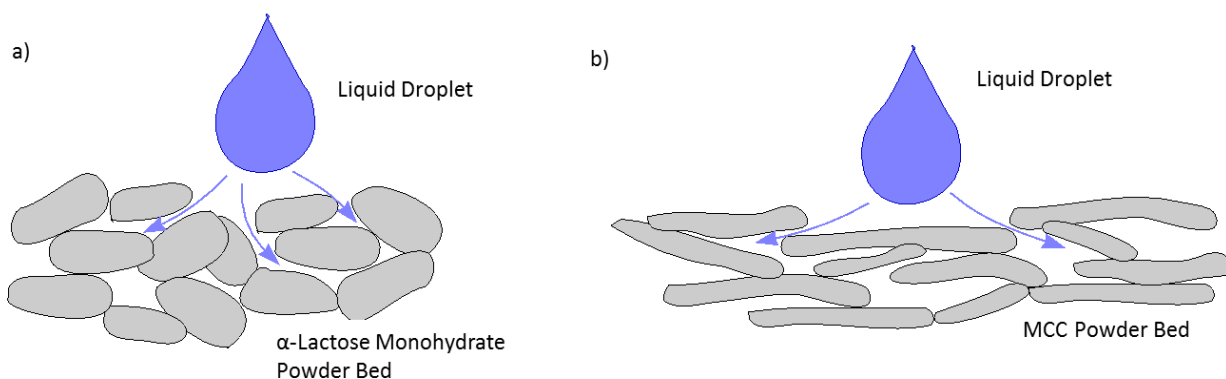
Figure 5.10: Schematic diagram of the penetration of a liquid binder droplet into powder beds of α-lactose monohydrate (a) and MCC (b).

The α-lactose monohydrate particles were somewhat rectangular and the powder bed would have many irregular shaped voids (Figure 5.10a). These voids would allow both horizontal and vertical migration of the liquid binder through the bed resulting in approximately spherical granule nuclei (Figure 5.6). For the MCC powder, many of the

fibres may be oriented horizontally (Figure 5.10b). This orientation would promote horizontal spreading of the liquid binder as it penetrated into the bed. Horizontal liquid movement would result in disc shaped MCC granule nuclei, as shown in Figure 5.6. Also, the hygroscopicity of MCC contributed to the disc shaped granule nuclei. The MCC fibres absorbed some of the liquid binder solution. As many of these fibres were oriented horizontally, they acted as "wicks" further promoting the migration of the liquid horizontally.
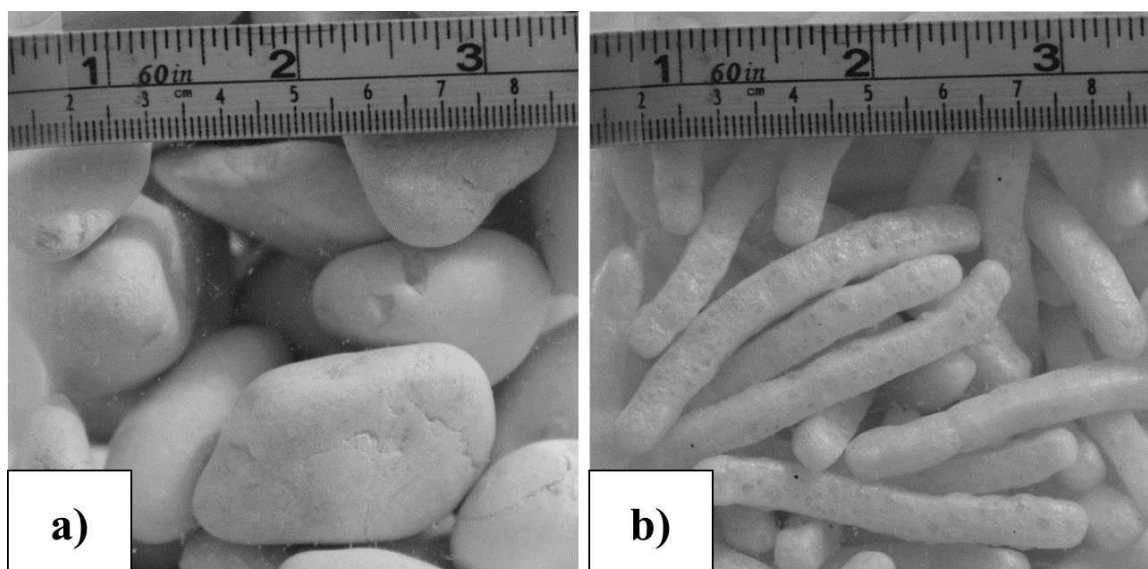
Figure 5.11 Images of model materials illustrating particle orientation for α-lactose monohydrate (a) and microcrystalline cellulose (b) powder beds. Material modeling α-lactose monohydrate powder beds show particles oriented both horizontally and vertically whereas material modeling microcrystalline cellulose show mainly particles oriented horizontally.

Figure 5.11 shows visual orientations of α-lactose monohydrate and microcrystalline cellulose particles modeled using material shapes similar to both powders. Both material particles were randomly placed into a container and photographed. The large and oval-shaped material modelling α-lactose monohydrate particles (Figure 5.11 a) show many and larger irregular shaped voids where liquid binder would allow for both vertical and horizontal migration through the powder bed. However, the model material to mimic

microcrystalline cellulose particles show particles oriented mainly horizontally (Figure 5.11 b) allowing for liquid to migrate horizontally within the powder bed.

5.4.2   Heterogeneous powder beds

The effective voidage of the powder bed increased approximately linearly as MCC was added to the powder bed, as shown in Figure 5.7. This was attributed to the different shapes of both powders. As shown in Figure 5.2, α-lactose monohydrate particles were more spherical than the MCC fibers. The voidage of the beds with spherical particles can vary from about 0.26 to 0.48 depending upon the packing condition [17]. The effective voidage for the α-lactose monohydrate bed was within this range. Random orientations of the irregular and very non-spherical MCC fibers created large voids within the bed increasing the voidage.

Drop penetration times for the heterogeneous power beds decreased as the effective voidage increased as shown in Figure 5.8. Decreasing drop penetration times were also observed in Rocca et al. [11] using a pure lactose monohydrate and MCC powder beds as well as a 50/50 mixture with a foam binder. The relationship between the drop times and effective voidage was non-linear, suggesting a complex relationship between the voids and liquid binder velocity. According to Equation 5.4, this relationship should be linear. Although the effective voidage of the bed changed almost linearly with the MCC fraction, due to the shapes and possible orientations of the two particles, the relationship with void geometry and radii may be complex and affect the drop penetration.

Figure 5.9 shows a decrease in granule size as the effective voidage and thus fraction of MCC in the powder bed increased. This decrease reflected the increasing amount of MCC within the bed. Although the higher voidage of the bed increased the potential velocity of the liquid binder through the voids, the liquid penetration was limited by the absorption by the hygroscopic MCC fibres. Fewer particles were therefore sufficiently wetted to form the liquid bridges to create a large granule. Observations also showed that the granule shape quickly progressed from approximately spherical granules of α-lactose monohydrate particles to disc shaped granules as the fraction of MCC in the powder increased. As MCC fibres were introduced into the powder bed, the geometry of the

voids changed to promote more horizontal migration of the liquid binder. The size and shape of the granules did not vary linearly with voidage or fraction of MCC in the bed; even a small amount of MCC in the powder mixture had an effect on granule formation. The quick drop in size and change in shape with the introduction of MCC in the powder suggested that the granule nuclei may contain a disproportionate amount of MCC.

5.5   Conclusions

Liquid binder drop penetration and subsequent granule nuclei formation were studied using α- lactose monohydrate and MCC powders and HPMC solutions as the liquid binders. Drop penetration time increased with the addition of HPMC in the liquid binder as the increasing liquid viscosity decreased the liquid velocity through the voids in the powder beds. The drop penetration time was shorter for MCC than for α-lactose monohydrate powder beds due to the high effective voidage, but granule nuclei were smaller as the hygroscopic MCC fibres partially absorbed some of the liquid binder minimizing the amount at the surface available for forming liquid bridges with other particles. In addition, MCC granule nuclei were disc shaped as the fibres promoted the horizontal migration of the liquid binder into the powder bed. In the heterogeneous powder beds, the hygroscopic MCC again minimized the formation of liquid bridges resulting in smaller, disc shaped granule nuclei that may have contained disproportionate amounts of MCC.

5.6   References

1. J. Litster, B. Ennis, L. Lian, The science and engineering of granulation processes, Springer (2004).

2. S.M. Iveson, J.D. Litster, K. Hapgood, B.J. Ennis, Nucleation, growth and breakage phenomena in agitated wet granulation processes: a review, Powder Technology, 117 (2001) 3-39.

3. K.P. Hapgood, J.D. Litster, S.R. Biggs, T. Howes, Drop penetration into porous powder beds, Journal of Colloid and Interface Science, 253 (2002) 353-366.

4. T. Nguyen, W. Shen, K. Hapgood, Drop penetration time in heterogeneous powder beds, Chemical Engineering Science, 64 (2009) 5210-5221.

5. P. McEleney, G.M. Walker, I.A. Larmour, S.E.J. Bell, Liquid marble formation using hydrophobic powders, Chemical Engineering Journal, 147 (2009) 373-382.

6. K.P. Hapgood, B. Khanmohammadi, Granulation of hydrophobic powders, Powder Technology, 189 (2009) 253-262.

7. K.P. Hapgood, L. Farber, J.N. Michaels, Agglomeration of hydrophobic powders via solid spreading nucleation, Powder Technology, 188 (2009) 248-254.

8. S. Ardizzone, F.S. Dioguardi, T. Mussini, P.R. Mussini, S. Rondinini, B. Vercelli, A. Vertova, Microcrystalline cellulose powders: structure, surface features and water sorption capability, Cellulose, 6 (1999) 57-69.

9. J. Kristensen, T. Schaefer, P. Kleinebudde, Direct pelletization in a rotary processor controlled by torque measurements. II: Effects of changes in the contest of microcrystalline cellulose, Aaps Pharmsci, 2 (2000) art. no.-24.

10. T.M. Chitu, D. Oulahna, M. Hemati, Rheology, granule growth and granule strength: Application to the wet granulation of lactose-MCC mixtures, Powder Technology, 208 (2011) 441-453.

11. K.E. Rocca, S. Weatherley, P.J. Sheskey, M.R. Thompson, Influence of filler selection on twin screw foam granulation, Drug Development and Industrial Pharmacy, 41 (2015) 35-42.

12. H. Li, M.R. Thompson, K.P. O'Donnell, Progression of Wet Granulation in a Twin Screw Extruder Comparing Two Binder Delivery Methods, Aiche Journal, 61 (2015) 780-791.

13. R.C. Rowe, P.J. Sheskey, S.C. Owen, A.P. Association, Handbook of pharmaceutical excipients, Pharmaceutical press London (2006).

14. A. Alkhatib, L. Briens, Modelling liquid binder drop penetration into heterogeneous powder beds. In preparation for submission; 2015.

15. A. Crouter, L. Briens, The Effect of Moisture on the Flowability of Pharmaceutical Excipients, AAPS Pharmscitech, 15 (2014) 65-74.

16. J. Callahan, G. Cleary, M. Elefant, G. Kaplan, T. Kensler, R. Nash, Equilibrium moisture content of pharmaceutical excipients, Drug Development and Industrial Pharmacy, 8 (1982) 355-369.

17. F.A. Dullien, Porous media: fluid transport and pore structure, Academic press (1991).

Chapter 6

6 Modelling liquid binder drop penetration into heterogeneous powder beds

6.1 Introduction

Wet granulation, the process of agglomerating powder particles using a liquid binder to form granules, is used extensively in the pharmaceutical industry. Granulation occurs in three simultaneous rate processes: wetting and nucleation, consolidation and growth, and breakage and attrition [1]. The behavior of droplets impacting upon a powder bed, called the wetting and nucleation stage, and the subsequent granules that form are essential to controlling and designing the wet granulation process [2]. Wetting and nucleation have received significant attention, as these processes are crucial to developing optimal granules with a narrow size distribution and content uniformity.

Wetting and nucleation occur primarily in the spray zone of a granulator, where the liquid binder initially contacts the powder bed [3]. The droplets penetrate into the powder bed where the binder forms liquid bridges between the powder particles to create granule nuclei. In the spray zone, granule nuclei formation is important, where poor powder and liquid combinations can lead to difficulty in reproducibility of granulation processes [4]. Operation should occur in the drop controlled regime, where ideal nucleation is achieved when one liquid binder forms one granule nucleus.

Regime maps have been developed to determine the operation regime of granulation processes [4-10]. Regime maps for granule nucleation are a function of both the formulation as well as process parameters of the granulation process, where two criteria need to be satisfied in order to operate in the desired drop controlled regime and obtain granules with a narrow size distribution [4]: (i) Relatively little overlap of droplets or a low spray flux and (ii) Fast drop penetration into the bed or short drop penetration times

Fast drop penetration into the bed promotes the formation of one granule nucleus from one droplet in the drop controlled nucleation regime. With an approximately constant droplet size, the resulting nuclei size distribution is narrow, which positively impacts growth into final granules with an optimal size range. Powder properties, such as wettability, and liquid properties, such as viscosity, have been shown to affect nucleation kinetics [11-13].

6.1.1   Theoretical Model Development

Middleman et al. [14] developed a simple model to describe the penetration of a liquid droplet into a powder bed. For this model, the voids between the particles of the powder bed are assumed to be bundles of parallel cylindrical capillaries. The driving force for the liquid flow through these capillaries was the capillary pressure difference due to surface tension and described by the Young-Laplace equation and, for a spherical droplet, by:

$$\Delta P = \frac{2\gamma \cos \theta_d}{R} \tag{6.1}$$

where γ is the surface tension of the liquid, R is the radius of the droplet and is the dynamic contact angle which measures the flow of a liquid through capillary voids [16].

The liquid flow through the capillaries was assumed to be Newtonian and laminar with an average velocity given by:

$$U = \frac{dx}{dt} = \frac{R^2 \Delta p}{8\mu x} \tag{6.2}$$

or

$$U = \frac{dx}{dt} = \frac{R\gamma \cos \theta_d}{4\mu x} \tag{6.3}$$

where U is the average velocity, x is the distance of liquid travelled, t is the time, R is the average radius of the voids formed between particles, θ_d is the measured dynamic contact angle, and μ is the viscosity of the liquid.

The drop penetration time, τ, is defined as the time required for a liquid droplet to penetrate completely into a powder bed with no liquid remaining at the bed surface. The drop penetration time can be obtained through integration of Equation 6.3 to give Equation 6.4:

$$\tau_{CDA} = 1.35 \frac{V_o^{2/3}}{\varepsilon^2 R_{pore}} \frac{\mu}{\gamma_{LV} \cos \theta_d} \tag{6.4}$$

where V_o is the drop volume, ε is the powder bed voidage and R_{pore} is the size of the voids in the powder bed. This integration assumes a constant drawing area, CDA, where the droplet radius remains constant while the contact angle decreases as the droplet penetrates into the powder bed [16, 17]. A CDA assumption means that the number of capillaries available for the liquid droplet to penetrate remains constant.

Hapgood et al. [18] recognized the limitations of the model developed by Middleman et al. [14]: powder beds do not have uniform parallel capillary voids and therefore liquid penetration into the voids is more complex than described by this simple model. The voids of a powder bed in a granulator are not uniform and the radii of these voids can vary and change. Hapgood et al. [18] proposed that sudden increases in the void radius will stop liquid migration through that void, changing the pathway of the liquid penetration and increasing the penetration times. To account for these variations in void sizes, Hapgood et al. [18] defined an effective voidage, ε_{eff}, to estimate the fraction of voids within a powder bed that have a radius that allows liquid flow. They proposed that this effective voidage could be obtained from the bed voidage, ε, and its tap voidage, ε_{tap}:

$$\varepsilon_{eff} = \varepsilon_{tap}(1 - \varepsilon + \varepsilon_{tap}) \tag{6.5}$$

$$\varepsilon = 1 - \frac{\rho_{bulk}}{\rho_{true\ particle\ density}} \tag{6.6}$$

$$\varepsilon_{tap} = 1 - \frac{\rho_{tap}}{\rho_{true\ particle\ density}} \tag{6.7}$$

Adapting the Kozeny approach to estimating voidage allows an effective radius of the voids to be:

$$R_{eff} = \frac{\phi d_{3,2}}{3} \frac{\varepsilon_{eff}}{(1-\varepsilon_{eff})} \tag{6.8}$$

where ϕ is the shape factor of the particles and $d_{3,2}$ is the surface mean particle diameter. Modification of the Middleman et al. [14] model then provided a new estimate of a drop penetration time based upon a constant drawing area:

$$\tau_{CDA,M} = 1.35 \frac{V_o^{2/3}}{\varepsilon_{eff}^2 R_{eff}} \frac{\mu}{\gamma_{LV} \cos \theta_d} \tag{6.9}$$

Hapgood et al. [18] applied this modified drop penetration model to powders ranging from glass ballotini to lactose monohydrate, zinc oxide and titanium dioxide. The predicted values were higher and provided generally better estimates of the drop penetration times.

6.1.2   Drop Penetration Studies

Several researchers have studied the penetration of liquid droplets into powder beds. Effects of parameters such as drop impact, powder wettability, granule agglomeration, voidage of the powder bed and liquid viscosity on drop kinetics have been considered [11, 18-32]. Studies on drop impact using single droplets penetrating into a static powder showed varying drop penetration mechanisms for changing droplet velocities [19-21]. Hapgood et al. [18] measured the drop penetration time of systems of many different homogeneous powder beds and liquid binders to acquire data to improve existing drop penetration models. Nguyen et al. [11] examined heterogeneous powder beds of salicylic

acid and lactose monohydrate with distilled water as the liquid binder; adding more salicylic acid to the lactose monohydrate increased the hydrophobicity of the powder bed and the drop penetration times correspondingly increased. Powder hydrophobicity was also studied by several other research groups, where extreme hydrophobicity led to liquid marble formation and longer drop penetration times [22-25].

Both Marston et al. [27] and Charles-Williams et al. [28] investigated the effect of powder moisture content on drop penetration as, during granulation, liquid binder droplets will impact upon and penetrate into beds of increasing moisture content. Marston et al. [27], using glass ballotini and water, found that the drop penetration time decreased as the moisture content of the bed increased while Charles-Williams et al. [28] found the opposite trend with powder beds of lactose monohydrate. The results provided in the literature to date indicate that penetration of liquid droplets into powder beds is complicated and can depend on many factors.

A few studies have used the model by Hapgood et al. [18] to predict drop penetration times for their respective systems. Nefzaoui et al. [29] found that increasing viscosity of the liquid binder resulted in larger deviations of the predicted drop penetration times from measured results. Oostveen el al. [30] also found differences between measured and predicted drop penetration times for various powder starches. They then attempted to improve the model by replacing the effective voidage with a voidage measured using microCT imaging. This resulted in better agreement with the measured values.

Studies on void morphology of pharmaceutical powder beds do not appear in the literature. However, the effect of void morphology of porous media on drop penetration has been studied for other applications such as ink printing onto porous paper [31]. It has been found that sharp discontinuities in the void morphology may have been a more significant effect upon drop penetration rate than void size [32]. The orientation of the voids affects the penetration rate and depth where a large number of vertical voids promote faster rates with deeper penetration.

Microcrystalline cellulose (MCC) and lactose monohydrate are commonly used excipients in the pharmaceutical manufacturing of tablets. Our previous work examined drop penetration times and granule nuclei formation using MCC and lactose monohydrate system with several binder solutions. Increases in liquid binder viscosity led to longer drop penetration times and increasing bed effective voidage decreased drop penetration times. In addition, granule nuclei size and shape were affected. Nuclei were smaller than expected with an increase in the amount of MCC as MCC partially absorbed the liquid binder reducing the amount available for forming the liquid bridges between particles to create granule nuclei. The void structure in a MCC powder bed promoted horizontal migration over vertical liquid migration resulting in disk shaped nuclei compared to the more spherical nuclei formed with lactose monohydrate powder.

Rapid drop penetration into powder beds is important for establishing drop controlled nucleation during granulation. Models to predict drop penetration times have been developed and examined, primarily using ideal powders such as glass ballotini. The goal of this research was to examine the models developed by Middleman et al. [14] and Hapgood et al. [18] using more complex powder bed systems of MCC and lactose monohydrate, two excipients commonly used in commercial formulations.

6.2   Materials and Methods

6.2.1   Material Characterization

6.2.1.1   Particle Size and Shape

Microcrystalline cellulose (Avicel PH-101, FMC BioPolymer) and α- lactose monohydrate (EMD Emprove) were used in this study. Images of the powders were taken using a Hitachi S-4500 field emission scanning electron microscope; the powders were mounted on a plate and coated with gold before examination. Particle size measurements for the MCC and α- lactose monohydrate were analyzed in triplicate using a Malvern Mastersizer 2000. The shape factor was determined as the ratio of the actual projected surface area of the particle (A) to the area of a circle with a diameter of maximum length (ML) [34]:

$$Shape\ factor\ (\phi) = \frac{4\ A}{\pi \cdot (ML)^2} \tag{6.10}$$

The surface area and maximum length diameter of the particles were determined using Image-Pro Premier software and the scanning electron microscope images and were analyzed in triplicates.

Powder properties are summarized in Table 6.1.

Table 6.1: Summary of powder properties

wt/wt% MCC	wt/wt% α-lactose monohydrate	$d_{3,2}$ (μm)	ρ_{bulk} (g/cm³)	ρ_{tap} (g/cm³)	ε_{bed} (-)	ε_{tap} (-)	$\varepsilon_{effective}$ (-)	ϕ (-)
0	100	98.7±0.61	0.76±0.00	0.91±0.01	0.51±0.00	0.41±0.01	0.37±0.00	0.51±0.00
20	80	87±0.47	0.61±0.01	0.78±0.01	0.61±0.01	0.5±0.01	0.44±0.00	0.47±0.01
40	60	75.32±0.33	0.49±0.01	0.68±0.02	0.68±0.01	0.56±0.01	0.5±0.01	0.42±0.01
60	40	63.64±0.22	0.43±0.01	0.58±0.01	0.73±0.00	0.63±0.01	0.57±0.00	0.38±0.00
80	20	51.97±0.16	0.36±0.00	0.52±0.00	0.77±0.00	0.67±0.00	0.6±0.00	0.33±0.01
100	0	40.29±0.23	0.33±0.01	0.45±0.01	0.79±0.01	0.71±0.01	0.66±0.01	0.29±0.00

6.2.1.2   Density and Voidage

The true particle density of the α-lactose monohydrate and MCC were obtained through comparison with literature values and calculations described by Nguyen et al. [11] for determining true particle densities of heterogeneous mixtures [35]. Values ranged between 1.55 g/cm³ for pure α-lactose monohydrate particles to 1.58 g/cm³ for pure MCC particles.

Bulk density was determined by measuring the powder weight when loosely filled in a 100 mL graduated cylinder. Tap density was determined by agitating the powder in 100 mL graduated cylinders and determining the change in volume.

6.2.1.3   Liquid Binder Measurements

Liquids used for drop penetration experiments were water and 2 wt%, 6 wt%, and 8 wt% hydroxypropyl methylcellulose (HPMC) aqueous solutions (Shin-Etsu Chemical Company, Grade 603). Solutions were prepared by heating water to over 85° C, then

gradually adding HPMC powder while stirring until the powder fully dissolved. Solutions were cooled to 20°C before conducting experiments. A blue dye that did not affect the liquid properties was added to enhance visualization during the drop penetration trials.

Densities of liquid binders were measured using a Gamma-Sphere, Type X (Viscone Instruments, CH-5605 Dottikon). 10 mL liquid samples were measured and a 10 g sphere was inserted into the liquid sample. Displacement measurements were recorded to obtain density values. Viscosity measurements were conducted using a Brookfield Viscometer at 20 rpm with a 61 spindle. Dynamic surface tension was measured using a KRUSS Bubble Pressure Tensiometer and surface tension values were used at a surface age of 37 ms.

Liquid binder properties are summarized in Table 6.2.

Table 6.2: Summary of liquid binder properties

Liquid Solution	Surface Tension (mN/m)	Viscosity (Pa s)	Density (g/cm^3)
Water	73.67±0.30	0.0012±0.21	0.996±0.00
2 wt % HPMC	56.13±0.16	0.0042±0.42	1.002±0.01
6 wt % HPMC	55.28±0.17	0.0231±1.27	1.012±0.00
8 wt % HPMC	55.14±0.36	0.0429±0.85	1.017±0.00

6.2.1.4   Dynamic Contact Angle Measurements

Dynamic contact angle (θ_d) measurements were conducted using the Washburn method [36-38]. The dynamic contact angle was calculated by measuring the mass increase in powder during contact with liquid binder using the following equation:

$$m^2 = c \frac{\rho^2 \gamma_{LV} \cos\theta_d}{\mu} t \tag{6.11}$$

where m is the mass of the liquid at time t, ρ is the liquid density, γ_{LV} is the liquid-vapor surface tension of the liquid , μ is the liquid viscosity and c is the material constant. The

material constant was measured using hexane, a wetting fluid giving a dynamic contact angle of 0 for both the α-lactose monohydrate and MCC [38, 39].

A cylindrical metal vessel was loaded with 10 g sample powder and a filter was attached to one end of the vessel. The powder was packed using a shaker at 1500 rpm for 1 hour in order for similar orientation of powder in the vessel. The metal vessel was attached to a balance and liquid solution contacted the filter end of the vessel. Liquid was allowed to absorb into the powder and the change in mass over time was collected at 1 s intervals. Measurements were complete when mass remained constant and the liquid had fully absorbed into the powder bed.

Dynamic contact angles for the powder ratios were determined using a method developed by Cassie et al. [40] to calculate the apparent contact angle of heterogeneous powder beds:

$$\cos \theta_{apparent} = f_1 \cos \theta_1 + f \cos \theta_2 \tag{6.12}$$

where f_1 and f_2 are the fractions of powder 1 and 2 in the binary mixture and θ_1 and θ_2 are the dynamic contact angles of powder 1 and 2.

6.2.2   Drop Penetration Measurements

Drop penetration time measurements were conducted using a procedure similar to that described in Hapgood et al. [18]. The powders were manually mixed and sieved through a 1.70 mm sieve into a petri dish. Powder was allowed to freely settle into the petri dish as to mimic a granulation process where powder is not compressed. Excess powder was scraped off using a spatula. A 25 gauge needle syringe was mounted 0.5 cm above the powder bed and a liquid droplet (V_o=0.0048 mL) was gently placed onto the powder bed. Syringe height was placed just above the powder bed as to avoid the effects of drop impact observed in previous studies [19-21]. Drop penetration was filmed using a Canon EOS 60D camera with a macro lens, capturing images at 30 frames per second (fps). The procedure was repeated in triplicate. Figure 6.1 shows a schematic of the drop penetration set up. The drop penetration time was determined as the time at which the liquid droplet

was no longer visible at the powder bed surface. The images were carefully examined for changes in grayscale to help determine this time.
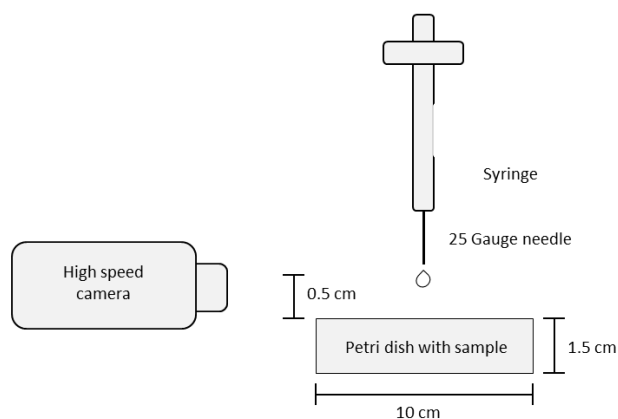
Figure 6.1: Schematic of the drop penetration measurements

6.3 Results

Figure 6.2 shows the particle size distributions, and Figure 6.3 shows the scanning electron images of the α-lactose monohydrate and MCC powders.
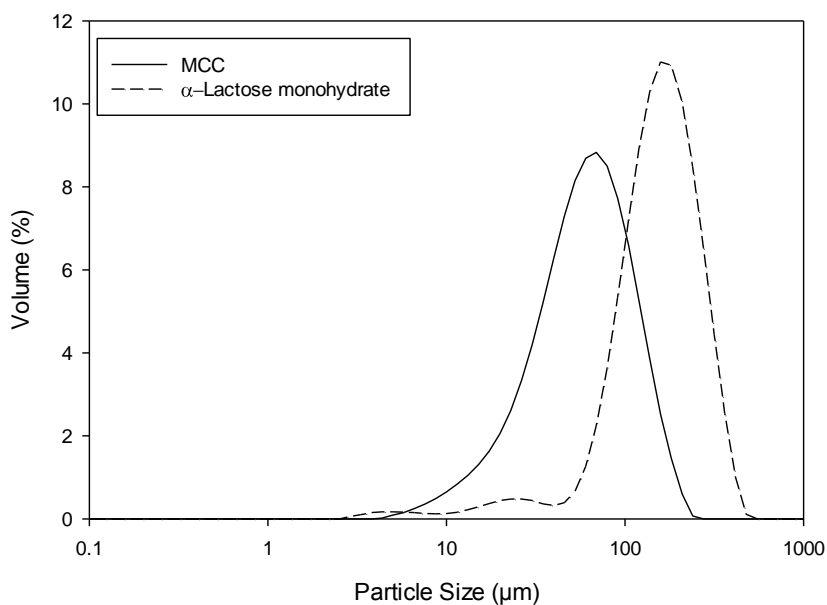
Figure 6.2: Particle size distributions for microcrystalline cellulose and α-lactose monohydrate

Most α-lactose monohydrate particles were near 170 μm with some smaller particles while MCC particles were overall smaller with a narrow distribution around 56 μm. α-lactose monohydrate particles had a smooth surface and a somewhat rectangular shape. MCC particles, in contrast, were irregular fibres. The size and shape of α-lactose monohydrate particles were considerably different than that of MCC, contributing to the change in effective voidage of the powder bed (Table 6.1).
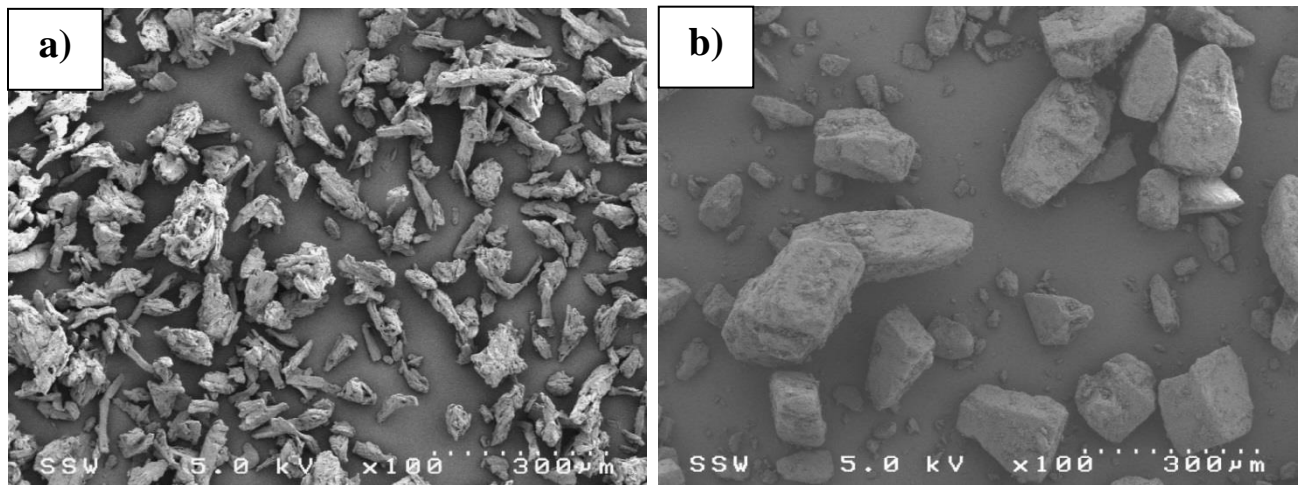
Figure 6.3: Scanning electron micrograph images of (a) microcrystalline cellulose and (b) α-lactose monohydrate

Figure 6.4 shows the effect of both liquid binder solution viscosity and effective voidage of the powder bed on the measured drop penetration times. Drop penetration times ranged between 0.12 s to 3.29 s, where increasing viscosity resulted in longer drop penetration times. An increase in α-lactose monohydrate powder in the bed, and hence decrease in effective voidage also resulted in longer drop penetration times.
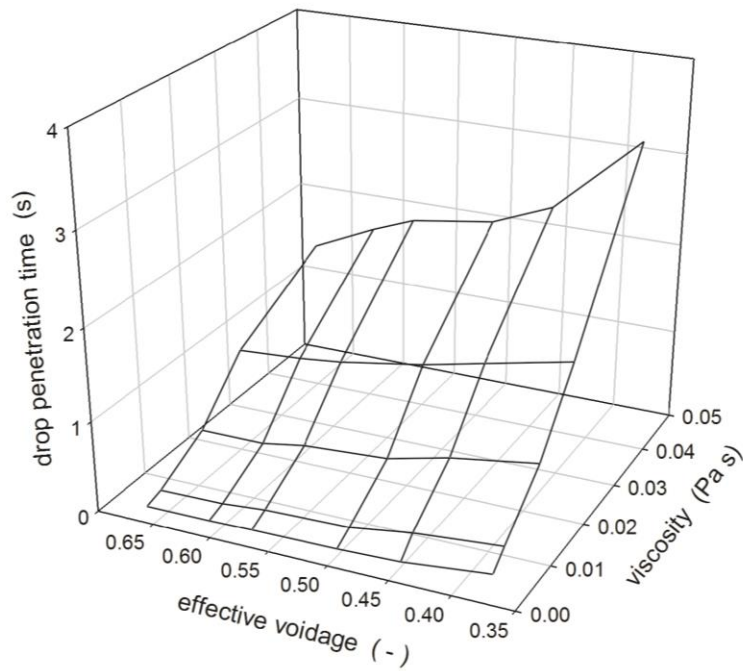
Figure 6.4: Measured drop penetration times for various powder bed effective voidages and liquid binder solution viscosities

Figure 6.5 compares the measured drop penetration times with the predicted times from the model by Middleman et al. [14], (Equation 6.4) and the model modification by Hapgood et al. [18], (Equation 6.9). Regression analysis allowed for the line of best fit to the data.
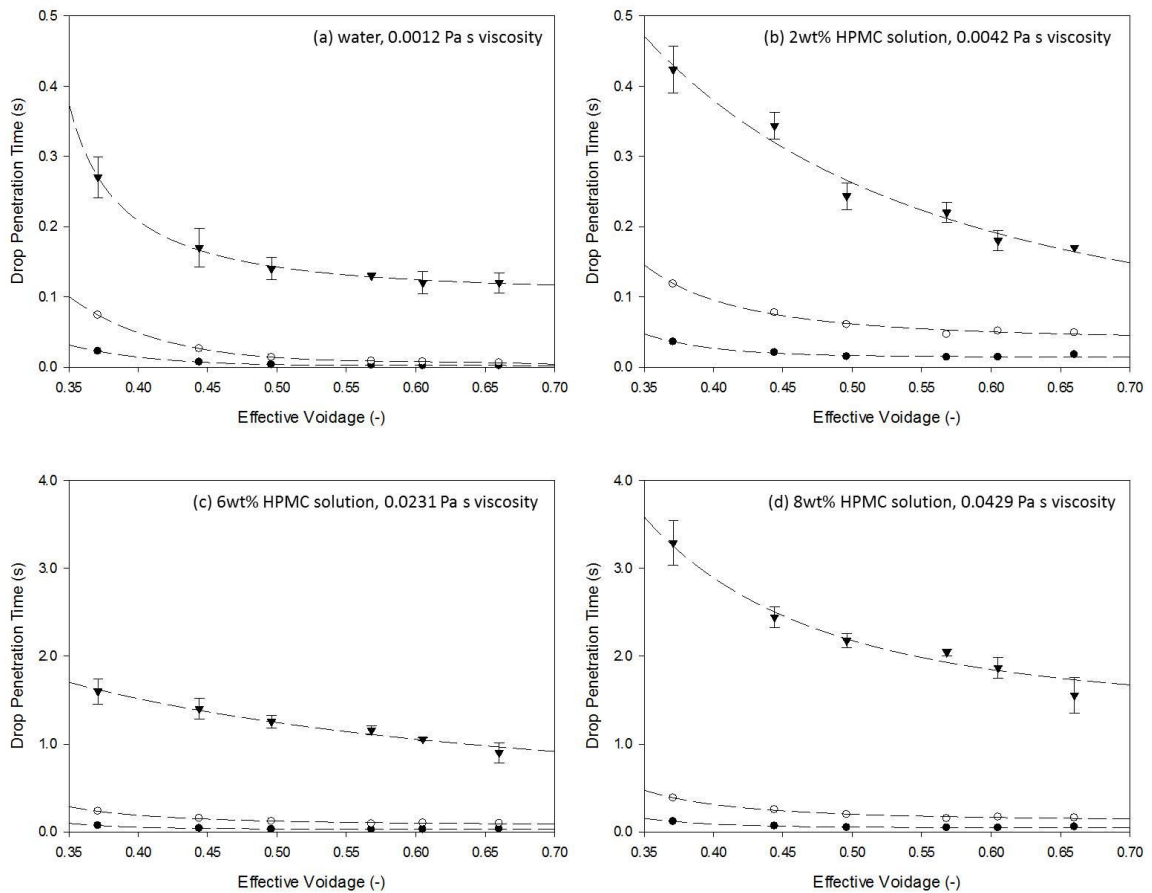
Figure 6.5: A comparison of measured drop penetration times (▼) with the predicted times using the model from Middleman et al. [14] (●) and modification by Hapgood et al. [18] (○).

6.4   Discussion

Figure 6.4 shows that increasing the effective voidage of the powder slightly decreased the drop penetration times. Powder beds with a high voidage would have many voids and/or many with large radii that would allow for faster migration of the liquid binder solution through the powder bed and corresponding decrease in drop penetration time.

The liquid binder solution viscosity increased from 0.0012 Pa s as HPMC was added until a viscosity of 0.0429 Pa s for an 8 wt% HPMC solution (Table 6.2). Figure 6.4 also shows the effect of liquid binder solution viscosity on the measured drop penetration times. The drop penetration times increased from 0.12 s to 3.29 s as the liquid binder

solution viscosity increased. As the viscosity increased, the velocity of the solution migrating through the voids of the powder bed decreased, which, in turn, increased the drop penetration times. Hapgood et al. [18] also measured longer drop penetration times of high viscosity binder solutions into homogenous powder beds.

Measured drop penetration times were compared with predicted times using equations 4 and 9 (Figure 6.5). The predicted times using the model modifications by Hapgood et al. [18] were slightly higher than predictions from the model by Middleman et al. [14]. Both model predictions, however, significantly underestimated the drop penetration times. The differences between the measured and predicted times were larger for the powder beds of low effective voidage and also larger as the liquid binder solution viscosity increased. Nguyen et al. [11] also found that predicted drop penetration times were lower than measured values for powder beds of varying ratios of salicylic acid and lactose monohydrate with water as the binder liquid. For many of their systems, Hapgood et al. [18] reported higher measured drop penetration times than predicted values. Their model modification improved the predicted values for powder beds of glass ballotini spheres and within an order of magnitude for homogenous powder beds of lactose monohydrate. Predicted times remained significantly lower for zinc oxide and titanium dioxide powder beds; these exceptions were attributed to the complex powder bed microstructures. The model assumptions and parameters do not adequately model many powder bed and liquid binder systems, especially complex powder systems that would be used for many pharmaceutical applications.

The Middleman et al. [14] model assumed that the voids were bundles of parallel cylindrical capillaries and liquid flowed uniformly through these capillaries. Hapgood et al. [18] improved this model by incorporating the possibility of non-uniform flow due to sudden changes in the size of the voids. Liquid will flow through the powder bed relatively easily if the voids are approximately equal in size or monotonically decrease in size, as in the beds with uniform shaped particles with a relatively narrow size distribution that have been arranged in a random slow packing pattern. For powder beds that are irregularly packed, there will be a wide range of void sizes. Liquid flow through the bed will stop if the void size increases suddenly to a macro-void. Macro-voids within

the powder beds will increase drop penetration times as the liquid must then migrate through other voids to penetrate into the bed. Hapgood et al. [18] accounted for the effect of macro-voids by incorporating an effective voidage into the model. This modification increased drop penetration times, improving predictions, but still failed to adequately predict drop penetration times for complex powder systems.

The α-lactose monohydrate and MCC powders had particles of very differently sizes and shapes which contributed to a range of effective voidages in the powder beds. Proposed schematic diagrams of the powder beds are given in Figure 6.6.
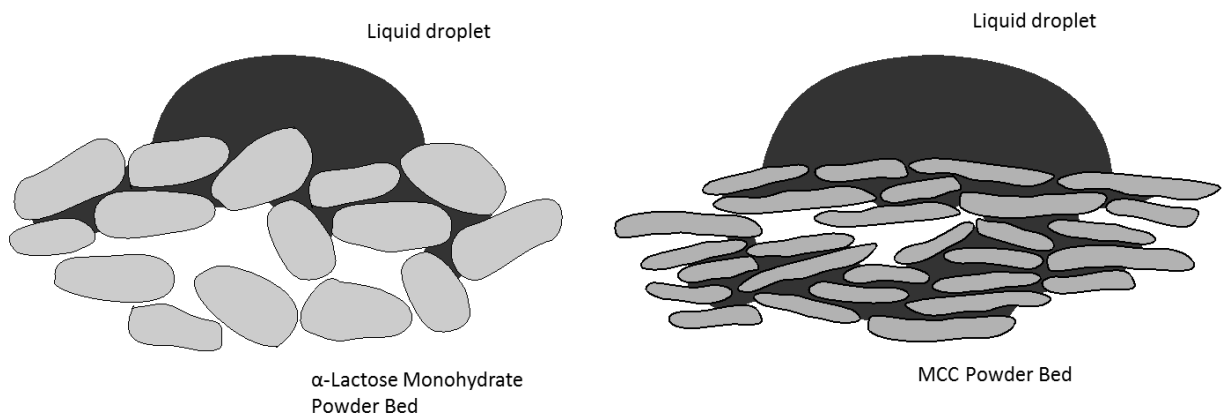
Figure 6.6: Schematic diagrams of the α-lactose monohydrate and MCC powder beds

Due to the size and shape of α-lactose monohydrate particles, a powder bed with many macro-voids and irregular shaped voids is proposed. In contrast, it is proposed that the small needle shaped MCC particles would primarily align horizontally thereby creating a powder bed with fewer macro-voids.
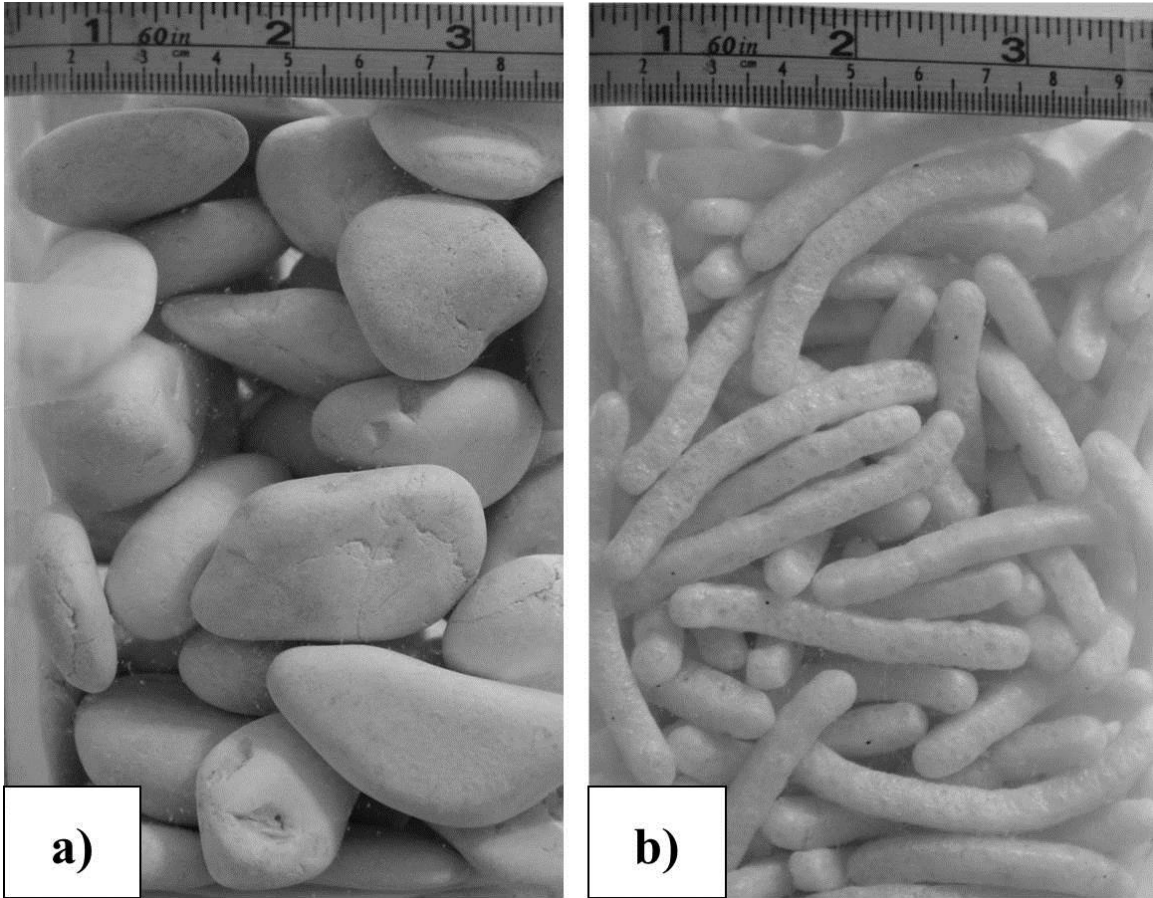
Figure 6.7: Images of model materials illustrating particle orientation for α-lactose monohydrate (a) and microcrystalline cellulose (b) powder beds. Material modeling α-lactose monohydrate powder beds show many irregular shaped voids much larger in size compared with material modeling microcrystalline cellulose.

Figure 6.7 shows visual orientations of α-lactose monohydrate and microcrystalline cellulose particles modeled using material shapes similar to both powders. Both material particles were randomly placed into a container and photographed. The large and oval-shaped material modelling α-lactose monohydrate particles (Figure 6.7 a) show many and larger irregular shaped voids compared with the model material to mimic microcrystalline cellulose particles which shows particles oriented mainly horizontally (Figure 6.7 b) allowing for fewer and smaller macro-voids.

Hapgood et al. [18] improved the Middleman et al. [14] model by trying to incorporate the effect of macro-voids in the powder beds through the introduction of an effective

voidage term. This improved the model, but the effect of macro-voids on the drop penetration time was still underestimated for beds with many macro-voids as proposed for α-lactose monohydrate powder beds.

Differences between the measured and predicted drop penetration times increased with increasing viscosity of the liquid binder solution. As the viscosity of the liquid binder solution increased, its migration velocity through the voids decreased due to higher resistance to flow. When a liquid encountered a macro-void, the flow stopped and the liquid then flowed through other voids to continue to penetrate into the bed. As the high viscosity liquids had more resistance to flow, stopping the flow in the direction of the macro-void and then changing directions to flow through other voids was very difficult. Drop penetration times of high viscosity liquids into powder beds with many macro-voids were therefore very long and much higher than model predictions.

The Middleman et al. [14] model assumed that voids were bundles of parallel cylindrical capillaries. The modification proposed by Hapgood et al. [18] partially accounted for sudden changes in the diameter of the void to create a macro-void. Neither model, however, accounts for irregular shaped voids. It has been proposed that sharp changes in the geometry of the voids may have a more significant effect on liquid penetration into a porous medium than void size [31]. As shown in the proposed schematics for the α-lactose monohydrate and MCC powder beds, the voids are irregular in shape especially in the α-lactose monohydrate powder bed. These irregular shape voids may therefore have also contributed to the differences between the measured and predicted drop penetration times.

Previous studies [29, 30] as well as the current results have all shown differences between measured and predicted drop penetration times thereby showing the need to even further improve the models. The results from α- lactose monohydrate and MCC powder beds indicate that the models need to consider more macro-voids and possibly irregular shaped voids. A parameter, ω, to account for these voids was introduced and coupled to the effective voidage term:

$$\tau_{CDA,new} = 1.35 \frac{V_O^{2/3}}{(\omega\varepsilon_{eff})^2 R_{eff}} \frac{\mu}{\gamma_{LV} \cos\theta_d} \tag{6.13}$$

This ω parameter can be adjusted for powder beds of different voidages. For the α-lactose monohydrate- MCC powder system with measured effective voidages between 0.37 and 0.66, ω was selected varying linearly between 0.42 and 0.32 according to:

$$\omega = -0.34\varepsilon_{eff} + 0.54 \tag{6.14}$$

Figure 6.7 shows that the predictions of drop penetration time using the model modified to include the parameter ω compared with Equation 6.9 correspond well with the measured drop penetration times. The parameter ω accounts for more macro-voids and/or irregular shaped voids that can be present in complex powder bed systems.
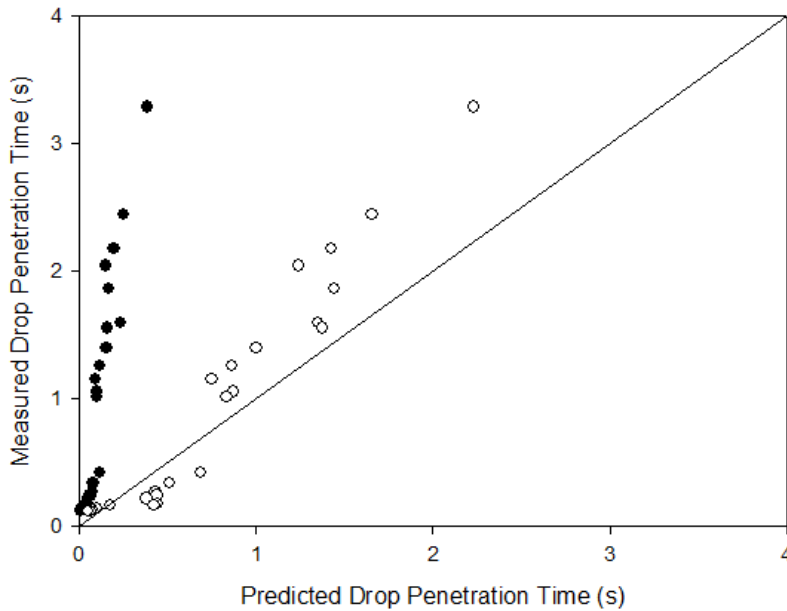
Figure 6.8: Measured drop penetration times compared with predicted times using the Hapgood equation (•) and the improved model equation to include the parameter, ω (○).

This model modification was also applied to the complex zinc oxide powder bed system using a viscous polyethylene glycol liquid binder solution from Hapgood et al. [18]. The model from Hapgood et al. [18] using this system highly underestimated the measured

drop penetration times and was attributed to the complex powder bed formed with the ZnO. To improve the predicted value, our semi-empirical model was applied to this system using the provided value of effective voidage of 0.41 and Equation 6.14, the value for the parameter ω was estimated to be 0.40. Measured drop penetration time was reported at 19.7 s and the Hapgood model predicted the drop penetration time to be 1.7 s. The prediction using our semi-empirical model was significantly improved to now 10.59 s for polyethylene glycol droplet penetration time into the zinc oxide bed. Although the source of the powder and detailed shape information was not provided, from the given data of small diameters with a high surface area, it was concluded that the particles would have irregular shapes thereby possibly forming powder beds with many macro-voids and/or irregular shaped voids. Accounting for these structures in the powder beds by incorporating the parameter ω provided better estimate of the drop penetration time.

6.5   Conclusions

Drop penetration times were measured using water and increasing hydroxypropyl methylcellulose liquid binder solutions into powder beds of α-lactose monohydrate and microcrystalline cellulose. A comparison of the measured times with predicted times from the models by Middleman et al. [14] and Hapgood et al. [18] showed that these models always underestimated the drop penetration times. The longer measured times were attributed to complex powder beds that have many macro-voids and/or irregular shaped voids that inhibit the path of the liquid binder solutions. A parameter ω that represents these complex void structures was introduced into the model by Hapgood et al. [18], coupled with the effective voidage term. The addition of the parameter ω to the model provided predictions of drop penetration times that corresponded well to measured times for powder beds of α-lactose monohydrate and microcrystalline cellulose. The modification was also applied to complex powder bed systems provided in the literature and significantly improved the predictions. The developed semi-empirical model with the new parameter ω reliably predicts drop penetration times for complex powder bed systems and therefore can be useful in the selection of granulation process parameters for optimum operation and yields of granules.

6.6   References

1. J. Litster, B. Ennis, L. Lian, The science and engineering of granulation processes, Springer2004.

2. S.M. Iveson, J.D. Litster, K. Hapgood, B.J. Ennis, Nucleation, growth and breakage phenomena in agitated wet granulation processes: a review, Powder Technology, 117 (2001) 3-39.

3. S.H. Schaafsma, P. Vonk, N.W.F. Kossen, Fluid bed agglomeration with a narrow droplet size distribution, International Journal of Pharmaceutics, 193 (2000) 175-187.

4. K.P. Hapgood, J.D. Litster, R. Smith, Nucleation regime map for liquid bound granules, Aiche Journal, 49 (2003) 350-361.

5. K.P. Hapgood, Nucleation and binder dispersion in wet granulation, (2000).

6. S.M. Iveson, J.D. Litster, Growth regime map for liquid-bound granules, Aiche Journal, 44 (1998) 1510-1518.

7. S.M. Iveson, P.A.L. Wauters, S. Forrest, J.D. Litster, G.M.H. Meesters, B. Scarlett, Growth regime map for liquid-bound granules: further development and experimental validation, Powder Technology, 117 (2001) 83-97.

8. S.L. Rough, D.I. Wilson, D.W. York, A regime map for stages in high shear mixer agglomeration using ultra-high viscosity binders, Advanced Powder Technology, 16 (2005) 373-386.

9. S.L. Rough, D.I. Wilson, A.E. Bayly, D.W. York, Mechanisms in high-viscosity immersion-granulation, Chemical Engineering Science, 60 (2005) 3777-3793.

10. W.D. Tu, A. Ingram, J. Seville, S.-S. Hsiau, Exploring the regime map for high-shear mixer granulation, Chemical Engineering Journal, 145 (2009) 505-513.

11. T. Nguyen, W. Shen, K. Hapgood, Drop penetration time in heterogeneous powder beds, Chemical Engineering Science, 64 (2009) 5210-5221.

12. S.J.R. Simons, R.J. Fairbrother, Direct observations of liquid binder-particle interactions: the role of wetting behaviour in agglomerate growth, Powder Technology, 110 (2000) 44-58.

13. T. Schaefer, C. Mathiesen, Melt pelletization in a high shear mixer .8. Effects of binder viscosity, International Journal of Pharmaceutics, 139 (1996) 125-138.

14. S. Middleman, Modeling axisymmetric flows: dynamics of films, jets, and drops, Academic Press 1995.

15. P. Joos, P. Vanremoortere, M. Bracke, The kinetics of wetting in a capillary, Journal of Colloid and Interface Science, 136 (1990) 189-197.

16. A. Marmur, The radial capillary, Journal of Colloid and Interface Science, 124 (1988) 301-308.

17. M. Denesuk, G.L. Smith, B.J.J. Zelinski, N.J. Kreidl, D.R. Uhlmann, Capillary penetration of liquid droplets into porous materials, Journal of Colloid and Interface Science, 158 (1993) 114-120.

18. K.P. Hapgood, J.D. Litster, S.R. Biggs, T. Howes, Drop penetration into porous powder beds, Journal of Colloid and Interface Science, 253 (2002) 353-366.

19. J.O. Marston, S.T. Thoroddsen, W.K. Ng, R.B.H. Tan, Experimental study of liquid drop impact onto a powder surface, Powder Technology, 203 (2010) 223-236.

20. S. Agland, S.M. Iveson, The impact of liquid drops on powder bed surfaces, Chemeca 99: Chemical Engineering: Solutions in a Changing Environment, (1999) 218.

21. A.C.S. Lee, P.E. Sojka, Drop Impact and Agglomeration Under Static Powder Bed Conditions, Aiche Journal, 58 (2012) 79-86.

22. K.P. Hapgood, L. Farber, J.N. Michaels, Agglomeration of hydrophobic powders via solid spreading nucleation, Powder Technology, 188 (2009) 248-254.

23. N. Eshtiaghi, J.S. Liu, W. Shen, K.P. Hapgood, Liquid marble formation: Spreading coefficients or kinetic energy?, Powder Technology, 196 (2009) 126-132.

24. N. Eshtiaghi, J.J.S. Liu, K.P. Hapgood, Formation of hollow granules from liquid marbles: Small scale experiments, Powder Technology, 197 (2010) 184-195.

25. K.P. Hapgood, B. Khanmohammadi, Granulation of hydrophobic powders, Powder Technology, 189 (2009) 253-262.

26. S.H. Schaafsma, P. Vonk, P. Segers, N.W.F. Kossen, Description of agglomerate growth, Powder Technology, 97 (1998) 183-190.

27. J.O. Marston, J.E. Sprittles, Y. Zhu, E.Q. Li, I.U. Vakarelski, S.T. Thoroddsen, Drop spreading and penetration into pre-wetted powders, Powder Technology, 239 (2013) 128-136.

28. H.R. Charles-Williams, R. Wengeler, K. Flore, H. Feise, M.J. Hounslow, A.D. Salman, Granule nucleation and growth: Competing drop spreading and infiltration processes, Powder Technology, 206 (2011) 63-71.

29. E. Nefzaoui, O. Skurtys, Impact of a liquid drop on a granular medium: Inertia, viscosity and surface tension effects on the drop deformation, Experimental Thermal and Fluid Science, 41 (2012) 43-50.

30. M.L.M. Oostveen, G.M.H. Meesters, J.R. van Ommen, Quantification of powder wetting by drop penetration time, Powder Technology.

31. T.J. Senden, M.A. Knackstedt, M.B. Lyne, Droplet penetration into porous networks: Role of pore morphology, Nordic Pulp & Paper Research Journal, 15 (2000) 554-563.

32. H. Kent, M. Lyne, Influence of paper morphology on short term wetting and sorption phenomena, Fundamentals of Papermaking: Transactions of the Ninth Fundamental Research Symposium, Cambridge, 1989, pp. 895-920.

33. M. Cavinato, E. Andreato, M. Bresciani, I. Pignatone, G. Bellazzi, E. Franceschinis, N. Realdon, P. Canu, A.C. Santomaso, Combining formulation and process aspects for optimizing the high-shear wet granulation of common drugs, International Journal of Pharmaceutics, 416 (2011) 229-241.

34. K. Iida, Y. Hayakawa, H. Okamoto, K. Danjo, H. Leuenberger, Evaluation of flow properties of dry powder inhalation of salbutamol sulfate with lactose carrier, Chemical & Pharmaceutical Bulletin, 49 (2001) 1326-1330.

35. R.C. Rowe, P.J. Sheskey, S.C. Owen, A.P. Association, Handbook of pharmaceutical excipients, Pharmaceutical press London2006.

36. D.F. Steele, R.C. Moreton, J.N. Staniforth, P.M. Young, M.J. Tobyn, S. Edge, Surface Energy of Microcrystalline Cellulose Determined by Capillary Intrusion and Inverse Gas Chromatography, Aaps Journal, 10 (2008) 494-503.

37. E. Nowak, G. Combes, E.H. Stitt, A.W. Pacek, A comparison of contact angle measurement techniques applied to highly porous catalyst supports, Powder Technology, 233 (2013) 52-64.

38. A. Siebold, A. Walliser, M. Nardin, M. Oppliger, J. Schultz, Capillary rise for thermodynamic characterization of solid particle surface, Journal of Colloid and Interface Science, 186 (1997) 60-70.

39. J. Kiesvaara, J. Yliruusi, The use of the washburn method in determining the contact angles of lactose powder, International Journal of Pharmaceutics, 92 (1993) 81-88.

40. A. Cassie, Contact angles, Discuss. Faraday Soc., 3 (1948) 11-16.

Chapter 7

7 Influence of process parameters and powder properties on initial granule nuclei formation during high shear granulation

7.1 Introduction

High shear wet granulation is the process of the agglomeration of particles using a liquid binder in order to form multi-particle granules. The granules are important for preventing segregation, improving flowability, and compaction, as well as for stabilizing mixtures [1]. Poor granulation causes problems in downstream processes that eventually lead to substandard tablets that must be discarded. High shear wet granulation is a common step in the manufacture of many pharmaceutical tablets. The granulator bowl is loaded with specific powder excipients and after an initial mixing period, the liquid binder is sprayed onto the powder bed to form granule nuclei that grow until the process is stopped. The granules are then dried and further processed as part of the solid dosage form manufacturing pathway.

The formation of granules in high shear granulators has been studied by several research groups. This research has been summarized in a review article by Iveson et al. [2]. Granulation starts with wetting and nucleation. The liquid binder impacts upon the powder surface in the granulator bowl, ideally as small droplets, and then penetrate into the powder bed to form granule nuclei. The penetration time of the liquid binder into the powder bed affects the formation of granule nuclei and is dependent on powder bed voidage, particle size and orientation in the bed, as well as both the properties of the liquid and powder [3].

Properties of the powders can influence granule nuclei formation. Iveson et al. [2] explain that a liquid binder can preferentially wet the more hydrophilic particles of a formulation. Therefore, if the powder surface in initial contact with the liquid binder contains a mixture of powders with different surface properties, granule formation and growth with hydrophilic particles would be promoted over granules containing hydrophobic particles. A study of the drop penetration of a heterogeneous powder mix of hydrophilic and

hydrophobic powders by Nguyen et al. [4] found that increasing the hydrophobicity led to longer drop penetration times.

The influence of hygroscopicity on drop penetration time has been studied using heterogeneous mixtures of α-lactose monohydrate and hygroscopic microcrystalline cellulose (MCC) [5]. Drop penetration times decreased as the fraction of hygroscopic MCC in the mixture increased. The granule size also decreased as the MCC particles readily absorbed the liquid binder leaving less liquid to migrate through the powder bed voids and form liquid bridges between powder particles. Granule size and uniformity can therefore be impacted by hygroscopic powders.

Considering that the contact between the liquid binder and the surface of the powder bed influence granule formation, it is important to determine the flow and composition of this powder surface. Studies of particle flow in a bladed mixer by Zhou et al. [6] found that initial arrangement of particles affected mixing kinetics, but not the final quality of the mixture. Three different initial arrangements were investigated with a horizontal layering arrangement showing the fastest mixing time. Koller et al. [7] also investigated initial arrangements on mixing of an acetyl salicylic acid and lactose monohydrate binary mixture. Horizontal arrangement of powders found mixing to occur in two stages: a convective vertical mixing between layers followed by diffusive mixing. Cavinato et al. [8] studied the powder flow of lactose monohydrate and microcrystalline cellulose in bladed mixers of two sizes using impeller torque, current consumption and particle image velocimetry. The effect of mass fill and impeller clearance were studied and mass fill was found to contribute to changes in powder flow patterns.

Segregation in a bladed mixer was studied by Conway et al. [9]. Mixtures of glass beads of varying diameter were used in their study. It was found that the larger particles segregated to the powder surface and then to the bowl perimeter. This pattern was observed independently of powder loading. Impeller velocities only up to 50 rpm were tested. At higher impeller velocities typically used in high shear granulators, it would be expected that the high centrifugal effects would segregate the large particles near the bowl perimeter.

Mixing in a PMA-1 high shear granulator was studied using different size sugar spheres [10]. Dry mix time, particle load order, particle size ratio and impeller speed were varied using a design of experiments methodology. Impeller speeds at 300 rpm and 700 rpm resulted in a bumping and roping regime introduced by Litster et al [11]. During the bumping regime, larger particles segregated to the centre of the granulator bowl. The roping regime resulted in larger particles segregating near the surface of the toroid. The study recommended larger particles to be loaded first and dry mix for short times at high impeller speeds to minimize segregation.

Both process parameters and powder properties during granulation were studied by Cavinato et al. [12]. The influence of formulation properties such as particle size distribution, hygroscopicity and solubility and process parameters on granule growth and final drug distribution were studied in high shear wet granulation. The distribution of three actives in final granules were analysed. Formulations with longer liquid penetration times lead to selective agglomeration and retarded granule growth. Shorter drop penetration times led to faster granule growth, but inconsistency in granule uniformity. Process parameters such as granulation time and impeller speed were found to influence the final granule formation properties such as granule strength.

A study by Oka et al [13] found non-homogeneity of granules to form due to powder segregation at the powder bed surface. Samples were collected at the surface of the powder bed to determine the surface composition at impeller speeds of 225 and 300 rpm using a design of experiments. Percolation of smaller particles to the bottom of the powder bed allowed for the larger particles to the bed surface and therefore non-homogeneity of granules. The study by Oka et al. [13] did not consider particle mixing and subsequent granule formation in both the bumpy and roping regimes. Impeller speeds used at 225 rpm and 300 rpm were both relatively low compared to conventional pharmaceutical processes. Therefore, powder mixing and subsequent initial granule nuclei behavior in both the bumpy and roping regimes need to be considered.

The objective of this research was to examine conditions that could influence granule nuclei formation in high shear wet granulation. The process parameters that were varied

included impeller speed, mixing time, and loading order of the particles. The formulation consisted of primarily α-lactose monohydrate and MCC, two commonly used excipients in pharmaceutical tablets. Impeller speeds in both the bumpy and roping regimes were considered. Through drop penetration measurements, the effect of the process parameters on the powder bed surface composition was investigated. Measurements after only a few minutes of granulation allowed the effect of the process parameters on granule nuclei formation to be investigated.

7.2 Materials and Methods

7.2.1 Equipment

An Aeromatic-Fielder PMA-1 (GEA Pharma Systems, Wommelgem Belgium) high shear granulator shown schematically in Figure 7.1 was used for all the trials. This vertical shaft granulator had a bottom mounted three bladed impeller. An optional side mounted chopper was not used for this study.
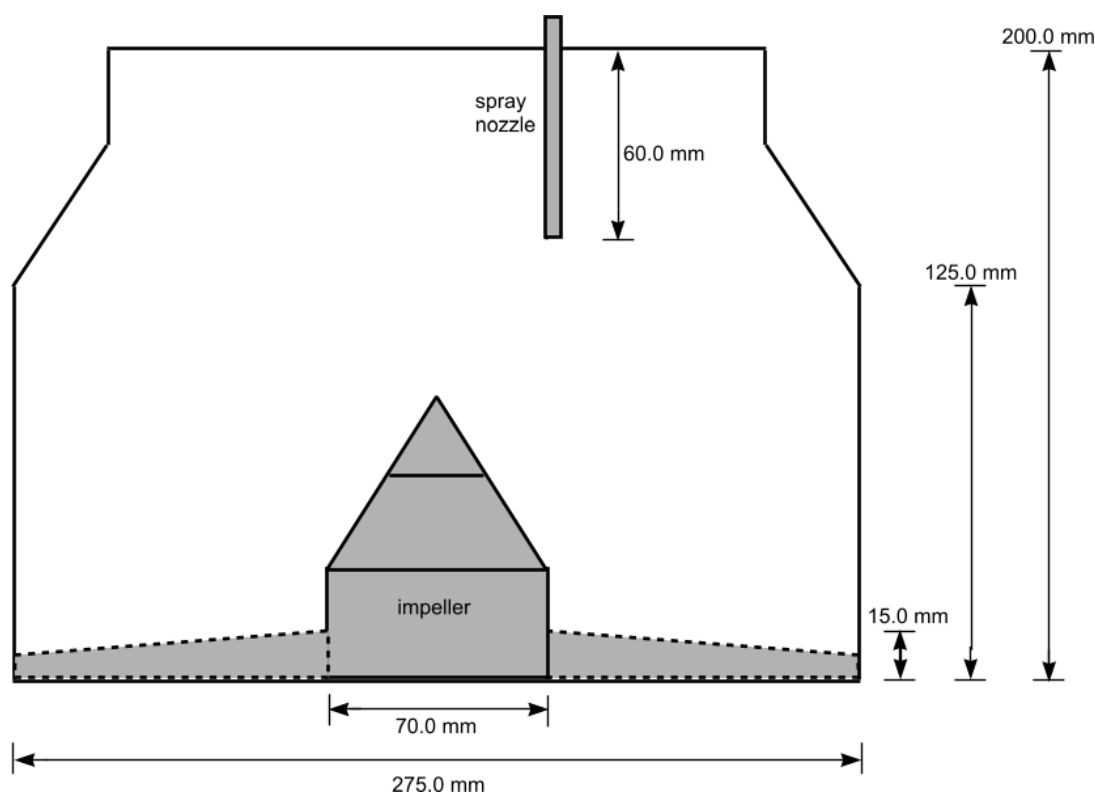
Figure 7.1: Schematic diagram of the PMA-1 high shear granulator

The experimental work was divided into two sections, drop penetration measurements and granulation measurements. The drop penetration measurements were designed to complement previous research on drop penetration into heterogeneous powder beds and to allow examination of initial granule nuclei in a high shear granulator. The granulation measurements extend our research on the effect of process parameters on segregation during dry mixing in a granulator while incorporating the effect of the powder properties on granule nuclei formation.

7.2.2   Drop Penetration Measurements

α-lactose monohydrate (EMD Emprove) and microcrystalline cellulose MCC (Avicel PH-101, FMC BioPolymer) were used as the powders for the drop penetration measurements.   A binary mixture of these powders with a total batch size of 1.5 kg powder was carefully loaded horizontally into the granulator bowl with either α-lactose monohydrate or MCC loaded first as specified in the experimental design given in Table 7.1. The impeller speed was set to either 300 or 700 rpm and the powders were allowed to dry mix through the action of the impeller for either 10 or 120 s. After mixing, the drop penetration measurements were conducted with the powder remaining in the granulator bowl.

Table 7.1: Experimental design for the drop penetration measurements

Trial	Impeller Speed (rpm)	Loading Order		Dry Mix Time (s)
		Top Layer	**Bottom Layer**	
1	300	α-lactose monohydrate	MCC	10
2	300	α-lactose monohydrate	MCC	120
3	300	MCC	α-lactose monohydrate	10
4	300	MCC	α-lactose monohydrate	120
5	700	α-lactose monohydrate	MCC	10
6	700	α-lactose monohydrate	MCC	120
7	700	MCC	α-lactose monohydrate	10
8	700	MCC	α-lactose monohydrate	120

Drop penetration measurements were conducted using a syringe with a 25 gauge needle positioned 0.5 cm above the powder bed in the granulator bowl. A 0.00048 mL droplet of liquid was then carefully dropped onto the powder bed surface. Images of the droplet penetration were recorded using a Canon 60D camera with a macro lens at 30 frames per

second to determine the time for the droplet to completely penetrate into the powder bed. An 8 wt% hydroxypropyl methylcellulose solution (Shin-Etsu Chemical Company, Grade 603), with a measured viscosity of 0.0429 Pa s, was used as the liquid for the measurements. Using a high viscosity solution for the liquid increased the drop penetration times allowing easier and more accurate measurements.

Drop penetration measurements were conducted at twelve locations, four at each of three different radial coordinates (Figure 7.2). The four measurements were averaged to provide an average value for each radial coordinate.
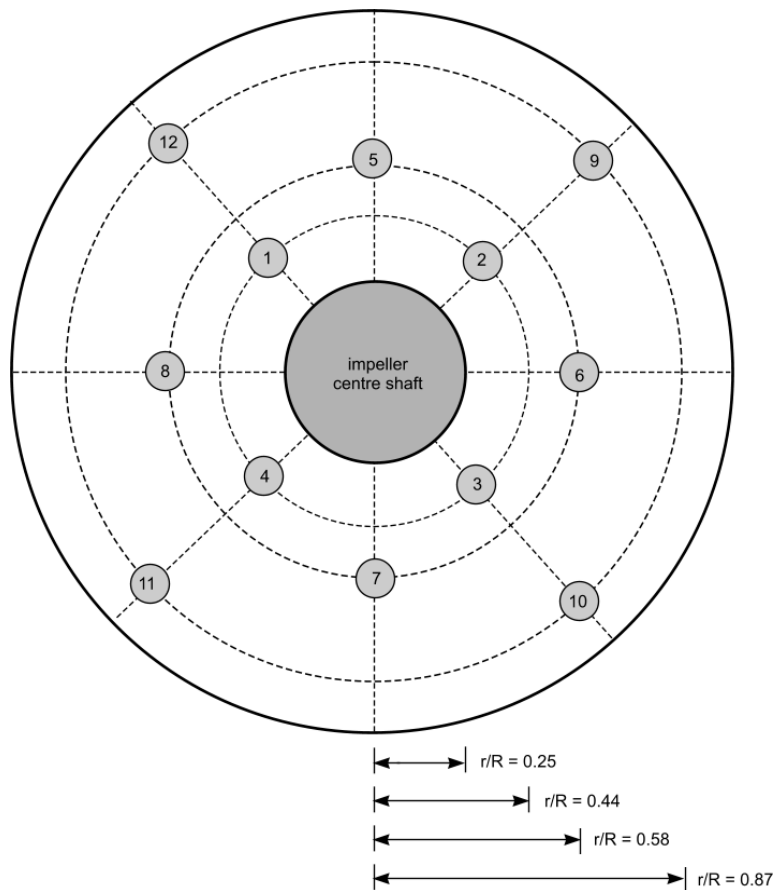
Figure 7.2: Locations for drop penetration measurements

7.2.3   Granulation Measurements

The formulation used for the granulation measurements was 50 wt% α-lactose mmonohydrate (EMD Emprove), 45 wt% microcrystalline cellulose (Avicel PH-101, FMC BioPolymer), 4% w/w hydroxypropyl methylcellulose (Shin-Etsu Chemical Co.Ltd.) and 1 wt% carboxymethyl cellulose sodium salt (Alfa Aesar). The batch size for all trials was 1.5 kg. Water was used as the liquid binder.

The powders were horizontally loaded into the granulator bowl with either α -lactose monohydrate first and MCC last or vice versa as outlined in Table 7.1. The small amounts of hydroxypropylmethyl cellulose and carboxymethyl cellulose sodium salt were added in the middle.

The impeller speed was set to either 300 or 700 rpm and the powders allowed to dry mix for either 10 or 120 s (Table 7.1). Liquid binder addition was then started at a flowrate of 67 mL/min and continued for 6 minutes.   Stopping the trials at 6 minutes wetting time allowed only granule nuclei and early growth granules to be isolated. The granulated material was removed from the bowl, dried on trays at a temperature of 23°C until the moisture content was below 2 wt%.

Images of the granule nuclei were obtained using a scanning electron microscope (Hitachi S-4500 field emission SEM with a Quartz XOne EDX system).   Samples were placed on a plate and coated with gold prior to examination. The size distribution of the granule nuclei was measured through sieving with 18 mesh cuts ranging from 38 to 3350 μm.

7.3   Results and Discussion

7.3.1   Formulation

Figure 7.3 shows the scanning electron micrograph images of α -lactose monohydrate and MCC. The size and shape of these two powder particles were very different. The α-lactose monohydrate particles had a smooth surface and an average length to width ratio of about 1.5. MCC particles were porous fibres of smaller primary particles. The surface

texture was rough and the average length to width ratio was 3 to 4 [13, 14]. The particle size distributions are shown in Figure 7.4. The median particle sizes for α-lactose monohydrate and MCC were 170 µm and 56 µm, respectively. This provided a particle size ratio of about 3.
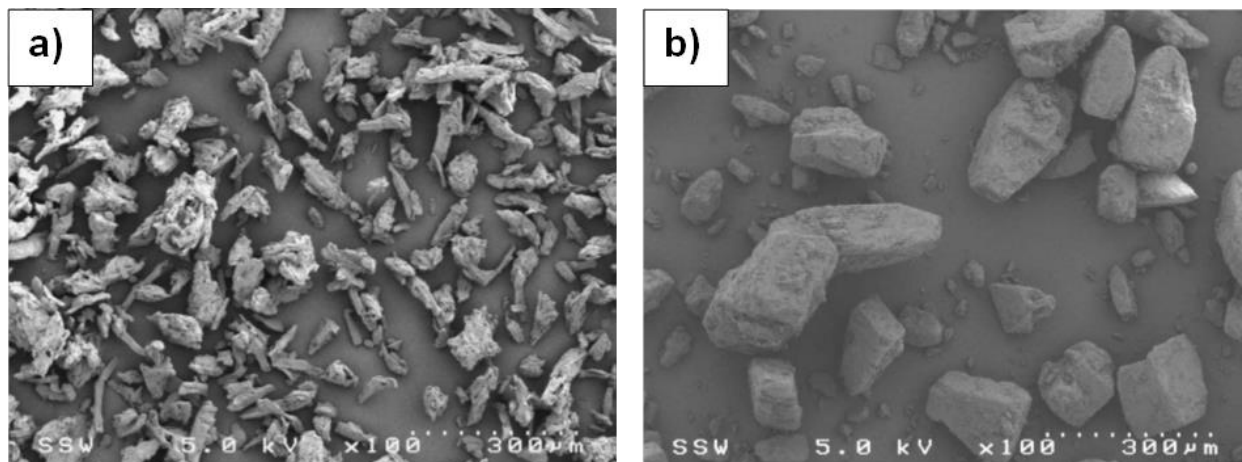
Figure 7.3: Scanning electron micrograph images of the individual components: (a) microcrystalline cellulose, (b) α-lactose monohydrate
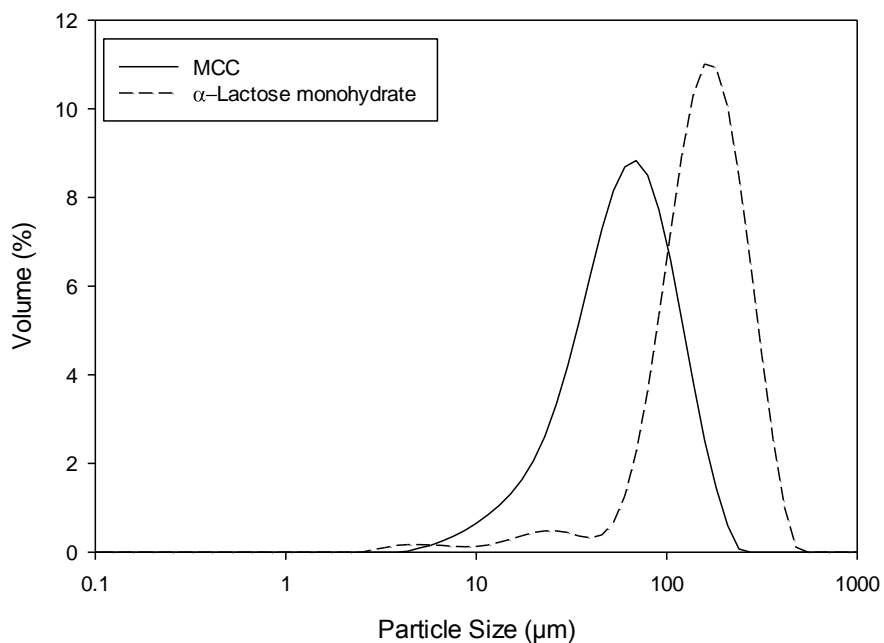
Figure 7.4: Particle size distribution for α- lactose monohydrate and MCC powders

7.3.2   Drop Penetration Measurements

Figure 7.5 shows the average times from the drop penetration measurements and compares them to values from homogeneous powder beds of α -lactose monohydrate and MCC. Standard deviations for trials at 300 rpm ranged from 0.03 to 0.59 and at 700 rpm 0.33 to 1.02. Drop penetration times of an 8 wt% HPMC solution into an α -lactose monohydrate powder bed averaged 3.2 s while the times were lower at 1.6 s for a MCC powder bed. The results showed that the powder bed surface at all locations and at both impeller speeds consisted of both **α** -lactose monohydrate and MCC.
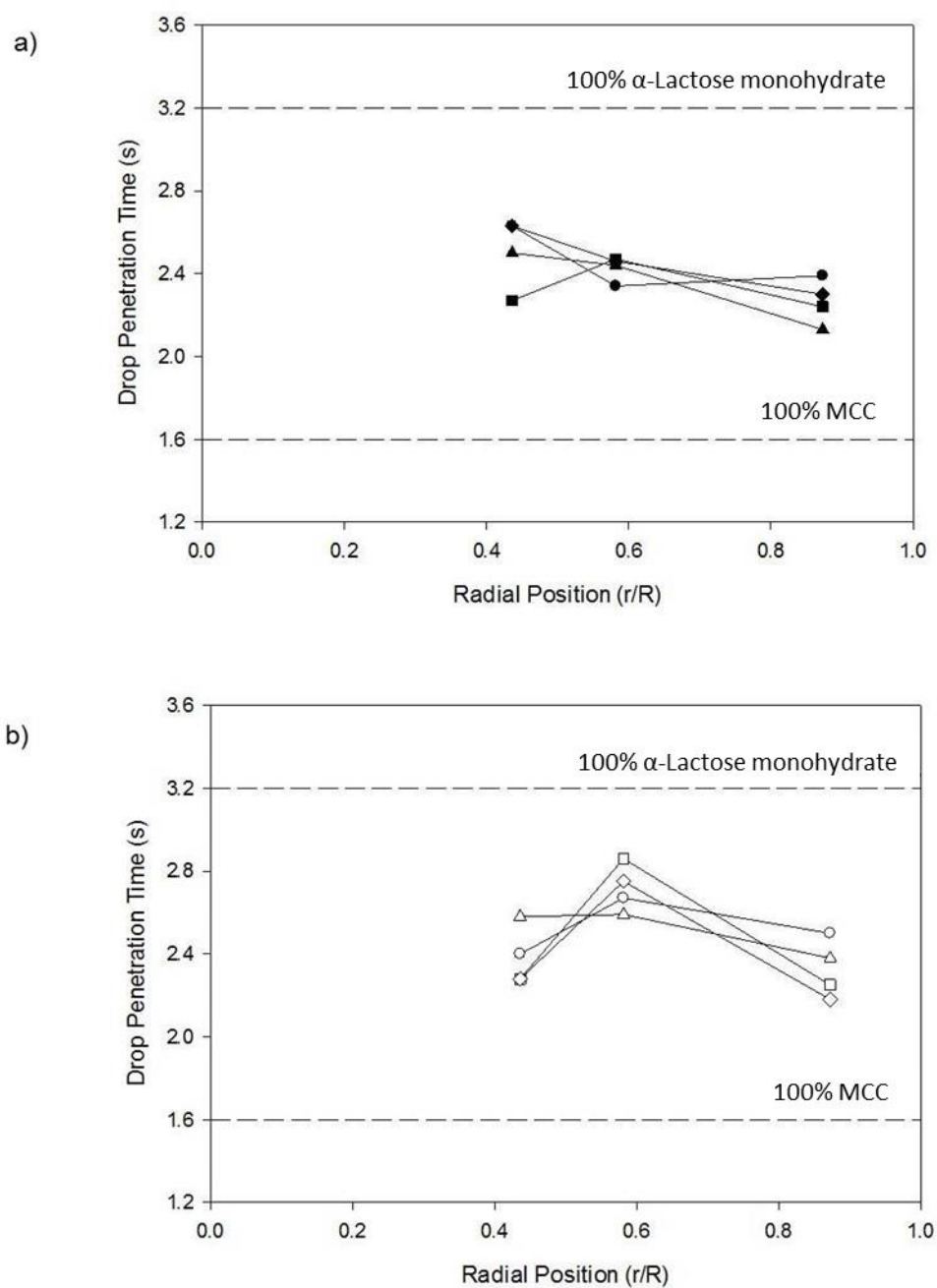
Figure 7.5: Drop penetration times for trials at an impeller speed of a) 300 rpm and 700 rpm. Trials indicated as follows: Trial 1 (●), Trial 2 (■), Trial 3 (▲), Trial 4 (♦), Trial 5 (○), Trial 6 (□), Trial 7 (△), Trial 8 (◇)

At an impeller speed of 300 rpm, the drop penetration times into the powder bed in the granulator bowl were generally higher near the centre than near the perimeter of the bowl (Figure 7.5a). These results indicated that α-lactose monohydrate was slightly overrepresented near the centre while slightly more MCC collected near the bowl perimeter. Experiments with sugar spheres showed that, at an impeller speed of 300 rpm, segregation can occur resulting in a disproportionate amount of large particles collecting near the centre of the granulator bowl [10]. The impeller disturbed the powder bed especially near the centre which promoted percolation segregation of the small particles to the bottom of the bed.

The profiles of the drop penetration times were different for the trials conducted at impeller speeds of 300 and 700 rpm. This reflected the difference in powder flow regimes: at the low impeller speed the powder followed a bumpy flow regime while at the high impeller speed a roping flow developed. The results shown in Figure 7.5b suggested that α-lactose monohydrate was slightly overrepresented at the powder bed surface at an intermediate radial position. Experiments with sugar spheres indicated that particle segregation in roping flow was complicated; a toroid with larger particles at its surface could develop. The crest of the toroid was near the radial position of 0.58 and particle movement at this location was very dynamic. The results also showed slightly different profiles for the measurements after 10 s compared to after 120 s of mixing. This indicated that the toroid structure took more than 10 s to fully form and stabilize.

Shear caused by the impeller blades can also lead to dilation of the powder bed, where dense matter has been observed to expand within the bed [16, 17]. The expansion of the powder bed would then allow for an increase in bed voidage of the MCC/ α-lactose monohydrate mixture during dry mixing. The increase in the bed voidage could potentially affect the drop penetration times and therefore granulation measurements were needed to supplement the drop penetration results.
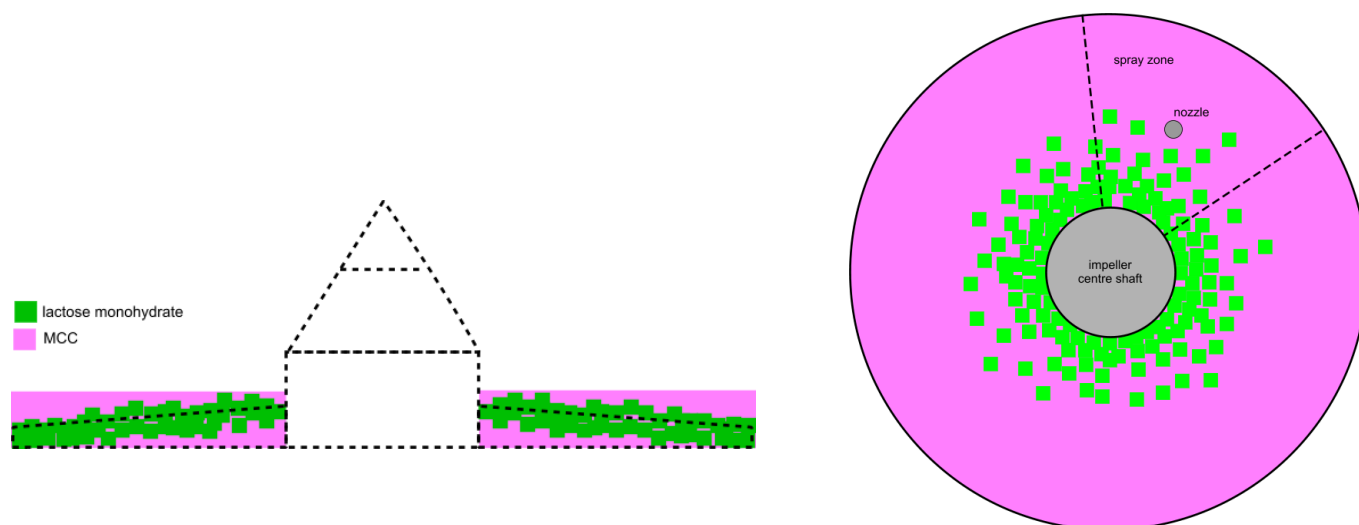
7.3.3   Granulation Measurements

The granule nuclei from the granulation trials were visualized using scanning electron microscopy. At an impeller speed of 300 rpm, the images showed that MCC particles had agglomerated into granule nuclei while the α-lactose monohydrate remained as individual particles and was not incorporated into nuclei (Figure 7.6). From the images, it was difficult to determine any effect of dry mixing time or loading order on the granule nuclei.
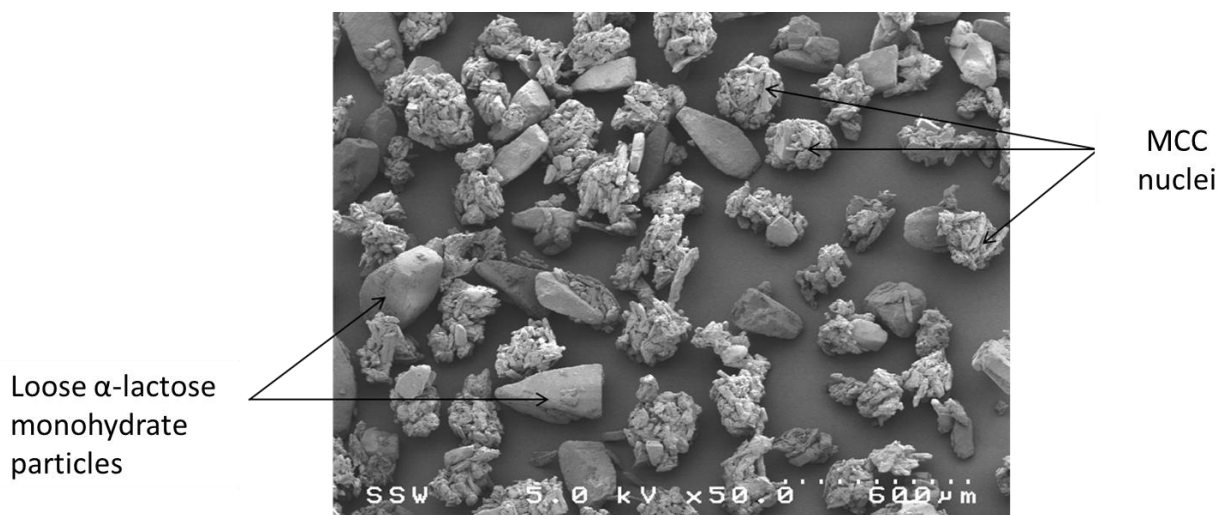
Figure 7.6: SEM image of the powder from the granulation measurements at 300 rpm showing mainly MCC nuclei as well as loose α -lactose monohydrate particles

The results from experiments with sugar spheres and from the drop penetration measurements indicated that, at an impeller speed of 300 rpm, the α -lactose monohydrate particles would segregate to the centre of the bowl while more MCC particles would be present at the powder bed surface near the bowl perimeter. The spray zone was identified as a wedge with an angle of about 60° and an area of about 8900 mm^2. As shown in Figure 7.7, this combination allowed more MCC particles to be wetted with the liquid binder spray. As MCC is hygroscopic, it easily absorbed the liquid binder droplets and quickly reached a critical liquid content that promoted coalescence into granule nuclei.

Figure 7.7: Schematic diagrams of the powder bed and spray zone at an impeller speed of 300 rpm

SEM images of the powder from the granulation measurements at an impeller speed of 700 rpm are provided in Figure 7.8. There was a mixture of granule nuclei of MCC, granule nuclei incorporating both MCC and α -lactose monohydrate and loose α -lactose monohydrate particles. At an impeller speed of 700 rpm, a toroid formed with α- lactose monohydrate particles overrepresented at its surface. As shown in Figure 7.9, this resulted in more exposure of the α-lactose monohydrate particles to the liquid binder spray compared to the MCC particles. The α-lactose monohydrate particles became sufficiently wetted to allow coalescence with other particles to form granule nuclei. α - lactose monohydrate is non-hygroscopic while MCC is hygroscopic. This property allowed MCC to easily absorb the liquid binder. Therefore, although only a small fraction of MCC was exposed to the spray, some granule nuclei of MCC were formed. The higher powder velocity at an impeller speed of 700 rpm allowed more frequent particle collisions at higher energies that promoted coalescence. Wetted α-lactose monohydrate particles could then coalesce, forming nuclei of MCC and creating granule nuclei incorporating both particles.
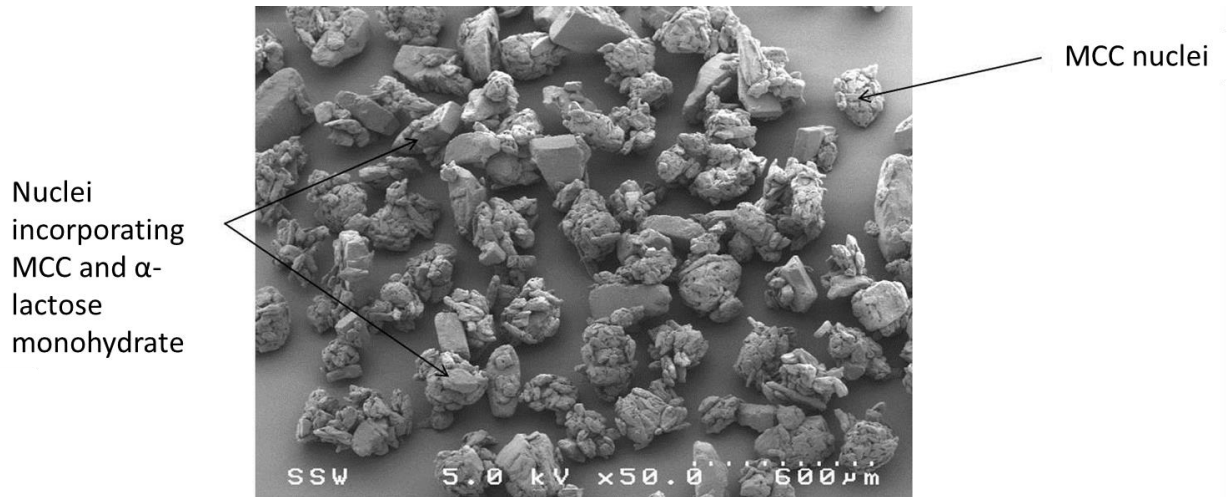
Figure 7.8: SEM image of the powder from the granulation measurements at 700 rpm showing mainly nuclei incorporating MCC and α -lactose monohydrate as well as some MCC rich nuclei.
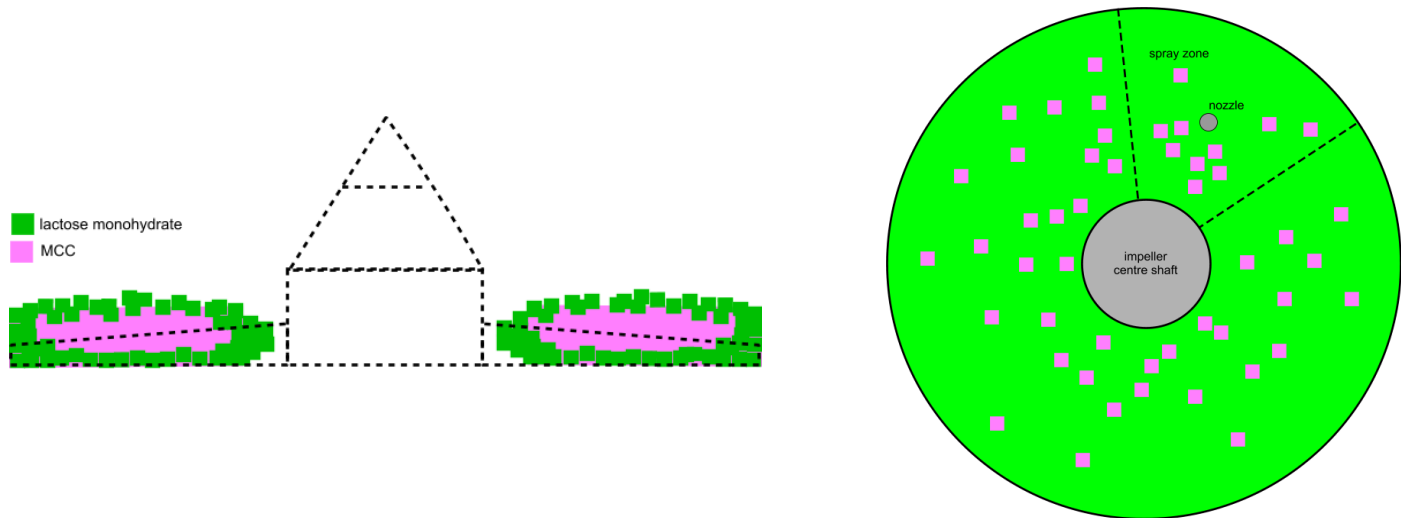

Figure 7.9: Schematic diagrams of the powder bed and spray zone at an impeller speed of 700 rpm

The incorporation of α -lactose monohydrate particles into granule nuclei at an impeller speed of 700 rpm was reflected in the size distribution measurements. As shown in Figure 7.10, the median particle sizes from the granulations at an impeller speed of 300 rpm ranged from 105 μm to 107 μm while those from the granulations at an impeller speed of 700 rpm ranged from 130 μm to 143μm.
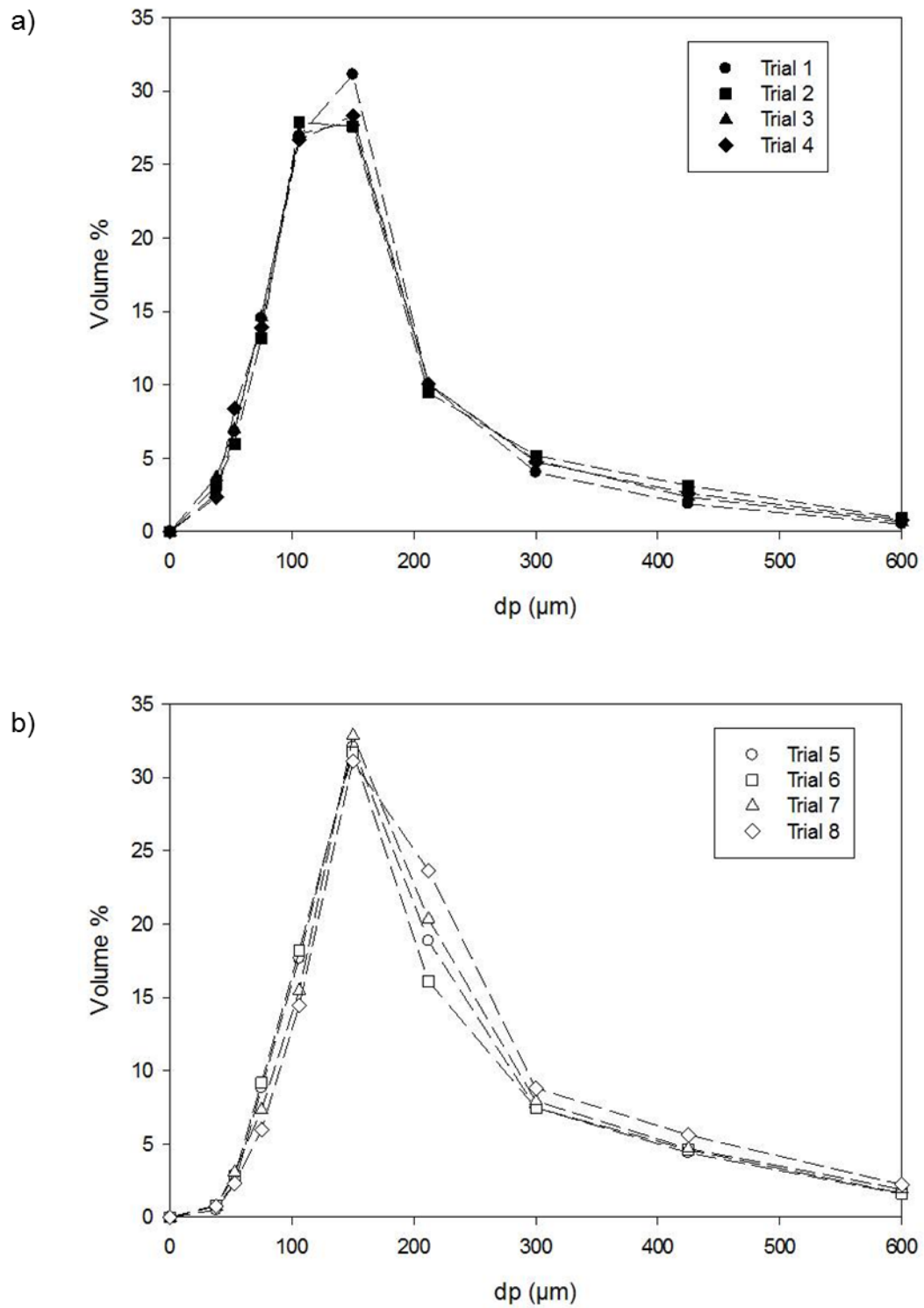
Figure 7.10: Particle size distributions for the granulation measurements at impeller speed of 300 rpm (a) and 700 rpm (b)

7.4   Conclusions

Nucleation is a critical process during high shear wet granulation as the formation of granule nuclei affects the properties of the final granules. Nucleation, however, is a complex process that is not yet fully understood. The objective of this research was therefore to investigate the influence of process and formulation properties on initial granule nuclei formation using two common pharmaceutical excipients, α- lactose monohydrate and microcrystalline cellulose.

Through drop penetration measurements, the effect of the process parameters on the powder bed surface composition was investigated. At a low impeller speed of 300 rpm, in the bumpy flow regime, the powder segregated such that α- lactose monohydrate particles were slightly overrepresented near the centre of the bowl. At a high impeller speed of 700 rpm, in the roping flow regime, the powder formed a toroid with α- lactose monohydrate particles segregating near the surface of the toroid.

Measurements after only a few minutes of granulation allowed the effect of the process parameters on granule nuclei formation to be investigated. At an impeller speed of 300 rpm, segregation caused more MCC particles to become wetted and therefore most granule nuclei were composed of only MCC particles. At an impeller speed of 700 rpm, α -lactose monohydrate particles were now exposed to the liquid binder spray and granule nuclei incorporating α -lactose monohydrate particles were also formed.

It is recommended that the initial dry mixing time of high shear wet granulation be conducted at an impeller speed high enough to ensure powder flow in the roping regime. This flow pattern allows better contact between all the components of the formulation and the liquid binder spray zone. Granule nuclei that contain all the components can therefore be formed providing the basis for growth into final granules with optimal properties.

7.5   References

1. D. Daniher, L. Briens, A. Tallevi, End-point detection in high-shear granulation using sound and vibration signal analysis, Powder Technology, 181 (2008) 130-136.

2. S.M. Iveson, J.D. Litster, K. Hapgood, B.J. Ennis, Nucleation, growth and breakage phenomena in agitated wet granulation processes: a review, Powder Technology, 117 (2001) 3-39.

3. K.P. Hapgood, J.D. Litster, S.R. Biggs, T. Howes, Drop penetration into porous powder beds, Journal of Colloid and Interface Science, 253 (2002) 353-366.

4. T. Nguyen, W. Shen, K. Hapgood, Drop penetration time in heterogeneous powder beds, Chemical Engineering Science, 64 (2009) 5210-5221.

5. A. Alkhatib, L. Briens, Granule nuclei formation in pharmaceutical powder beds of varying hygroscopic powders, In preparation for submission (2015).

6. Y.C. Zhou, A.B. Yu, R.L. Stewart, J. Bridgwater, Microdynamic analysis of the particle flow in a cylindrical bladed mixer, Chemical Engineering Science, 59 (2004) 1343-1364.

7. D.M. Koller, A. Posch, G. Hoerl, C. Voura, S. Radl, N. Urbanetz, S.D. Fraser, W. Tritthart, F. Reiter, M. Schlingmann, J.G. Khinast, Continuous quantitative monitoring of powder mixing dynamics by near-infrared spectroscopy, Powder Technology, 205 (2011) 87-96.

8. M. Cavinato, R. Artoni, M. Bresciani, P. Canu, A.C. Santomaso, Scale-up effects on flow patterns in the high shear mixing of cohesive powders, Chemical Engineering Science, 102 (2013) 1-9.

9. S.L. Conway, A. Lekhal, J.G. Khinast, B.J. Glasser, Granular flow and segregation in a four-bladed mixer, Chemical Engineering Science, 60 (2005) 7091-7107.

10. A. Alkhatib, L. Briens, Alkhatib, The effect of operational parameters on mixing in wet high shear granulation. In preparation for submission (2015)

11. J.D. Litster, K.P. Hapgood, J.N. Michaels, A. Sims, M. Roberts, S.K. Kameneni, Scale-up of mixer granulators for effective liquid distribution, Powder Technology, 124 (2002) 272-280.

12. M. Cavinato, R. Artoni, M. Bresciani, P. Canu, A.C. Santomaso, Scale-up effects on flow patterns in the high shear mixing of cohesive powders, Chemical Engineering Science, 102 (2013) 1-9.

13. S. Oka, H. Emady, O. Kaspar, V. Tokarova, F. Muzzio, F. Stepanek, R. Ramachandran, The effects of improper mixing and preferential wetting of active and excipient ingredients on content uniformity in high shear wet granulation, Powder Technology, (2015).

14. L. Shi, Y. Feng, C.C. Sun, Origin of profound changes in powder properties during wetting and nucleation stages of high-shear wet granulation of microcrystalline cellulose, Powder Technology, 208 (2011) 663-668.

15. A.M. Bouwman, M.J. Henstra, D. Westerman, J.T. Chung, Z. Zhang, A. Ingram, J.P.K. Seville, H.W. Frijlink, The effect of the amount of binder liquid on the granulation mechanisms and structure of microcrystalline cellulose granules prepared by high shear granulation, International Journal of Pharmaceutics, 290 (2005) 129-136.

16. K. Sakaie, D. Fenistein, T.J. Carroll, M. van Hecke, P. Umbanhowar, MR imaging of Reynolds dilatancy in the bulk of smooth granular flows EPL (Europhysics Lett). 84 (2008) 38001

17. T. Dunstan, J.R.F. Arthur, A. Dalili, O.O. Ogunbekun, R.K.S. Wong, Limiting mechanisms of slow dilatant plastic shear deformation of granular media, Nature, 336 (1988) 52-54.

8   General discussion and conclusions

High shear wet granulation is a common manufacturing step in the pharmaceutical industry, where liquid binder is used to agglomerate particles into granules. Granulation has the advantages of minimizing dust and segregation while improving flowability [1]. The process begins by adding a powder mixture to a granulator bowl and dry mixing. Liquid binder is then sprayed onto the powder bed, where droplets contact the particles to allow formation of granule nuclei.

The granulation process begins with the wetting and nucleation stage, where liquid binder initially contacts the powder bed. Liquid binder droplets fall onto the powder and allow for an initial granule nucleus to form. Powder particles then agglomerate to the initial nucleus, allowing for granules to grow in size. Ideally, every granule should contain the same proportion of excipients as the original powder mixture, where non-uniformity in granule formation could lead to potentially substandard tablets that need to be discarded.

Granulation has always been proven to be challenging, as both the influence of process parameters and formulation variables affect the granulation process and subsequent granule formation [2-4]. The objective of this research was to study the influence of several process and formulation parameters on powder mixing and initial granule nuclei formation during high shear wet granulation. This thesis investigates i) the influence of process parameters on dry mixing prior to liquid addition ii) formulation influence on granule nuclei formation and drop kinetics, iii) comparison of experimental drop penetration data with literature models and iv) the influence of both operational and formulation parameters on initial granule formation.

Initially there was a need to study the effects of operational parameters on dry mixing (Chapter 4). Sugar spheres were mixed in an Aeromatic-Fielder PMA-1 granulator varying the impeller speed, particle size ratio, dry mix time, and particle load order. At a low impeller speed of 300 rpm, powder flow followed the bumpy regime and large particles tended to segregate near the centre of the bowl. At a high impeller speed of 700 rpm, powder followed the roping flow regime and larger particles segregated near the

surface of the toroid. To minimize segregation, large particles should be loaded first into the bowl and the dry mixing conducted only for short times at high impeller speeds. Minimizing segregation during the initial dry mixing helps to ensure that granule nuclei contain the correct proportions of each component of the formulation and therefore likely to grow and develop into granules with the correct proportions. It should be noted that the illustrations presented in this work are conceptually based on given knowledge found with both radial and surface bed sampling.

The influence of formulation variables was investigated to further understand initial granule nuclei behavior of two commonly used pharmaceutical excipients, α -lactose monohydrate and microcrystalline cellulose (Chapter 5). The drop penetration technique was used to study initial granule nuclei behavior using liquid solutions with increasing viscosities. Liquid binders at increasing viscosities contributed to longer drop penetration times as the average velocity of the liquid would decrease with viscosity. It was also found that increasing the bed voidage through increasing the fraction of MCC in the powder bed led to shorter drop times as the increase in voidage provided more pathways for the liquid to penetrate into the powder bed. Granule size decreased with an increase of MCC in the powder bed as the hygroscopic MCC partially absorbed some of the liquid solution, leaving less liquid to travel through the voids and potentially contact other particles to form liquid bridges and thus larger granules.

For a granulation process to produce optimum granules, operation should proceed in the drop controlled regime [5]. To operate in this regime, two criteria must be satisfied: i) relatively little overlap of droplets or a low spray flux and ii) fast drop penetration into the bed or short drop penetration times. The prediction of drop penetration times was investigated where measured drop penetration times using MCC and α -lactose monohydrate and several liquid binder solutions were compared with models from literature (Chapter 6). Measured times were found to be much higher than predicted times. The models did not account for complex void structures formed within the powder bed. Therefore, a correction parameter (ω), to account for the many macro-voids and/or irregular shaped voids was introduced to incorporate these complex void structures. The new semi-empirical model then provided excellent predictions of drop penetration times

into the α -lactose monohydrate and MCC powder beds. The semi-empirical model was also applied to data from the literature and improved the prediction of the drop penetration times. A drop penetration model that reliably predicts times provides important information about granule nucleation can be used to further understand and improve granulation processes.

Investigation of both process and formulation properties on initial granule nuclei formation in a high shear granulator was studied, with the aim of developing a better understanding of nucleation using a formulation of primarily α- lactose monohydrate and microcrystalline cellulose (Chapter 7). Drop penetration measurements and granulation at short times, were used to study nuclei formation at low impeller speeds (300 rpm) and high impeller speeds (700 rpm). A bumping flow regime was observed at 300 rpm, where α -lactose monohydrate was slightly overrepresented at the center of the bowl. Roping of the powder was observed at 700 rpm, where powder formed a toroid and α -lactose monohydrate particles segregated near the surface of the toroid. It should be noted that the illustrations presented in this work are conceptually based on given knowledge found using drop penetration and granulation methods. Granulation measurements found more MCC particles to become wetted due to particle segregation at lower impeller speeds. However, at higher impeller speeds α -lactose monohydrate was exposed to the spray zone and thus incorporation of both MCC and α- lactose monohydrate to the granule nuclei were observed. It was recommended that the initial dry mixing period be conducted at high enough impeller speeds to ensure a roping regime and thus better incorporation of all powders into granule nuclei.

Future work to be conducted includes:

1) Allow for powder to be placed in the bowl vertically and study the effect this may have on initial granule formation. Compare horizontal loading with vertical loading.

2) Use different formulations to further determine the extent of segregation and nuclei formation behaviour in a high shear granulator.

a) Caffeine, paracetamol, or acetylsalicylic acid could be used with α -lactose monohydrate where analytical techniques from literature have been determined to study content uniformity [4]. This technique could be adapted to the work presented to study initial dry mixing and granule nuclei formation.

3) Utilize a Process analytical technique (PAT) to monitor mixing of powders during high shear granulation and determine possible powder segregation

8.1   References

1. C. Mangwandi, J. Liu, A.B. Albadarin, R.M. Dhenge, G.M. Walker, High shear granulation of binary mixtures: Effect of powder composition on granule properties, Powder Technology, 270 (2015) 424-434.

2. H. Charles-Williams, R. Wengeler, K. Flore, H. Feise, M.J. Hounslow, A.D. Salman, Granulation behaviour of increasingly hydrophobic mixtures, Powder Technology, 238 (2013) 64-76.

3. K. van den Dries, H. Vromans, Experimental and modelistic approach to explain granulate inhomogeneity through preferential growth, European Journal of Pharmaceutical Sciences, 20 (2003) 409-417.

4. M. Cavinato, E. Andreato, M. Bresciani, I. Pignatone, G. Bellazzi, E. Franceschinis, N. Realdon, P. Canu, A.C. Santomaso, Combining formulation and process aspects for optimizing the high-shear wet granulation of common drugs, International Journal of Pharmaceutics, 416 (2011) 229-241.

5. K.P. Hapgood, J.D. Litster, R. Smith, Nucleation regime map for liquid bound granules, Aiche Journal, 49 (2003) 350-361.

Curriculum Vitae

Name:	Aveen Alkhatib

Post-secondary Education and Degrees:

Kansas State University
Manhattan, Kansas USA
2002-2006 Bachelors of Science

Oregon State University
Corvallis, Oregon, USA
2007-2009 Masters of Science

Western University
London, Ontario, Canada
2010-2015 Doctor of Philosophy

Honours and Awards:

Western Graduate Research Scholarship (WGRS)
Western University, London, Ontario
2010-Present

Graduate Research Thesis Award
Western University, London Ontario
2013

Best Poster in Research Bridges Conference
Sarnia Research Bridges Symposium Sarnia, Ontario
2013

1st place Glaxo Smith Kline Most Industrially Relevant Poster
5th International Granulation Conference, Lausanne Switzerland
2011

Related Work Experience

Teaching Assistant
Western University
2010-2014

Teaching Assistant
Oregon State University
2007-2009

R&D Intern-Filling and Freeze Drying
Bayer HealthCare
Summer 2008

Production Engineering Intern-Manufacturing
Dow Chemical
Summer 2006

Team Advisor Intern-Manufacturing
Schreiber Foods
Summer 2005

Conference Presentation

1. **Alkhatib, A**. and Briens, L., "The Influence of Powder Hygroscopicity on Granule Formation in Pharmaceutical High Shear Wet Granulation." American Institute of Chemical Engineering (AIChE) Annual Meeting, Atlanta Georgia, (2014)

2. **Alkhatib, A.** and Briens, L., **"**Empirical Model Development of Drop Penetration of a Liquid into a Hygroscopic Powder Bed." 64th Canadian Chemical Engineering Conference, Niagara Falls Canada, (2014)

3. **Alkhatib, A**., and Briens, L., "Initial Mixing on Granule Properties." 5th International Granulation Conference, Lausanne Switzerland, (2011)

Conference Posters

1**. Alkhatib, A**. and Briens, L., "Influence of dry mixing and various process parameters on initial granule nuclei formation in High Shear Granulation." Research Bridges Symposium, London Ontario, (2013)

2. **Alkhatib, A**., and Briens, L., "Initial Mixing on Granule Properties." 5th International Granulation Conference, Lausanne Switzerland, (2011)